A Comprehensive Review on Thermal and Hygro/Hydrothermal Aging of Plant Fiber Composites: Properties, Degradation Mechanisms, and Service Life Prediction

Amine Fourari, Mouad Chakkour, Mohamed Ould Moussa, Ismail Khay, Tarak Ben Zineb

A Comprehensive Review on Thermal and Hygro/Hydrothermal Aging of Plant Fiber Composites: Properties, Degradation Mechanisms, and Service Life Prediction

Amine Fourari[1] | Mouad Chakkour[2,3] | Mohamed Ould Moussa[1] | Ismail Khay[1] | Tarak Ben Zineb[4]

[1]Laboratory of Renewable Energies and Advanced Materials LERMA, College of Engineering and Architecture, International University of Rabat, Sala Al Jadida, Morocco | [2]Arts et Métiers Campus of Rabat, Research Center S3I, Sala Al Jadida, Morocco | [3]Nantes Université, Ecole Centrale de Nantes, CNRS, GeM, Saint-Nazaire, France | [4]Université de Lorraine, CNRS, Arts et Métiers Institute of Technology, LEM3, Nancy, France

Correspondence: Mohamed Ould Moussa (mohamed.ouldmoussa@uir.ac.ma)
Funding: This study was supported by the International University of Rabat.
Keywords: bio-sourced composite | degradation mechanism | durability | hydrothermal aging | hygrothermal aging | plant fiber | service life prediction

ABSTRACT

Recently, the growth of plant fiber-reinforced composites (PFRCs) has a great impact on composite research and innovation. As these materials have various applications in several engineering fields, it would be of great interest to understand the multi-physical properties of plant fiber composites under real-life conditions. In this context, several efforts have been made to shed light on the multi-physical properties of bio-composites under synergetic aging environments. For this reason, the current review examines the hygro/hydrothermal and thermal aging of plant fiber polymer composites. Interestingly, the mechanical and physical (i.e., morphology chemical composition, crystallinity, thermal stability, moisture absorption...) properties of bio-composites and their constituents are scrutinized to better understand material response under harsh environments. Several analytical models (i.e., Arrhenius, time–temperature superposition principle ...) used for predicting the lifespan of the aforementioned materials are critically reviewed. This review paper is intended to provide new insights into the durability of plant fiber composites with a view to widespread industrial integration. More importantly, future directions are also provided to trigger new research areas.

1 | Introduction

Nowadays, global societal awareness regarding environmental impact, sustainability, and the rising energy demand has significantly increased, highlighting the urgent need for eco-friendly materials that are durable, biodegradable, and lightweight. A combination of renewable materials such as plant fibers instead of synthetic ones, and polymeric matrices has been shown to meet these properties. Accordingly, over the years, plant fiber composites have been considered in various engineering fields (e.g., automotive, aeronautics, aerospace, construction, and wind energy ...) [1–6].

A variety of plant fibers are available and relevant to the composite industry, including bast fibers (flax, hemp, jute, ramie, and kenaf, etc.), seed fibers such as coconut and kapok, leaf fibers (abaca, banana, pineapple, and sisal, etc.), grass fibers such as bamboo and corn, and wood fibers (softwood and hardwood) [7–9]. Typically, these plant fibers are structurally composed of multilayered cell walls considered as natural composites. The cell walls vary in thickness and chemical composition, containing lignin, hemicellulose, and pectins as a matrix, and cellulosic fibrils as reinforcement, working together to provide the structural integrity of plant fibers. Herein, with this complex feature,

Summary

- Hygro/hydrothermal conditions influence the multi-physical properties of fibers.
- Plant fibers' chemical composition governs their behavior under thermal stress.
- Fiber-matrix debonding is a turning point in composite performance.
- Accelerated aging tests and analytical models help to predict PFRCs' service life.

comprising a flexible outermost primary cell wall and thicker secondary wall, the multi-physical properties of plant fibers are very sensitive to environmental conditions (temperature and humidity) [5, 10, 11]. However, their intrinsic hydrophilicity makes them highly sensitive to such conditions and vulnerable to structural modifications, involving challenges to their long-term durability in practical applications [7, 12–19]. Eventually, Le Duigou et al. [13] reported that the multi-scaled architecture of fibers governs the durability of fibers in a wet environment, and long-term aging involves many multi-physical degradation steps. More importantly, Cadu et al. [16] stated that fluctuations in temperature and humidity stress the multi-walled structure of fibers and modify their chemical composition. Furthermore, the crystallinity that is a key parameter determining the mechanical properties is further susceptible to changes in the hot/wet environment. Thuault et al. [17] reported an interaction between the moisture and the microfibrillar network of fibers. Even so, temperature is involved in the modification of the microfibrillar network during thermal exposure [20]. In addition, the thermal exposure holds sway over hygroscopic conditions, accelerating degradation and changing fibers' structural integrity.

Besides, regarding the thermal stability of plant fibers, their embedding inside a matrix for the formulation of composites involves using two types of polymeric matrices (i.e., thermoplastics and thermosets). Thermoplastics (e.g., PP, PLA, LDPE, and HDPE) that soften and thermosets (i.e., epoxy, polyester, vinylester, and other phenolic resins) that can be cured below the temperature of 200°C are the most widely used [9, 21]. Matrices protect plant fibers from the hot/wet conditions and transfer the load to reinforcement. However, exposure to these conditions leads to potential degradation of composites' strength and durability, involving multiple physicochemical degradation mechanisms targeting both the polymeric matrix and plant fibers. These degradation mechanisms were documented in the literature [9–11, 13, 16, 22–33]. Herein, the issue remains on how to control the degradation. It alters multiple properties at once: crystallinity, morphology, as well as mechanical response. Cai et al. [26] reported an example of these mechanisms in unidirectional flax-reinforced phenolic composites aged over a long period in water at different temperatures. They affirmed that damage initiates at different levels of the composite, neither in the fibers nor the thermoset matrix. Li and Xue [27] confirmed that the temperature and aqueous environment induce stress and trigger different degradation mechanisms, noting differential expansion between flax and epoxy. Moreover, Xian et al. [32] shed light on an important region in the composite, which is the fiber/matrix interface. It plays a key role in transferring the mechanical load when composites are used in outdoor applications. They showed that with hygrothermal conditions, this part of ramie/phenolic composites was subjected to most of the stress and governed degradation over time. Furthermore, some PFRCs were adopted in certain applications that demand exposure to hygro/hydrothermal or high thermal conditions, for instance, in aerospace and automotive structural components where composites are used in fuselage, wings, hood, and control surfaces. These conditions led to moisture and water ingress, promoted corrosion at the interfaces, and led to structural failure upon mechanical loadings [25].

However, with all these challenges faced by composites and their structural components, understanding their durability is relevant to the composites industry in terms of predicting long-term performance, ensuring reliability, and guiding the development of more resilient and sustainable materials. This underscores the necessity of developing robust predictive models to better understand their durability. As research advances, analytical models have been developed to predict their long-term performance [34–36], including time–temperature superposition principles (TTSP) enabling the extrapolation of material physical property over extended timeframes while accounting for temperature variations, and the Arrhenius equation, emphasizing the degradation rate. Additionally, finite element modeling techniques have provided insights into water diffusion behavior and mechanical property degradation [37–39]. Indeed, there is a noticeable lack of comprehensive review articles that systematically address the durability of PFRCs, particularly in the context of environmental aging [22, 33, 40]. Most existing review papers deal with the general properties of plant fibers and their composites. However, there is a lack in the assessment of their durability, leaving a gap in understanding how plant fiber composites with their components respond to long-term exposure to hygro/hydro or thermal conditions. Closing this gap will enable researchers to develop improved materials with greater resilience to environmental factors.

This review presents a comprehensive analysis of the factors influencing the long-term performance of PFRCs, with a focus on the effects of aging under harsh conditions on their physicochemical, morphological, and mechanical properties across different scales. Predictive modeling techniques and accelerated aging methodologies are examined to estimate composite lifespan and describe their behavior in hot and wet environments. The review also outlines future research directions, including strategies to mitigate PFRC degradation in severe conditions and the development of advanced simulation tools for more accurate predictions of service life in real-world applications.

2 | Hygro/Hydrothermal and Thermal Aging of Plant Fiber Composites and Their Constituents

2.1 | Fibers

The surrounding environment is characterized by fluctuations in humidity and temperature. Those stressors have a prominent effect on fibers' multi-physical properties. The hydrophilic nature of plant fibers allows high absorbance of moisture that

results in the modification of the properties of their internal structure. Herein, with prolonged exposure to environmental stressors, the chemical composition and crystallinity of plant fibers are also susceptible to variations. In fact, extensive research has been devoted to the impact of various environmental conditions (hygro/hydro and thermal) on plant fibers' mechanical, physicochemical, and thermal properties, with more concerns about the effect induced by high temperatures. Table 1 summarizes studies evaluating the physical properties of plant fibers after exposure to hygrothermal stresses.

Aside from that, the evolution of each of the fiber's properties after exposure to severe conditions will be described in the next sections concerning the fibers.

2.1.1 | Moisture Absorption and Swelling

The water sorption behavior of plant fibers offers valuable insights into their hygrothermal characteristics. Several authors assessed the evolution of plant fiber's saturation moisture content with the change in relative humidity [10, 47, 53, 57, 58, 61, 64], and ascertained the mechanisms governing the transport of water. Based on sorption isotherms of plant fibers, authors explained that moisture absorption could result from different phenomena, adsorption in the free hydroxyl groups of fibers and diffusion by capillarity action. However, the sorption isotherms of plant fibers (Figure 1) typically exhibited a sigmoidal shape (type II-isotherm curves according to IUPAC classification), which represents the adsorption behavior of macro-porous and non-porous adsorbents [69]. In fact, for plant fibers, three sorption modes occur [10, 70, 71]. At low relative humidities (below 15%), water molecules bond with the specific sites of plant fibers (i.e., hydroxyl groups of amorphous cellulose and hemicellulose or carbonylic and carboxylic groups of pectins) which marks the slight and linear increase of the saturation moisture content with relative humidity. Besides, in a range of relative humidities between 15% and 70%, saturation moisture content continues its slight increase as water molecules infiltrate easily and in higher quantities through the hollow part (lumen), the porous structure of plant fibers, and adsorb to the hydrophilic sites resulting in fiber swelling. However, above that stage of relative humidities, water concentration within fibers exceeds a certain threshold and becomes too important, leading to the formation of water molecules' clusters in macropores and lumens, and a sharp increase in saturation water uptake. Otherwise, water molecules bound with cell walls and middle lamellae-free sites through hydrogen bonds over the full range of relative humidities. In fact, most of the absorbed moisture is held in the amorphous areas of the cellulose, hemicellulose, pectins, and lignin.

Garat et al. [10] have studied the sorption properties of different plant fibers at 23°C for different ranges of relative humidities using Dynamic Vapor Sorption (DVS) analysis for relative humidities between 0% and 90%, and the centrifugation method for the evaluation of Water Retention Value (WRV) (100 RH%). For all plant species, the sorption isotherms exhibited a sigmoidal shape (Figure 1), but the moisture content differed between plant species at 100 RH%. That was attributed to the difference in the morphological aspect of fibers, especially the amount and size of open pores and lumens. Indeed, the chemical composition might also have contributed to the substantial differences in water sorption of the cell walls. Nettle fiber bundles with a high amount of pectins exhibited elevated moisture content.

In another study, Jiang et al. [72] evaluated the sorption properties of flax and hemp fibers at 30°C, highlighting similar sorption isotherms (type II-isotherm curves). The study suggested that water bound to the cell walls of fibers could be removed without high temperature, as the enthalpy of heat sorption across the full range of relative humidities was greater than the heat of vaporization of water at 30°C. Additionally, the enthalpy of heat sorption at relative humidities below 33% was much higher than at high relative humidities.

Apart from that, few authors were interested in understanding the moisture sorption behavior inside plant fibers and exploring the diffusion phenomenon involved during their aging in a hygrothermal environment [70]. Among the models proposed in the literature, Fick's model was the most used to assess the diffusion phenomenon, but in certain conditions, Langmuir and dual-stage Fick's law were suitable when plant fibers exhibited an anomalous Fickian diffusion. Célino et al. [71] examined the diffusive behavior of four different plant fibers (hemp, flax, jute, and sisal) during aging in a hygrothermal environment (at 23°C/80 RH% and at 23°C/100 RH%). They used the three models to assess the diffusion kinetics. Fick's law and dual-stage Fick's law fit well with the moisture uptake of the different fibers when aged at 23°C/80 RH%. Herein, the dual-stage Fick law allowed determining two Fickian diffusion kinetics. In fact, the diffusion coefficient was higher for fibers having a high content of amorphous counterparts such as sisal and hemp, showing values of 2.14×10^{-6} mm^2/s and 4.00×10^{-6} mm^2/s, respectively. In contrast, the diffusion coefficients found for jute and flax were 1.12×10^{-6} mm^2/s and 1.19 mm^2/s, respectively. Besides, the Langmuir model which considers the two phases of water (mobile water corresponding to capillary condensation and bound water adsorbed to the free hydroxyl sites) involved during the exposure of fibers to severe humid conditions (100 RH%) has suitably captured the moisture uptake of all plant fibers during immersion.

Furthermore, under hygrothermal or hydrothermal conditions, the absorption of water molecules induces dimensional changes in plant fibers, predominantly manifested as transverse swelling due to the high sorption properties of the amorphous components of fibers such as hemicellulose. This leads to the orientation of microfibrils. According to Garat et al. [10], the transverse swelling of various plant fiber bundles follows a linear trend with RH. Between RHs of 20% and 73%, the cross-sectional swelling ranged from 20% for palm fibers to over 70% for nettle fibers, with intermediate expansion for sisal (~42%), hemp (~49%) and flax (~57%). Additionally, they evaluated the cross-sectional hygroexpansion coefficients of these fibers under the same hygrothermal conditions and hydrothermal conditions using a dimensional analysis apparatus. Nettle exhibited the highest coefficient of 1.70, while palm fibers showed the lowest value of 0.42. Intermediate values were recorded for flax (1.67), sisal (1.49), and hemp (0.92). Under hydrothermal conditions, these coefficients decreased, exhibiting values of 0.47, 0.84, 0.90, 1.07, and 0.72 for palm, sisal, hemp, flax, and nettle, respectively. The variability of these coefficients was attributed to differences

TABLE 1 | Literature studies investigated the evolution of the multi-physical properties of various plant fiber species under hygro/hydrothermal and thermal conditions.

Fibers	Pre-conditioning	Temperature of exposure (°C)	RH (%)	Treatment instrument	Duration (h)	Testing methods	Highlights	References
Cellulosic fibers from leaves of Moroccan (*Pennisetum alopecuroides*) plant	Oven drying at 60°C for 24 h	100	100	Immersion in distilled water	0.25, 0.5, and 1	Chemical composition, FTIR, SEM, XRD, TGA	– Hydrothermal conditioning induced an increase of 55% in crystallinity. – The surface morphology of the fibers changed from smooth to rough after 1 h of hydrothermal treatment.	[18, 41]
Tepa fibers (*Laureliopsis philipiana* Looser)		150	100	autoclave	1.5	Chemical composition	– Hydrothermal exposure induced change in Tepa fibers color. – The relative amount of lignin and cellulose increased as holocellulose decreased.	[19]
Bamboo fibers (*Phyllostachys edulis*)	Drying to 6% moisture content.	120, 140, 160 and 180	100	Superheated steam	2	SEM, XRD, bending test	– Crystallinity and elastic modulus increased slightly at temperatures between 120°C and 140°C and decreased at higher temperatures. – Temperature induced a decrease in strength.	[15, 42–47]

(Continues)

TABLE 1 | (Continued)

Fibers	Pre-conditioning	Temperature of exposure (°C)	RH (%)	Treatment instrument	Duration (h)	Testing methods	Highlights	References
Palm (*Elaeis guineensis*) Hemp (*Cannabis sativa* Flax (*Linum usitatissimum*)		0 to 6 cycle comprising humidification at ambient temperature and drying at 80°C	Humidification/drying (100/-)	Immersion in water/Oven	3/16	Single-fiber tensile test, TGA, FTIR, SEM, XRD	– Hygrothermal exposure induced a slight increase in cellulose content in hemp and palm with a decrease in ketones and organic matter content for all fibers. – The degradation temperature of cellulose in flax fibers was maintained at 375°C but shifted to 375°C for both hemp and palm from 330°C and 350°C respectively. – Lignin and hemicellulose were lost in flax fibers as hydrothermal treatment cycles increased, lignin degraded the most in palm and hemicellulose in hemp fibers. – The crystallinity of fibers improved better than that of hemp fibers. In contrast, crystallinity was diminished in palm fibers.	[48, 49] [48–53] [7, 12, 13, 16, 17, 48, 54]
		140, 190 and 250	—	Oven	0.13	Single-fiber tensile test, TGA, SEM	– Decrease in the mechanical performance (tensile strength and stiffness) at a temperature of 250°C as the internal structure was modified. – TGA showed that fibers' chemical composition remained constant without loss of matter.	
		−40, −20, 0, 20, 40, 60, 80, 100, 120, 140	60–63	Oven	4		– Tensile strength decreased at cold and high temperatures, while elastic modulus was altered at high temperatures beginning from 60°C. – The synergetic effect of temperature and humidity modified the microstructure of fibers.	
		25, 45, 65, 85	50	Climate chamber	4			
		105	—	Thermogravimetric analyzer	14	TGA	– Fibers lost 44% and 39% of their strength and failure strain, respectively. – The shear stress in the secondary cell wall dropped after thermal exposure from 45 MPa to 9 MPa.	

(Continues)

TABLE 1 | (Continued)

Fibers	Pre-conditioning	Temperature of exposure (°C)	RH (%)	Treatment instrument	Duration (h)	Testing methods	Highlights	References
Agave fibers (*Tequilina Weber Azul*)	Conditioning in laboratory conditions.	180	—	Forced air-oven	3	SEM, TGA, single-fiber test, DRX	– At 180°C, crystallinity increased, and the mechanical properties remained unchanged. – Heat treatment induced brittle behavior in the fiber.	[55–58]
Bamboo fiber bundles (*Phyllostachys pubescens*)	Oven drying at 65°C for 24 h	160, 180, 200 and 220	—	Oven	1	FTIR, SEM, Tensile test, Nanoindentation	– Tensile strength decreased with temperature, while elastic modulus increased below the temperature of 180°C, and decreased beyond that temperature. – The crystallinity correlated with the behavior of Young's modulus. – The fiber's fractured surface exhibited increased roughness following the temperature rise.	[15, 42–45]
Bamboo fibers (*Phyllostachys heterocycla*)	Oven drying at 50°C for 5 h.	100, 120, 140, 160, 180, 200, and 220	—	Oven	6	SEM, IRTF, Chemical composition, TGA	– At temperature of 220°C, cellulose content remained almost unchanged. Hemicellulose content decreased while lignin increased. – The crystallinity decreased mainly at 100°C compared to other treatment temperatures which was due to water release. – The microstructure was slightly altered.	
Sisal fibers (*Agave sisalana*)		20, 100, 150, 200, 250 and 300	—	Oven	3	SEM, XRD, Tensile test	– Sisal morphology altered slightly at the temperature of 200°C and sharply at 250°C. – Enhanced mechanical properties until 250°C.	[59–61]
Kenaf fibers (*Hibiscus cannabinus L*)		140–150	—	Drying oven	2.5, 5, 7.5, 10 and 12.5	XRD, single-fiber tensile test, SEM, AFM	– Heat treatment improved crystallinity and fiber strength. – Heat treatment during 10 h improved kenaf fiber tensile strength. – Impurities and extractives present on the kenaf fibers surface were removed.	[62–65]

(Continues)

TABLE 1 | (Continued)

Fibers	Pre-conditioning	Temperature of exposure (°C)	RH (%)	Treatment instrument	Duration (h)	Testing methods		Highlights	References
Oil palm empty fruit bench fibers (OPEFB)		28.5, 100 and 190	78% RH at 28.5	Oven	0.25	SEM, XRD, FTIR	–	Oven-heat treatment induced a decrease in hemicellulose content leading to an increase in cellulose content.	[66–68]

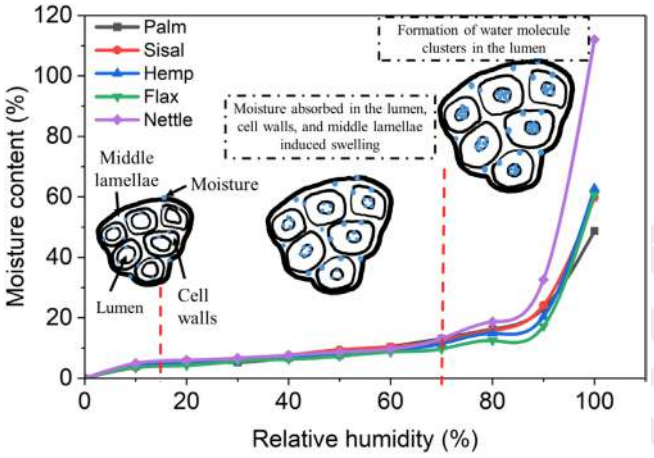

FIGURE 1 | Sorption isotherms of different plant fibers (palm, sisal, hemp, flax, and nettle) at 23°C adapted from Garat et al. [10] work.

in chemical composition and microfibrillar angle (MFA); fibers with higher lignin content and larger MFA tend to restrict water retention and swelling. Similarly, Joffre et al. [73] examined the local hygroexpansion coefficient of a lignified fiber (softwood) between 47 RH% and 80 RH% using tomography measurements, finding a coefficient of 0.45. These findings underline the contribution of fibers' chemical composition to the moisture-induced dimensional changes, opening interesting perspectives for the predictive modeling of PFRC durability by incorporating fiber dimensional changes, which are closely related to the structural features of the fibers.

2.1.2 | Crystallinity

Due to the importance of crystallinity on the mechanical performance of plant fibers, various techniques have been used for its evaluation including Fourier transform infrared spectroscopy (FTIR), differential scanning calorimetry (DSC), and x-ray diffraction (XRD). The latter was the most used technique, providing various methods for studying the crystallinity index (CrI) [74, 75]. Among these methods, the Segal peak height was adopted by several researchers due to its simplicity and its suitability to evaluate the effect induced by treatment or exposure to hygro/hydrothermal and thermal conditions, although, it is considered to overestimate the values of crystallinity when compared to other methods (Rietveld method and peak fitting method). In fact, the pitfall of this method arises from the variation of the crystal size in the lignocellulosic fibers [74]. The smaller crystals are generally considered amorphous material in the XRD pattern. Cellulose exists in two conformations in plant fibers as Iα and Iβ, but the latter remain the form existing [76]. Generally, the diffraction of plant fibers shows typical characteristic peaks of the crystalline cellulose at 110, $1\bar{1}0$, 120, 200, and 004. Figure 2 demonstrates each of those peaks, in addition to the amorphous region contributing in the calculation of CrI by Segal's empirical method (Equation 1) [77], where I_{200} represents the height of the 200 peak located between the scattered angles of $2\theta = 22°$ to 23°, constituting the sum of the crystalline and amorphous components, and I_{am} corresponding only to the amorphous component and represented by the

intensity at the minimum of about 18° between the 110 and 200 peaks.

$$CrI = \frac{I_{200} - I_{am}}{I_{200}} \times 100 \quad (1)$$

Beyond that, those peaks are subjected to modification when plant fibers withstand hygro/hydrothermal conditions revealing a change in crystallinity. Amorphous constituents of plant fibers become susceptible to leaching, which results in enhanced crystallinity. Interestingly, such observations have been ascertained in various research studies. Elmoudnia et al. [18] observed such behavior when exposing a cellulosic fiber for different lengths of time (0.25, 0.5, 1 h) at 100°C/100 RH%. As illustrated in Figure 2, the intensity of the peaks corresponding to cellulose revealed the increase in the relative amount of crystalline cellulose due to the removal of hemicellulose. Cadu et al. [16] spotlighted also an increased crystallinity because of the removal of fibers' amorphous counterparts with the hornification mechanism when aged flax fiber bundles in cyclic hygrothermal conditions (humidification for 3.5 days at 55°C/90 RH% and drying for the same period at 55°C/40 RH%). The apparent crystallinity increased by 2.5% during aging, more prominently between the 4th and 9th cycle. Otherwise, in the study of Ezugwu et al. [48], the crystallinity of various plant fibers (palm, hemp, and flax) behaved differently when exposed to hygrothermal cycles (humidification for 3 h at 100 RH% and drying at 80°C). Indeed, the XRD diffractogram of palm fibers shown in Figure 3a depicted 1 to 5 peaks depending on exposition to hygrothermal cycles. Meanwhile, 7 to 8 peaks corresponding to crystalline cellulose were observed for hemp and flax in Figure 3b,c at 2θ values: 14.5°, 16.5°, 20.5°, 34.6°, 45.0°, and 54.1° for flax, and 14.3°, 20.3°, 34.6°, 45.0°, and 54.1° for hemp fibers. However, both fibers exhibited the common cellulose peak at 22.6° with high intensity, but the peak between 16° and 17° was well-defined in flax, but not revealed for hemp. The latter presented a well-distinct cellulose peak at 32.2°. However, the crystallinity of palm fibers was supposed to remain unchanged with cyclic hygrothermal conditions as the peak at 21.5° and 34.6° remained stable, but after 6 cycles crystallinity dropped by 13%. Unlike palm, flax and hemp showed an increase in crystallinity by 19% and 2%, respectively, after hygrothermal cycles.

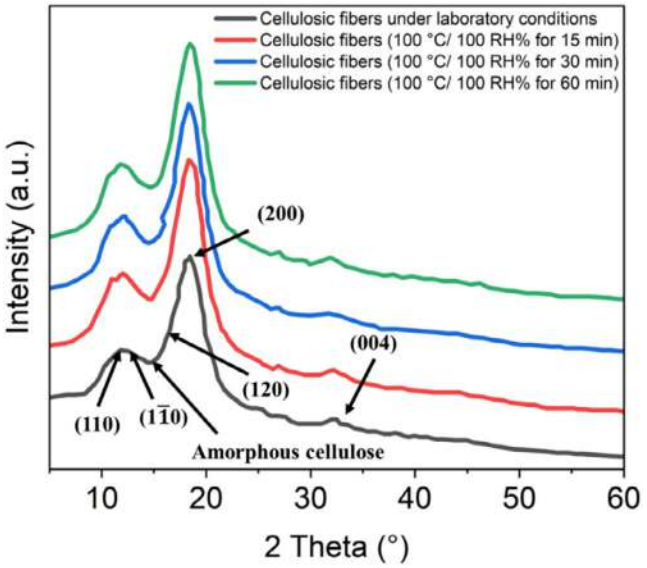

FIGURE 2 | XRD patterns of cellulosic fibers before and after exposure to hygrothermal conditions (100°C/100 RH%) for different durations (15, 30, and 60 min) adapted from Elmoudnia et al. [18] work.

Besides, numerous studies have demonstrated that temperature with the time of exposure influences crystallinity and induces structural changes to the crystalline cellulose [43, 44, 55, 56, 59, 65, 66, 78–80]. Cellulose Iβ exhibits anisotropic behavior upon temperature. This phenomenon is reversible, as the strain induced by temperature change does not involve any irreversible mechanism. Guillou et al. [78] demonstrated the reversibility of this behavior through temperature-controlled XRD analysis performed on flax fibers subjected to successive short isothermal exposures (ranging from 25°C to 230°C), followed by cooling. Their results showed that the 200 peak in XRD patterns shifted to a lower angle with increasing temperature and retrieved its initial position after cooling. Another important conclusion was that the interplanar distance between the (200) planes increases with temperature but returns to its

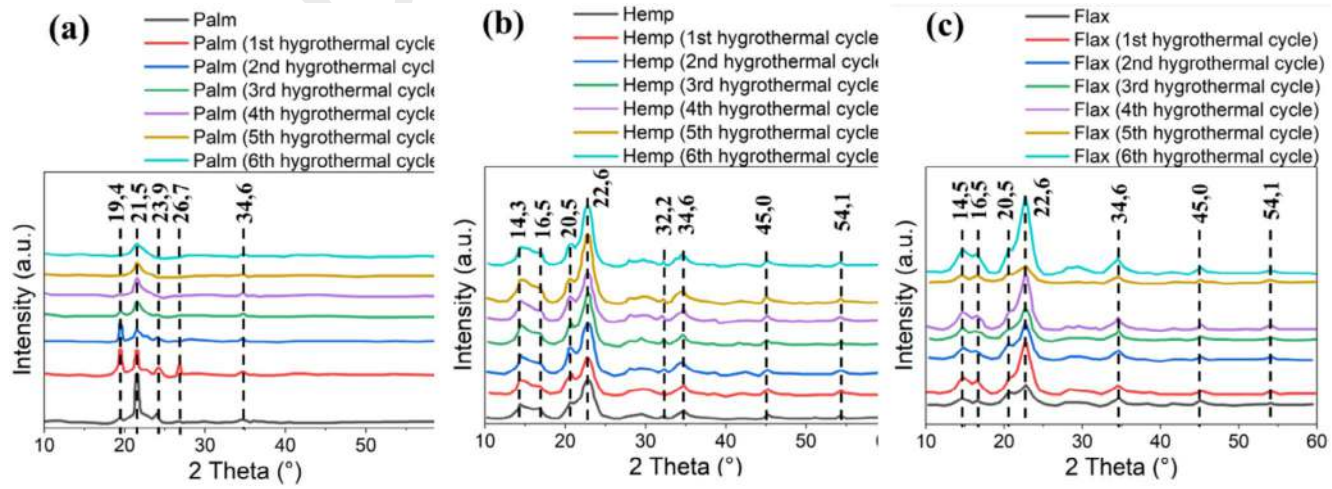

FIGURE 3 | XRD diffraction patterns of three different plant fibers (a) palm, (b) hemp, and (c) flax, undergone cyclic aging (humidification at 100 RH% for 3 h and drying for 16 h at 80°C) adapted from Ezugwu et al. [48] work.

initial value at 23°C. This behavior can be attributed to the molecular arrangement of cellulose chains, which enables them to approach one another and form a complex network consisting of numerous hydrogen and Van der Waals bonds. Temperature disrupts these bonds, particularly the weaker ones (Van der Waals interactions) along the [100] direction, contributing to the anisotropic thermal expansion of the crystalline cellulose. Dri et al. [79], using Density Functional theory (DFT) calculations, demonstrated the temperature-induced thermal expansion of cellulose. Their findings revealed that thermal expansion is more pronounced in the lateral direction compared to the [010] direction. Similarly, Wada et al. [80] experimentally observed the same trend and noted that cellulose Iβ undergoes a phase transition near 230°C. Additionally, thermal expansion along the a-axis [100] reached a value of 9.8×10^{-5} °C^{-1} below the phase-transition temperature and 19.8×10^{-5} °C^{-1}.

Regarding the effect of thermal aging on fibers' crystallinity, Figure 4 shows these changes for a variety of plant fibers for different exposure times. Langhorst et al. [55, 56] reported an increased crystallinity in blue-agave fibers after subjection to high temperatures for 3 h. The increase was related to the loss of hemicellulose. Interestingly, the crystallinity increased until a temperature of 180°C. However, they stated that the increase in crystallinity involved an enhancement of stiffness as the mobility of cellulose microfibrils in the cell walls was reduced at high temperatures [56]. Furthermore, the increase of crystallinity was also relevant in sisal fibers exposed for the same duration to temperatures ranging from 100°C to 300°C, as demonstrated by Ferreira et al. [59]. They explained such an increase by the occurrence of a hornification mechanism, which results in the bonding of cellulose chains to the amorphous counterparts (lignin and hemicellulose). Despite that, it was revealed that exposure to high temperatures such as 300°C leads to the degradation of cellulose, though a drop in crystallinity [81]. Hence, crystallinity increases in most cases. Carada et al. [65] featured an increased crystallinity in kenaf fibers exposed for 1 h to a temperature of 140°C. Solikhin et al. [67] also observed an increased crystallinity in oil palm empty fruit bunch stalk fibers (OPEFB) after withstanding temperatures (100°C and 190°C) for 15 min, as well as Yun et al. [44], who observed an increased crystallinity in bamboo fibers that faced high temperatures (120°C, 140°C, 160°C, and 180°C) for 2 h. That was attributed to the production of ether bonds at high temperatures by condensation reactions between hydroxyl groups present in the amorphous region of bamboo fibers. Eventually, Cui et al. [15] spotlighted the effect induced by exposure to high temperatures for 1 h on bamboo

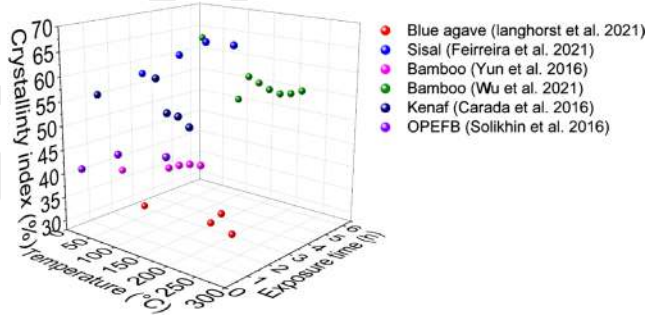

FIGURE 4 | Effect of thermal stress on the crystallinity index of plant fibers [43, 44, 55, 59, 67].

crystallinity. In fact, it was stated that the degradation of amorphous regions of cellulose and hemicellulose [82], and the rearrangement of the cellulose crystalline regions [83] lead to increased crystallinity. Indeed, exposure to high temperatures for a long time results in reduced crystallinity. Wu et al. [43] underlined the effect induced by exposure for long periods to high temperatures on the crystallinity of bamboo fibers. Crystallinity dropped drastically from the first-faced temperature of 100°C as water molecules were released and the cellulose crystalline region was partially removed. Ariawan et al. [62] subjected kenaf fibers to a temperature of 140°C for different periods (2.5 h, 5, 7.5, 10, and 12.5 h) and highlighted an increase in crystallinity values assuming that cellulose molecules were rearranged inside the quasi-crystalline amorphous regions [84, 85]. In fact, exposure for a long period of 12.5 h caused a drop in crystallinity since oxidation and dehydration reactions occurred, and that induced degradation with fiber cells shrinking and reduction of fiber density [85, 86].

2.1.3 | Chemical Composition

The alteration in crystallinity of plant fibers under hygrothermal conditions and thermal conditions is closely linked to their chemical composition. Plant fiber cell walls are composed of various components such as cellulose, non-cellulosic polymers like hemicellulose, water, lignin, protein, and in minor fractions waxes. Determining these components in plant fibers before and after their exposure to severe conditions helps in understanding the transformations that occur within the fiber cell walls. Consequently, several approaches in the literature have been adopted to analyze these changes and quantify the constitutive polymers of cell walls [87]. Figure 5 illustrates the methods used to assess the evolution of the chemical composition. Generally, FTIR and biochemistry analysis are the most widely used techniques, followed by TAPPI's method and colorimetric analysis. The analysis by FTIR involves monitoring the evolution of the bands corresponding to functional groups specific to fiber components [88–99]. Figure 5 shows the corresponding fiber component for each absorption band. In contrast, biochemical analysis involves deriving pentose and hexose monosaccharides which constitute cellulosic and non-cellulosic polymers using various solvents. These monosaccharides are then quantified and identified using high-performance liquid chromatography (HPLC) or Gas chromatography [54, 87]. The determination of cellulose content is typically based on quantifying its constitutive monomer, glucose. Changes in hemicellulose content are identified based on the quantities of xylose, mannose, and galactose, whereas pectic substances are characterized by the colorimetric method. Lignin is quantified separately, usually through calcination.

Ultimately, the application of these methods has demonstrated that hygrothermal and hydrothermal conditions significantly alter the ultrastructure of fibers. This alteration is often characterized by the leaching of non-cellulosic polymers, leading to an increase in the relative content of cellulose and lignin. For example, Crespo et al. [19] found that Tepa fibers exposed to hydrothermal conditions at 150°C for 90 min in an autoclave at a pressure of 430 kPa exhibited increases in cellulose content of 11.68% and 21.31%, respectively. Conversely, the amount of

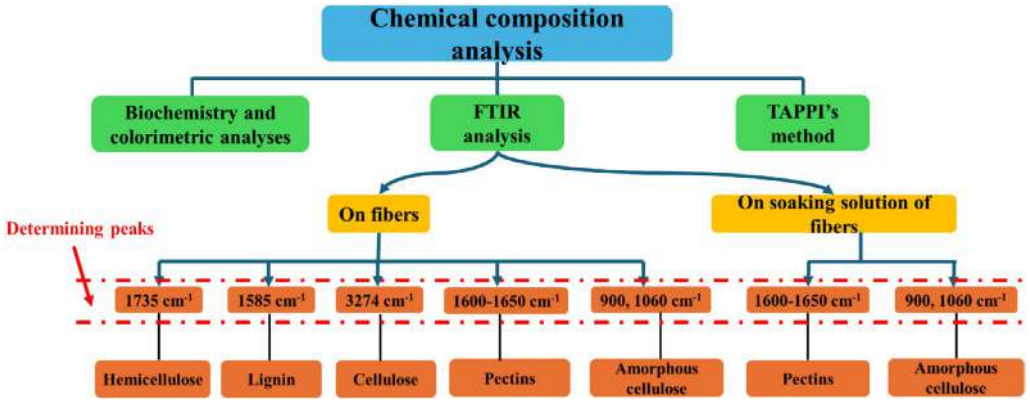

FIGURE 5 | Methods used in literature to assess the evolution of plant fiber's chemical composition during hygrothermal aging.

holocellulose (which include amorphous cellulose and hemicellulose) decreased by 3.9%. The degradation of these chemical components results in the formation of organic acids (e.g., acetic acid and formic acid), phenolic compounds, and other aromatic and extractive substances. These organic acids, in turn, catalyze the hydrolysis of pectins, hemicelluloses, and to a lesser degree amorphous cellulose. Le Duiguou et al. [13], using the colorimetric method, observed the release of significant amounts of polysaccharides corresponding to hemicellulose and pectins over time during hydrothermal aging at 23°C.

FTIR analysis has been employed to investigate both the bulk fibers and the soaking solutions after aging in hydrothermal environments. Analyzing the soaking solution is particularly useful for detecting the degradation products of fiber cell walls. Degradation is considered time- and temperature-dependent; with prolonged exposure and higher immersion temperatures, the degradation of the amorphous materials that make up the fibers' primary wall increases. Using FTIR analysis on cellulosic fibers, Elmoudnia et al. [18] observed a decrease in hemicellulose content after prolonged exposure to hydrothermal conditions at 100°C. Similarly, Li and Xue [27] analyzed soaking solutions used for aging flax fibers over 17 weeks at 23°C, 37.8°C, and 60°C, finding evidence of leaching of hemicellulose, non-esterified pectins, and poorly crystallized cellulose. Cadu et al. [16] also reported the removal of these constituents from flax after the 26th week of aging in cyclic hygrothermal conditions (1 cycle: 55°C/90 RH% for 3.5 days and 55°C/40% for 3.5 days). In fact, when fibers feature cyclic hygrothermal conditions, the leaching effect remains encountered. Ezugwu et al. [48] studied the effects of cyclic hygrothermal conditions (6 cycles of water immersion for 3 h at ambient temperature, followed by drying at 80°C) on palm, hemp, and flax fibers. FTIR results revealed an increase in cellulose and lignin content after several cycles, attributed to the leaching of hemicellulose and the dissolution of water-soluble ketones, particularly from palm fibers.

Other studies have explored the effects of high thermal exposure on fiber chemical composition, focusing on plant fibers such as flax, bamboo, and wood. Flax fibers, known for their gelatinous cell walls and thick S2 layer rich in cellulose (up to 90%), exhibit different degradation behaviors compared to lignified and xylan-rich fibers like bamboo and wood. Generally, thermal degradation begins with the removal of pectins, followed by the degradation of hemicelluloses, cellulose, and lignin. In lignified fibers, thermochemical reactions between xylan groups in hemicellulose and lignin result in crosslinking and lignin condensation at high temperatures [46, 47, 93]. Cui et al. [15, 42] demonstrated through FTIR analysis that bamboo fibers exposed to temperatures ranging from 160°C to 220°C for 1 h showed significant hemicellulose degradation, while cellulose remained relatively stable. This stability was attributed to the polymerization of free hydroxyl groups in the amorphous regions of cellulose via oxidation under high temperatures and atmospheric conditions. Similarly, Wu et al. [43] reported increases in cellulose and lignin content in bamboo fibers exposed to temperatures up to 200°C for 6 h due to hemicellulose removal. For fibers with gelatinous cell walls, Guillou et al. [78] conducted biochemistry analysis (acid hydrolysis and gas chromatography) on flax fibers subjected to successive thermal exposures at 170°C, 190°C, 210°C, and 230°C for 20 min each. The results indicated a marked decrease in thermosensitive polymers such as hemicelluloses and pectins with increasing temperature, particularly after 190°C. lignin content, measured using spectrophotometry via the acetyl bromine method, increased by 50% at 230°C relative to the dry matter of flax fiber bundles, though overall lignin content remained low in flax fibers.

2.1.4 | Morphology

In hygro and hydrothermal conditions, plant fibers undergo significant morphological changes, including surface alterations due to the leaching of amorphous content, defect development, and fiber decohesion caused by differential swelling stresses induced on the cell walls, which can intensify with prolonged exposure, as effectively assessed through Scanning Electron Microscopy (SEM). Thuault et al. [17] followed the evolution of flax fibers' surface in a hygrothermal environment (20°C/100 RH%). The findings revealed unchanged surface morphology after 1 day of exposure (Figure 6a). Herein, at that period water seeps through the surface defects and diffuses by capillarity action through the lumen and/or the cell wall interfaces. However, exposure of 7 days altered the surface of fibers, as some blisters appeared (Figure 6b), which were a result of the osmotic pressure generated in the outer wall of fibers. Indeed, after 4 weeks of aging, cracks were generated on the surface of fibers (Figure 6c) as the pockets busted and released the pressure. However, Le Duigou et al. [13] observed the fractured surface of flax fibers embedded in PLA matrix before (Figure 6d), and after exposure

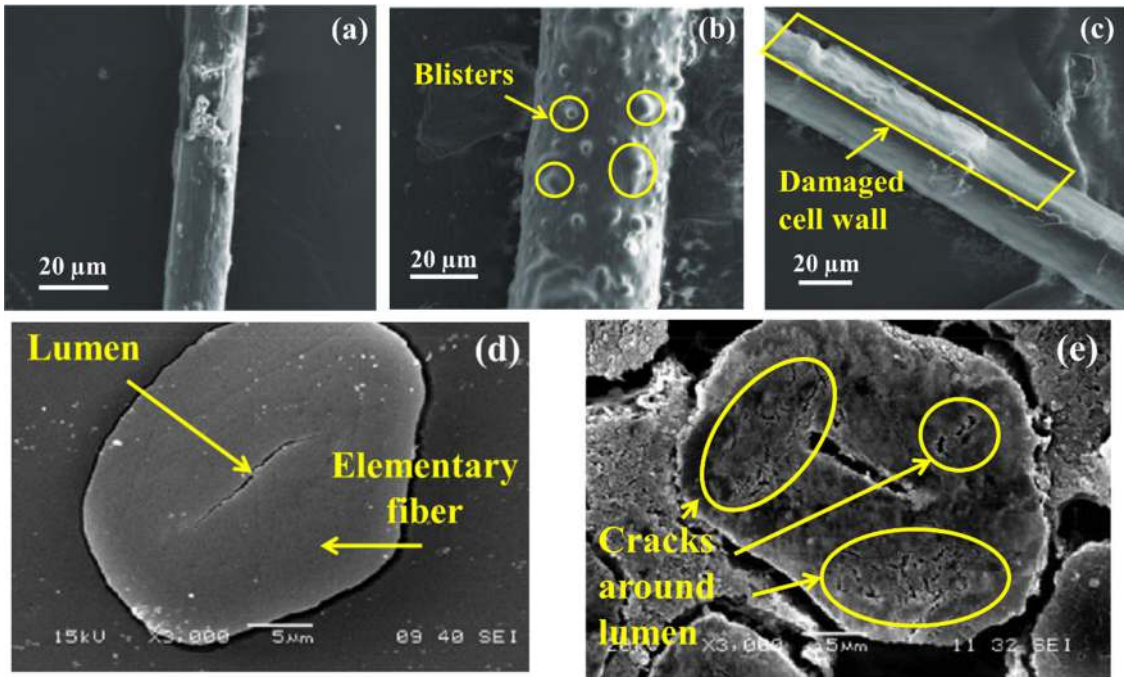

FIGURE 6 | Morphological changes of flax fibers aged for 1 day at 20°C/100 RH% (a), aged for 7 days (b) for 2 months (c) in the case study of Thuault et al. [17]; unaged flax (d), and aged for 2 months at 23°C/100 RH% (e) in Le Duigou et al. [13] work.

to hygrothermal conditions (23°C/100 RH%) for 2 months. The observations showed that those aging conditions caused the nucleation of cracks in the lumen area (Figure 6e). Indeed, the structural damage was a consequence of differential swelling stresses generated in fibers' cell walls. Nevertheless, Cai et al. [26] highlighted splitting of flax fibers surface after exposure to hygrothermal conditions (60°C/100% RH) for 2 months. Herein, in Ezugwu et al. [48] work, three types of fibers (flax, hemp, and palm) were subjected to cyclic hygrothermal conditions (humidification for 3 h at ambient temperature/100 RH% and drying for 16 h at 80°C). Exposure to 6 cycles of hygrothermal conditions resulted in the collapsing of fibers' surface and decohesion in flax and hemp. However, in palm fibers, the hygrothermal conditions caused the modification of their cell structure by their compaction, which was marked by the shrinkage of the lumen. In addition, flaws were developed in the surface of palm fibers as silica clusters collapsed.

Besides, with high thermal exposure, the structural integrity and fiber surface are subjected to severe modification. High temperatures embrittle fibers and induce a loss in the bonding strength between the non-cellulosic polymers of the plant fibers and the cellulosic microfibrils, which creates gaps between fiber cell walls and causes delamination. In fact, the embrittlement of fibers has been documented in numerous studies. For instance, Langhorst et al. [55] observed that after 3 h of exposure to 180°C, the fractured surface of blue-agave fibers transitioned from ductile to brittle failure. Otherwise, Ferreira et al. [59] reported that exposing sisal fibers to temperatures below 200°C for 3 h resulted in thermal deformation, leading to the formation of cracks, voids, and structural shrinkage in the middle lamellae. At 250°C, the internal structure of sisal fibers became more fused and compacted, with reduced porosity. Exposure to that temperature induced a phenomenon similar to the fusion between the middle lamellae and the secondary wall of the fibers, known as the plastification-vitrification process. However, at 300°C, cracks appeared in fiber cells, attributed to the loss of bonding between lignin and cellulosic fibrils. Differently, Cui et al. [42] explored the microstructural changes of bamboo fiber bundles extracted from different regions (inner, outer, and middle) in the radial direction of the stem after 1 h of exposure to high temperatures (160°C, 180°C, 200°C, and 220°C). The embrittlement of fibers was obvious after exposure to high temperatures. Herein, fiber bundles extracted from the outside region exhibited a serrated fractured surface with exposure of a large amount of fibers, below the temperature of 200°C revealing the ductility of fibers before the thermal exposure. It was reported that high temperature causes the degradation of fibers' main constituents, which results in weak bonding between the different layers of the cell walls. Recently, Cui et al. [15] have discovered such behavior when subjected bamboo samples to temperatures (160°C, 180°C, 200°C, and 220°C) for 1 h. The delamination of the cell walls was obvious at 160°C. However, at 180°C, the sublayers of the secondary wall of fibers were delaminated since hemicellulose degraded and volatile compounds were released, leaving gaps between the layers and causing their shrinkage. Eventually, at that stage of temperature, cellulosic microfibrils were exposed, but above 220°C, they were less and shorter due to twisting, cellulose degradation [100], and the softening of lignin. Such modification in the microstructure of fibers with high temperature begins with the weakening of the adhesion between lignin carbohydrate complexes (LCC), then between LCC and cellulosic microfibrils [101]. Wu et al. [43] reported unaltered surface morphology in short bamboo fibers exposed to high temperatures for a period of up to 6 h. Indeed, exposure for a long time to high temperatures was shown to develop mainly cracks and the degradation of cellulose. As observed by Oliveira et al. [102], cracks developed along fiber length in a fique fabric after exposure for 72 h and 120 h to a temperature of 170°C, and with prolonged exposure, microfibrils were exposed at the surface and collapsed

afterward. This was explained by the depolymerization of hemicellulose. However, Ariawan et al. [62] reported the removal of waxy and fatty substances after the subjection of Kenaf fibers to a temperature of 140°C for different durations (2.5, 5, 7.5, 10, 12.5 h) [8].

2.1.5 | Mechanical Properties

Despite the influence of factors such as the position of fiber extraction, plant growth conditions, chemical composition, and the processing methods used for extraction [8, 32, 47–50, 103], studies have shown that the mechanical behavior of plant fibers is also significantly affected by hygro and hydrothermal environments [87, 104–107]. Specifically, changes in crystallinity and chemical composition under extreme conditions govern their mechanical response. Tensile tests conducted on fiber bundles or elementary fibers have provided deeper insights into this behavior. Interestingly, their response to mechanical loadings reveals three types of humidity- and time-dependent stress–strain curves, as illustrated in Figure 7. The first type (Type I) represents fibers with elastic behavior; the second type (Type II) exhibits elastoplastic behavior. The third type (Type III), which is common among most lignocellulosic fibers, demonstrates an unusual pattern characterized by an initial non-linear region during the early loading stage, followed by a region where the tangent modulus increases progressively until failure. This phenomenon is often associated with an accommodation mechanism. Several hypotheses have been proposed to explain the non-linearity of this curve [12, 54, 108, 109]. The initial non-linear region is attributed to shear deformation within the amorphous regions and hardening due to the reorientation or modification of the MFA. Additionally, the presence of defects and dislocation zones within the ultrastructure of elementary fibers contributes to this behavior. These mechanisms may also lead to the breakage of intermolecular bonds between the amorphous components of the cell wall and the cellulose microfibrils, resulting in stress-induced crystallization, a phenomenon where crystallization occurs in response to mechanical loading. Studies on flax and hemp fibers have demonstrated that these stress–strain curve types are dependent on humidity levels. Placet et al. [106] conducted a quasi-static tensile test on single hemp fibers at varying relative humidity (10%, 25%, 50%, and 80%) and a temperature of 23°C. They found all three types of stress–strain curves, with type III being the most prevalent. As RH increased, the proportion of Type III curves also increased. Additionally, several studies highlighted the effects of hygro and hydrothermal conditions on tensile strength, modulus, and fracture modes of fibers. The hydration state of fibers, swelling, and plasticization of cell walls play crucial roles in determining their mechanical properties [7, 10, 106, 110]. Garat et al. [104] examined various plant fibers under different hygrothermal conditions at 23°C and observed that cell wall saturation and plasticization led to a decrease in Young's modulus as RH increased, primarily due to the flexibilization of the cellulose network. They also found that the hydration state, specifically, the saturation of hydroxyl groups governs the strength and strain at failure. Both properties increased until a saturation threshold (between 50 RH% and 73 RH%). Similarly, Thuault et al. [17] observed an increase in the tensile strength of flax fibers with RH up to 68 RH%, while Van Voorn et al. [111] reported a similar trend in flax and sisal fibers up to 70 RH%. Placet et al. [106] also noted an increase in the strain at failure of hemp fibers as RH increased from 2.34% at 10 RH% to 2.67% at 80 RH%. Guicheret-Retel et al. [107] studied the creep behavior of single hemp fibers under hygrothermal conditions (20%, 40%, 60%, and 80% RH at 20°C), concluding that humidity activates the viscoelastic properties of fibers and increases both primary and secondary creep strain rates.

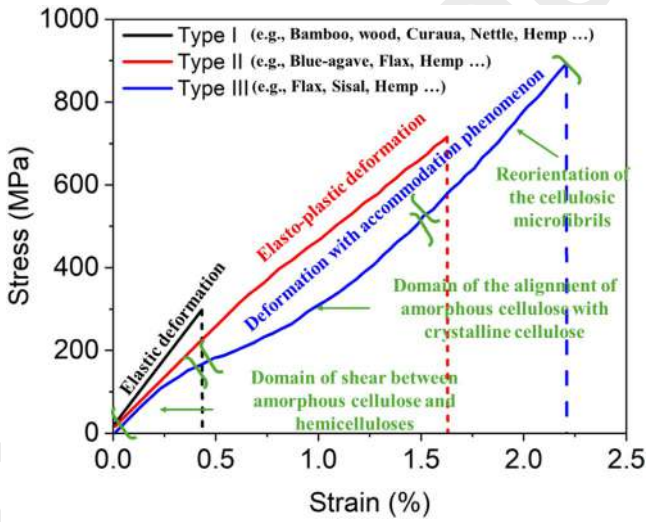

FIGURE 7 | Typical stress–strain curves of plant fibers at ambient temperature; Type I with the elastic response, Type II corresponding to elastoplastic deformation, and Type III with an accommodation phenomenon (elastic deformation at the beginning related to the shear stress-induced to amorphous cellulose and hemicellulose, non-linear region assigned to the alignment of amorphous cellulose, and final elastic stage corresponding to the reorientation of the cellulosic microfibrils).

Extended exposure to fluctuating hygro and hydrothermal conditions has been shown to degrade mechanical properties [16, 17, 48, 112]. Prolonged exposure can lead to ultrastructural degradation, including defect formation, microfibrillar network disorganization, and increased porosity due to high relative humidity. Cadu et al. [16] observed a 30% reduction in the tensile strength of flax fiber bundles after cyclic aging (humidification at 55°C/90 RH% for 3.5 days, followed by drying at 55°C/40 RH% for the same period). The tensile strength stabilized after 13 cycles (equivalent to 52 weeks), while Young's modulus decreased by 40% between the 4th and 13th cycles, likely due to the development of internal flaws such as decohesion. Ezugwu et al. [48] reported similar degradation in palm fibers exposed to cyclic hydrothermal conditions, with a 10.93% reduction in tensile strength after a single cycle (3 h immersion at room temperature, followed by 16 h of drying). They also noted that fibers with lower luminal porosity, such as flax and hemp, demonstrated greater resistance to strength loss compared to palm fibers.

Indeed, plant fibers are expected to endure prolonged mechanical stress and environmental variability when reinforcing composite materials. Several studies have shown that cyclic loading combined with varying hygrothermal environments induces mechanosorptive phenomena, where fiber deformation accelerates under repeated loading and environmental stress,

increasing fiber strain. Guicheret-Retel et al. [107] observed this effect in tensile creep tests on single hemp fibers under cyclic hygrothermal conditions (80 RH% to 15 RH%). Other studies have suggested that cyclic loading at constant RH affects fiber mechanical behavior by diminishing the non-linear response and reducing strain; an irreversible phenomenon that stiffens the fibers over time. Huguet et al. [105] confirmed the occurrence of such a mechanism when examining the mechanical response of flax fiber bundles by cyclic tensile test in hygrostatic conditions (23°C and 50 RH%). They suggested that the modification of the MFA, dislocations like defects, or crystallization contributes to the stiffening effect and the disappearance of the non-linearity response of fibers after 3 cycles.

Apart from that, extensive studies were conducted to study the effect of thermal exposure on the mechanical performance of plant fibers. They also ascertained that the response of plant fibers to mechanical load varies after subjection to high temperatures [15, 78]. Gourier et al. [54] analyzed the tensile properties of a batch of flax elementary fibers 23°C/48 RH% after thermal exposure for 8 min at temperatures (140°C, 190°C, and 250°C). The results revealed two types of stress–strain curves (Type II and Type III) but with more dominance of the Type III curve. In fact, it was inferred that flax fibers maintained their stability within that time of exposure to these temperature ranges. However, after exposure to 250°C, the tensile behavior changed, and the three typical stress–strain curves were observed with homogeneous distribution. That is because of the evolution of the cell wall structure involving a decrease in the polysaccharidic matrix's flow and consequently of the microfibrillar alignment. With that, important structural changes within the fibers occur, resulting in heterogenous stress distribution and defect generation. However, we mentioned before that the non-cellulosic polymers in the cell wall (lignin, hemicellulose, and pectins) are highly modified by temperature as they have a low glass transition temperature [113–116]. In this context, Baley et al. [12] have reported a decrease in tensile strength of about 44% after exposure to a temperature of 105°C for 14 h, but the stress–strain curve remained unchanged after the thermal exposure and exhibited the Type III curve (see Figure 8a). Teixeira et al. [60] performed tensile tests on different types of fibers (hemp, curaua, and sisal) before and after thermal exposure for 24 h at temperatures of 100°C, 150°C, and 200°C. The stress–strain curves of curaua and hemp fibers which have small microfibrillar angle (MFA) corresponded to the Type I curve illustrated in Figure 8b,c, with brittle behavior, whereas that of sisal fibers exhibited the Type III curve. After exposure to 100°C, the tensile behavior of all fibers remained the same, but after 150°C, the stress–strain curve of sisal fibers exhibited a brittle behavior (Type I) curve. Langhorst et al. [55] evaluated the tensile properties of blue-agave fibers exposed to 180°C for 3 h. A brittle failure occurred in fibers at that temperature after they showed a bilinear-plastic behavior (Type II) before thermal exposure. Eventually, Cui et al. [42] investigated the tensile behavior of bamboo fiber bundles after conditioning for 1 h at different temperatures (160°C, 180°C, 200°C, and 220°C), and observed though, stress–strain curves similar to (TI) type implying brittle failure. However, from all those research works, it is obvious that high temperatures embrittle plant fibers and modify their internal structure.

Regarding the variations in mechanical properties, such as tensile strength and modulus, of plant fibers when exposed to high temperatures out of the range of relative humidities. Figure 9 illustrates the findings. Teixeira et al. [60] have found that the thermal exposure to 100°C of curaua, hemp, and sisal fibers for 24 h enhances their tensile strength by 94%, 18%, and 6%, respectively, as at that temperature there was a loss of moisture. Meanwhile, Young's modulus increased for all fibers. The thermal exposure above that temperature resulted in a loss of strength but an improvement of elastic modulus. However, the latter was affected when the fibers were exposed to a temperature of 200°C. Ferreira et al. [59] have reported also an enhancement of elastic modulus by 15% after exposure of sisal fibers to temperatures below 150°C for 3 h. Besides, the water loss leads to the densification of the fiber structure implying interactions between hydroxyl groups of the different cell walls resulting in improved mechanical performance [117]. Indeed, after exposure to high temperature of 250°C, sisal fibers' mechanical properties were depleted. Rong et al. [84] have also pointed out that exposure of sisal fibers to 150°C for 4 h improves mechanical performance. Apart from that, Langhorst et al. [55] have reported that thermal exposure of plant fibers results in the creation of uniform defect distribution inside fibers. They conducted tensile tests on agave fibers before and after their exposure to a high temperature of 180°C for 3 h and studied also the effect induced by the gauge length. In fact, the tensile properties of fibers that were not thermally exposed exhibited a decrease with the increasing gauge length. That is because of the "size effect phenomenon" [118, 119], which became more prominent in large fiber volumes. Flaws and serious defects are more encountered. However, thermal exposure loosens this phenomenon as flaws become more developed inside fibers resulting in size-insensitive tensile properties. Interestingly, Carada et al. [65] have found that an exposure of kenaf fibers to a temperature of 140°C for 1 h results in an improvement of tensile strength by about 7%. Whereas, at higher temperatures tensile properties decreased, more prominently above 200°C. Eventually, thermal exposure affected tensile modulus and resulted in its decrease. However, Ariawan et al. [62] subjected kenaf fibers to temperature of 140°C for different durations (2.5, 5, 7.5, 10, and 12.5 h). An evaluation of their tensile properties revealed that exposure to that temperature for up to 10 h enhances tensile strength and modulus by 23.5% and 16.8%, respectively, but drops down for extended time. Likewise, Cao et al. [63] have found that the tensile strength of kenaf fibers decreases after 10 h of exposure to 150°C. Otherwise, Cui et al. [42] have also reported a gradual decrease in the tensile strength of bamboo fiber bundles after subjection to temperatures above 160°C for 1 h. Specifically, the tensile strength was reduced by approximatively 55% at 220°C, attributing this to the degradation of cellulose and hemicellulose. Interestingly, the elastic modulus increased by 29%. The internal mechanical properties were further assessed using nanoindentation tests, which showed that both Young's modulus and hardness of fiber cell walls improved by 17.17% and 30.56%, respectively, from average values of 15.96 GPa and 0.36 GPa. It was suggested that under tensile loading, bamboo fiber cell walls undergo interlayer sliding governed by three successive mechanisms: (i) the formation of hydrogen bonds between the free hydroxyl groups of cellulose molecular chains, (ii) their breakage, and recombination as load increases, and eventually (iii) debonding of covalent bonds (C-C and C-O), leading to molecular chain

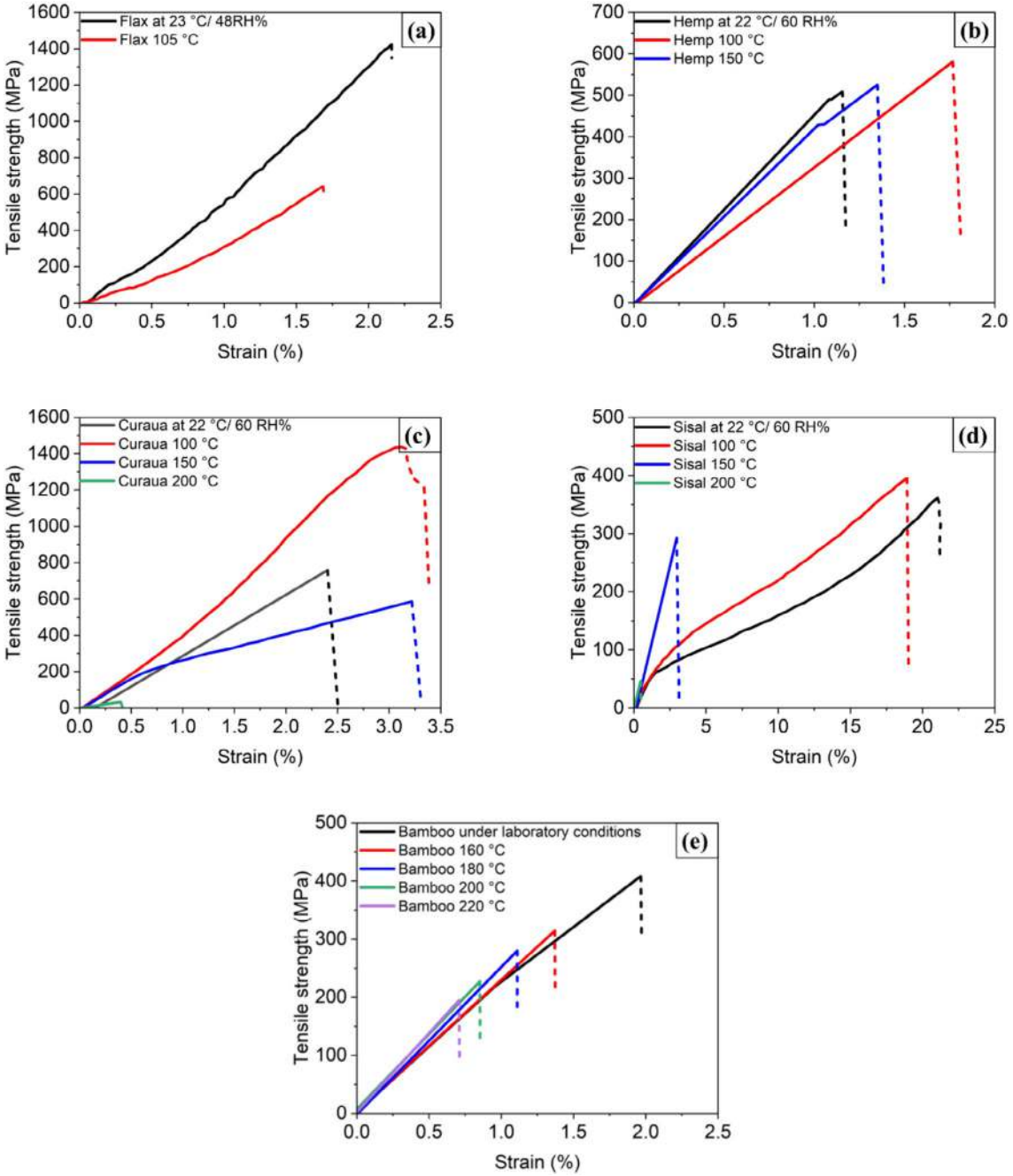

FIGURE 8 | Effect of temperature on the mechanical response of flax fibers (a) adapted from Baley et al. [12] work, hemp (b), curaua (c), sisal (d) adapted from Teixeira et al. [60] work, and bamboo fibers (e) adapted from Cui et al. 42 work [42].

scission. This process results in the collapse of the cell wall and the fracture of individual fibers, along with the disintegration of the crystalline cellulose skeleton [120]. Additionally, several studies have investigated the changes in the mechanical properties of flax fibers following thermal exposure. Gourier et al. [54] subjected flax fibers to temperatures of 140°C, 190°C, and 250°C for 8 min, and found a slight alteration of tensile strength and modulus at temperatures of 140°C and 190°C, but a prominent decline of about 68% in strength and about 31% in elastic modulus at 250°C. Baley et al. [12] observed a decrease of about 42% in strength, and about 8% of elastic modulus after 24 h of exposure to 100°C. Thuault et al. [17] investigated the tensile properties of flax fibers after exposure to both low and high temperatures, ranging from −40°C to 140°C, for 4 h. The results indicated a reduction in tensile strength at subzero temperatures, attributed to the hindrance of the plasticizing effect induced by water when its molecules were frozen. Additionally, the tensile strength decreased slightly at 40°C and significantly at 140°C, where it dropped by 58.5%. In contrast, the elastic modulus remained unaffected across the temperature range of −40°C to 20°C, maintaining a consistent value of approximatively 50 GPa. However, beyond 60°C, it declined to 27 GPa and then stabilized. The observed stiffening of the amorphous phases was attributed to water release, which limited microfibrils disorientation and led to increased brittleness as temperature rose. Furthermore as previously discussed, the deterioration in mechanical performance

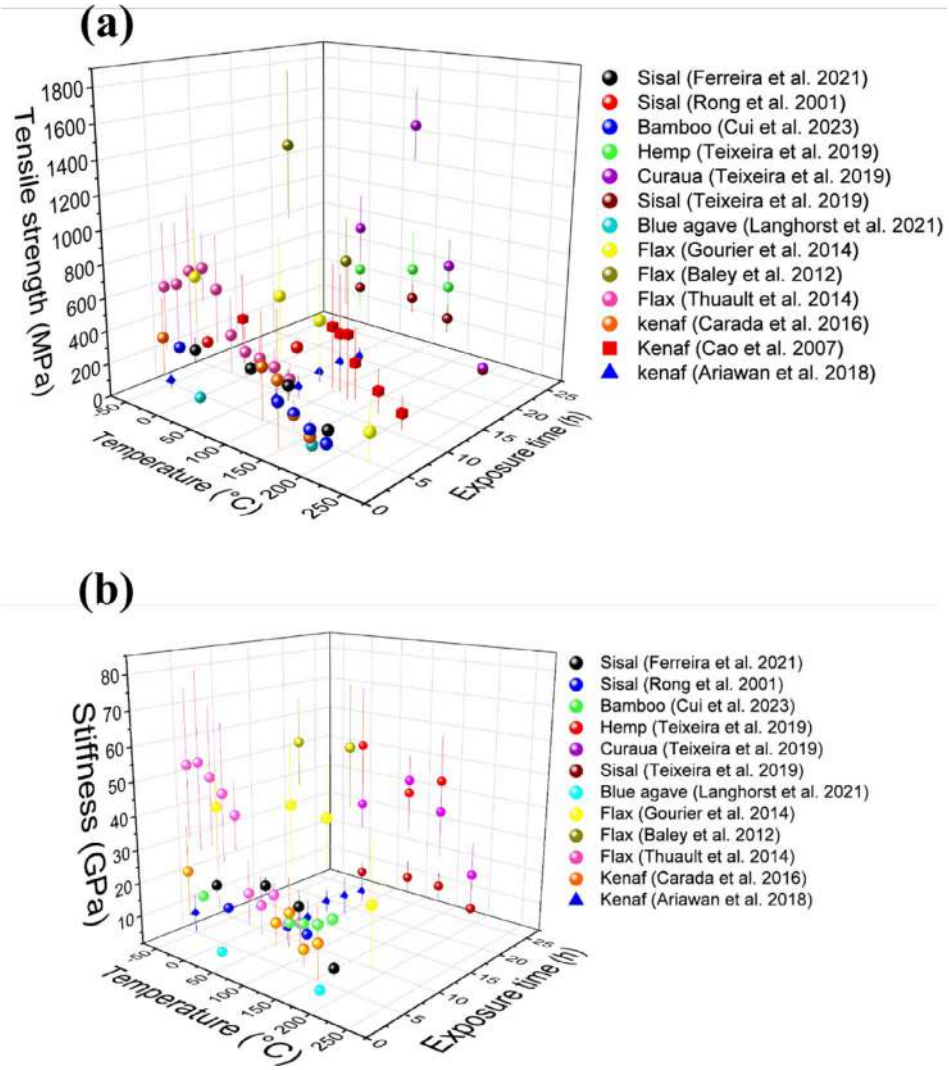

FIGURE 9 | Effect of temperature on tensile strength (a) and stiffness (b) of different plant fibers [12, 17, 42, 54, 55, 59, 60, 62, 63, 65, 84].

above 60°C may be linked to the removal or softening of fiber amorphous components with low glass transition temperatures, such as lignin (80°C–100°C) [113], hemicelluloses (60°C–138°C) [114], and pectins (−25°C to 20°C) [115, 116].

2.1.6 | Thermal Stability

Thermogravimetric analysis has been widely used to evaluate the thermal stability and composition of plant fibers. In fact, to the best of the author's knowledge, few studies considered the thermal stability of plant fibers after aging [43, 48, 56, 121]. However, it is known that the TGA of plant fibers exhibit three to four distinct weight-loss stages. The first stage, occurring below 150°C, is attributed to the evaporation of moisture and other volatile compounds. The second stage between 200°C and 350°C, involves the decomposition of hemicellulose and the initial degradation of cellulose. The third stage, from 350°C to 500°C, is characterized by the significant degradation of cellulose and lignin. In some cases, a fourth stage above 500°C can be observed, which is associated with the decomposition of residual lignin and the oxidation of char in an aerobic atmosphere. Indeed, the examination of the thermal stability of plant fibers after subjection to harsh conditions provided information about their durability. Interestingly, Wu et al. [43] have observed the three weight loss stages for bamboo fibers at 30°C–100°C, 200°C–350°C, 315°C–400°C related to water loss, decomposition of hemicellulose, cellulose, and lignin, respectively; However, the thermal stability of bamboo fibers exposed to high temperatures below 220°C for 6 h remained unaltered since the shoulder peak in TGA corresponding to hemicellulose degradation remained unchanged. The thermal stability was affected after exposure of fibers to temperatures above 220°C, as demonstrated by the decline in the shoulder peak corresponding to hemicellulose degradation and the shifting of cellulose peak at 360°C to lower temperatures, but the effect induced by thermal exposure wasn't more pronounced. Whereas, Langhorst et al. [56] observed improved thermal stability after exposing agave fibers to high temperatures for 3 h.

Ezugwu et al. [48] stated the three stages of weight loss in flax, hemp, and palm fibers, and ascertained the effect induced by hydrothermal cycles (1 cycle: humidification in water for 3 h at room temperature and 16 h of drying at 80°C) on the thermal stability. Hydrothermal conditions significantly affected hemp and palm fibers' thermal stability but slightly affected that of

flax fibers. The DTG of the latter fibers revealed that hydrothermal cycles maintained the cellulose degradation peak constant. On the other hand, the cellulose degradation peak of hemp shifted from 330°C to 375°C with the increase in hydrothermal cycles while its mass loss increased significantly. For palm fibers, hydrothermal cycles caused the reduction of the mass loss due to water evaporation, which was revealed by the rise in the DTG curve. Also, the DTG of palm fibers revealed two distinct peaks of hemicellulose that were absent in hemp and flax fibers. However, hydrothermal cycles caused a shifting of the hemicellulose and cellulose degradation peaks from 260°C to 298°C and from 350°C to 375°C, respectively. Such a shift was a result of the partial decomposition of lignin and hemicellulose. Thus, the thermal stability was improved.

One can note that the affectivity of the thermal stability by hygro or hydrothermal conditions is governed by the anisotropic thermal expansion of fibers, which results in modifications to the fiber microstructure. Saidane et al.'s [20] study showed that flax fibers present an anisotropic behavior upon hygrothermal conditions (50 RH% and different temperatures). They highlighted an important evolution of the transverse coefficient of linear thermal expansion ($75 \pm 5 \times 10^{-6}\,K^{-1}$) over the longitudinal coefficient of linear thermal expansion ($-1.2 \pm 0.1 \times 10^{-6}\,K^{-1}$). This behavior is attributed to the hierarchical microstructure and anisotropic properties of the cell wall components. Indeed, the differential behavior underscores how moisture and temperature interact to alter fiber microstructure and consequently, their thermal stability.

2.1.7 | Degradation Mechanisms of Fibers: A Summary

Literature surveys have claimed that hydrophilic plant fibers undergo significant degradation mechanisms when operated in severe conditions comprising different temperatures and humidity levels. Exposure to a hygro or hydrothermal environment invokes stresses to plant fiber cell walls, initiated by moisture adsorption in the non-cellulosic polymers, followed by diffusion in/between internal cell walls or in lumen and pores. However, continuous exposure to stress manifests in swelling, stiffening, and enhanced crystallinity. Otherwise, extended exposure aggravates moisture-induced stress, leading to the disorganization of the cellulosic fibrils and modification of the fiber's structural integrity. Both stiffness and crystallinity become susceptible to alteration. Indeed, long-term aging permits reaching a certain threshold of degradation, emerging in the leaching of amorphous constituents, and the development of flaws between microfibrils. Aside from that, a high operating temperature might involve different degradation mechanisms in fibers that depend on plant fibers' ultrastructure. Fibers with gelatinous cell walls lose their mechanical performance to high temperatures. In contrast, fibers with lignified cell walls experience many chemical reactions at elevated temperatures, namely condensation. Besides, exposition for a few minutes, accounting hours to temperature levels ranging from 200°C to 300°C, invokes the release of volatile compounds and hemicellulose. However, temperatures exceeding 300°C result in the degradation of the main components (i.e., cellulose and lignin). In fact, such degradation is also reached when aging fibers for a long time in a hygro or hydrothermal environment. Indeed, the damage is more prominent when cellulose degrades, leaving pores and voids inside fibers. In this context, the degradation mechanism of plant fibers is summarized in Figure 10. It also englobes the variation in the multi-physical properties to exposure time and hygro or hydrothermal, and high thermal conditions.

2.2 | Matrices and Composites

From what concerns matrices and composites, numerous research studies have performed accelerated tests under extreme hygro or hydrothermal conditions, providing valuable insights into the different degradation mechanisms that can occur during the service life of a composite. Hygro/hydrothermal aging is defined largely by three parameters: intensity of thermal loads, the extent of moisture uptake, and the aging time [22]. Hence, it was demonstrated that the absorbance of moisture or water sorption alters the mechanical properties at multiple levels, which deteriorate when the damage becomes evident at the fiber-matrix interface. In the early stages of aging, changes in the polymeric matrix, such as plasticization, may be encountered, and with prolonged time, these effects can worsen, leading to matrix cracking, molecular chain scissions, and hydrolysis [24, 29, 122–124]. Additionally, the deterioration of the fiber-matrix is accompanied by swelling of fibers, and that, as previously discussed, might involve the generation of osmotic pressure inside fiber cell walls and causes the leaching of the amorphous counterparts such as pectins, hemicelluloses, and some poorly crystallized cellulose, exacerbating the degradation of composites. Table 2 provides a summary of studies using accelerated aging tests (hygro and hydrothermal aging) to analyze the multi-physical properties of PFRCs. However, their findings revealed various degradation mechanisms regarding the polymeric matrix used, the amount of reinforcement, and the manufacturing process used for their elaboration. Herein, hygro and hydrothermal aging were shown to nucleate the damage from the interfacial region separating fibers from the matrix.

In the following sections, the variations of the mechanical and physical properties of PFRCs during aging in hygro and hydrothermal environments will be thoroughly detailed and discussed individually.

2.2.1 | Moisture Absorption

Recently, several research authors have assessed the moisture absorption kinetics of plant fiber composites under different environmental conditions [29, 131, 132]. They have explained that water molecules may diffuse through the matrix, the hollow structure of the plant fiber (lumen) as well as by capillary along the fiber-matrix interfaces, inducing damages to bio-composites by creating different stresses within both the matrix and fibers. In fact, the evaluation of the kinetic parameters of water absorption at different temperatures allowed authors to assess the diffusion mechanism involved during the aging process of composites as it follows a Fickian behavior, relaxation model, or other diffusion mechanisms [24, 26, 133–136], and also to evidence the effect caused by temperature on the diffusion behavior of bio-composites. Figure 11 illustrates different diffusion behaviors encountered in polymeric composites. Fickian diffusion remains the main form of diffusion encountered in composite and polymeric materials. It is characterized by rapid moisture

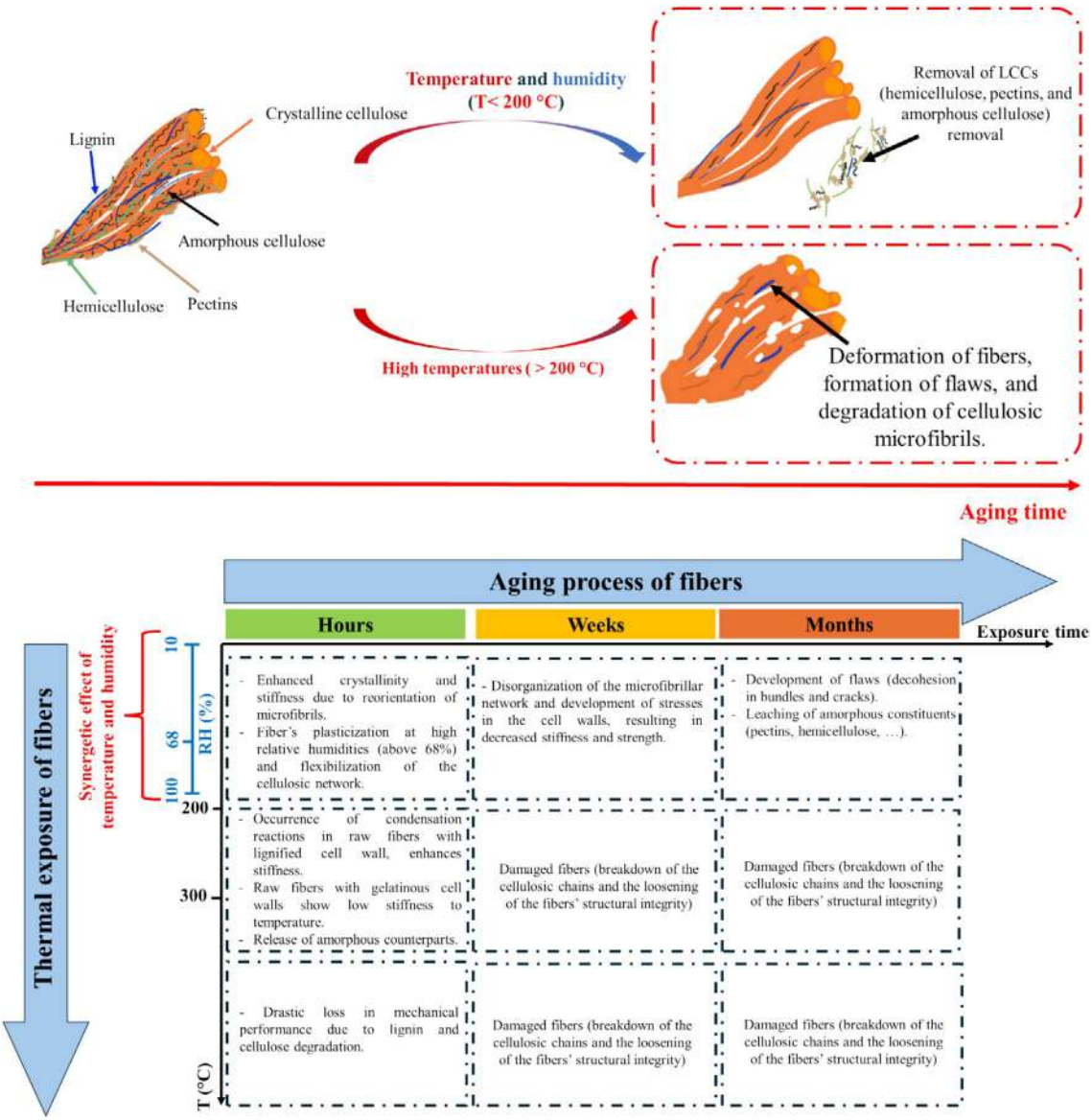

FIGURE 10 | Degradation mechanisms of plant fibers to temperature and physical properties evolution upon thermal and hygro/hydrothermal exposure.

uptake at the initial stages proportional to the concentration gradient of moisture and an equilibrium plateau when no damage occurs to the composite material (Figure 11a). Figure 11b shows a diffusion involving the relaxation of the molecular chains of the polymeric matrix and the interfacial region between fiber and matrix with plasticization of both fibers and matrix. The moisture uptake at the initial stage is similar to Fickian diffusion, characterized by rapid increase. Hence, due to relaxation, moisture uptake slows down and increases gradually. However, such diffusions might involve time-dependent structural damage (Figure 11c–e). A two-step diffusion (Figure 11c) englobes the initial stages of diffusion (rapid increase in moisture uptake and equilibrium stage), with the occurrence of structural damage with matrix cracking, which creates another pathway for moisture to diffuse at the later stages. Indeed, such a phenomenon might also be encountered simultaneously after the rapid increase in moisture content when the voids are big enough in the matrix, allowing an ease of fiber swelling. Herein, prolonged exposure to harsh hygro or hydrothermal conditions could alter the chemical properties of both fiber and matrix, inducing hydrolysis to the polymeric matrix and leaching of the amorphous constituents of plant fibers (hemicelluloses, pectins...), resulting in an anomalous diffusion (decrease in moisture uptake) (Figure 11e).

Li and Xue [27] have reported a diffusion behavior following Fick's law for both epoxy matrix and unidirectional flax fiber reinforced epoxy composite laminates aged in hydrothermal conditions at different temperatures (23°C, 37.8°C, and 60°C), with rapid absorbance of water during the first stages followed by an equilibrium plateau. Otherwise, in the same conditions of aging ((23°C, 37.8°C, and 60°C)/100 RH%), Cai et al. [26] observed a deviation from the normal diffusion for unidirectional flax fiber reinforced phenolic composites, which involved the viscoelastic effects of the phenolic matrix and caused the creation of free volume that allowed a gradual increase in moisture uptake after the first stage of rapid diffusion. However, a high temperature invoked during aging can damage composites and result in a

TABLE 2 | Studies investigated the effect of hygro/hydrothermal aging on the multi-physical properties of various PFRCs.

Type of composites	Aging conditions	Findings	References
Unidirectional flax fiber/phenolic composite	(23°C, 37.8°C, and 60°C)/100 RH%.	– Drop in the mechanical performance (strength and modulus) during 3 years of aging, with plasticization of fiber, and degradation of both the reinforcement and the matrix after reaching moisture equilibrium. – Elevated temperatures accelerate degradation.	Cai et al. [26]
Unidirectional flax/epoxy composite	(23°C, 37.8°C, and 60°C)/100 RH%.	– Weakening of the interfacial adhesion between fibers and matrix, and their plasticization, results in a decrease of composite's strength and stiffness at the first stages of aging. – Chemical degradation is achieved rapidly with high temperatures, manifesting in a drastic loss of mechanical performance.	Li and Xue [27].
Flax/polypropylene (PP) composite laminates	– Hydrothermal aging (70°C/100 RH%). – Thermal aging (120°C).	– Structural defects (voids, exposed fibers) due to composite manufacturing allows rapid water uptake and weakening of the fiber-matrix interface with the plasticization of fibers. – Propagation of cracks within the matrix as a result of fiber swelling. – Hydrolysis and leaching of flax fiber amorphous constituents after 14 days of aging causes a loss in bending properties (strength, stiffness, and strain at failure). – Flax fibers change color from yellow-brown to dark gray because of the biochemical modifications induced by metabolic activities [125]. – Thermal aging causes the weakening of the interfaces, but specifically results in the embrittled PP matrix and causes its oxidation.	Rousseau et al. [126]
Unidirectional flax/epoxy composite	Cyclic aging at 55°C (humidification for 3.5 days at 90 RH% and drying for 3.5 days at 40 RH%)	– Deterioration of the mechanical properties (strength, modulus, and strain) within cyclic aging, with the loss of the adhesion between fibers and matrix, and the degradation of fibers.	Cadu et al. [16]
Twisted bamboo fiber wound/epoxy composite	– Hydrostatic conditions (100 RH% at 20°C and 70°C). – Hygrostatic conditions (70°C/85 RH%).	– The durability of composites is affected by prolonged exposure to hygro and hydrothermal conditions. – High aging temperature aggravates fiber-matrix interface weakening, resulting in a drastic loss in composite performance.	Shi et al. [28]
Jute fiber/polylactic acid (PLA) composite	50°C/100 RH%.	– Embrittlement of the interfacial region between jute and PLA, differential swelling, and hydrolysis of the matrix by cleavage of its constitutive C-O bonds nucleates cracks, resulting in the formation of water channels and depletion in the mechanical properties (strength and stiffness) with preservation of plasticization.	Jiang et al. [29]

(Continues)

TABLE 2 | (Continued)

Type of composites	Aging conditions	Findings	References
Bidirectional plain-woven jute fabric/epoxy composite	(20°C and 40°C)/100 RH%.	– Tensile strength and stiffness decreases as the fiber-matrix interfaces weaken. – Increasing temperature of aging exacerbates degradation (appearance of more defects). – Hydrothermal aging in tap water results in the oxidation of the epoxy matrix mainly with the occurrence of molecular reorganization as a result of polymer chain scission.	Ma et al. [31]
Short wood fiber/high-density polyethylene (HDPE) composite	60°C/100 RH%	– Hydrothermal aging of wood fiber/HDPE composite until reaching saturation induced no changes in the structural properties. The loss of mechanical performance because of cyclic fatigue.	Mejri et al. [127]
Short ramie fiber/PLA composite	60°C/100 RH%	– Hydrothermal aging at a temperature above the glass transition temperature of the PLA matrix causes detrimental effects to the matrix and a decrease in the tensile and bending properties of composites. – The presence of ramie fibers inside composites accentuates degradation during hydrothermal aging.	Yu et al. [128]
Woven jute, kenaf, and hemp fiber/epoxy composite	90°C/97 RH%	– Frictional properties deplete within 1 month of exposure to hygrothermal conditions. – Jute/epoxy composite showed the highest frictional properties after aging.	Ugochukwu et al. [129]
Short sisal fiber/PLA composite	(60°C, 65°C, 70°C, 75°C, 80°C, and 85°C)/100 RH%	– Composites with a high amount of sisal fibers absorb a high amount of water. – Hydrothermal conditions enhance crystallinity and thermal stability, and allow the formation of transcrystalline regions between fibers and matrix. – Aging at temperatures above the glass transition temperature of PLA results in an anomalous diffusion of moisture.	Gil-Castell et al. [30, 122]
Nonwoven flax/epoxy composite laminates	45°C/100 RH%	– The evaluation of tensile properties at different temperatures (23°C, 50°C and 75°C) after saturation revealed that moisture combined with exposure to high temperatures result in a drastic loss of composite performance (strength and stiffness) but induce plasticization to the epoxy matrix.	Habibi et al. [130]
Unidirectional flax fabric/bio-epoxy composite	45°C/75 RH%	– Slight alteration of the flexural properties of composites in such hygrothermal conditions in 1 month.	Moudood et al. [24]
Fique fabric reinforced epoxy composite	170°C/-RH%	– Thermal aging deteriorates fiber-matrix interface and changes the intrinsic properties of epoxy matrix (temperature of glass transition).	Oliveira et al. [102]

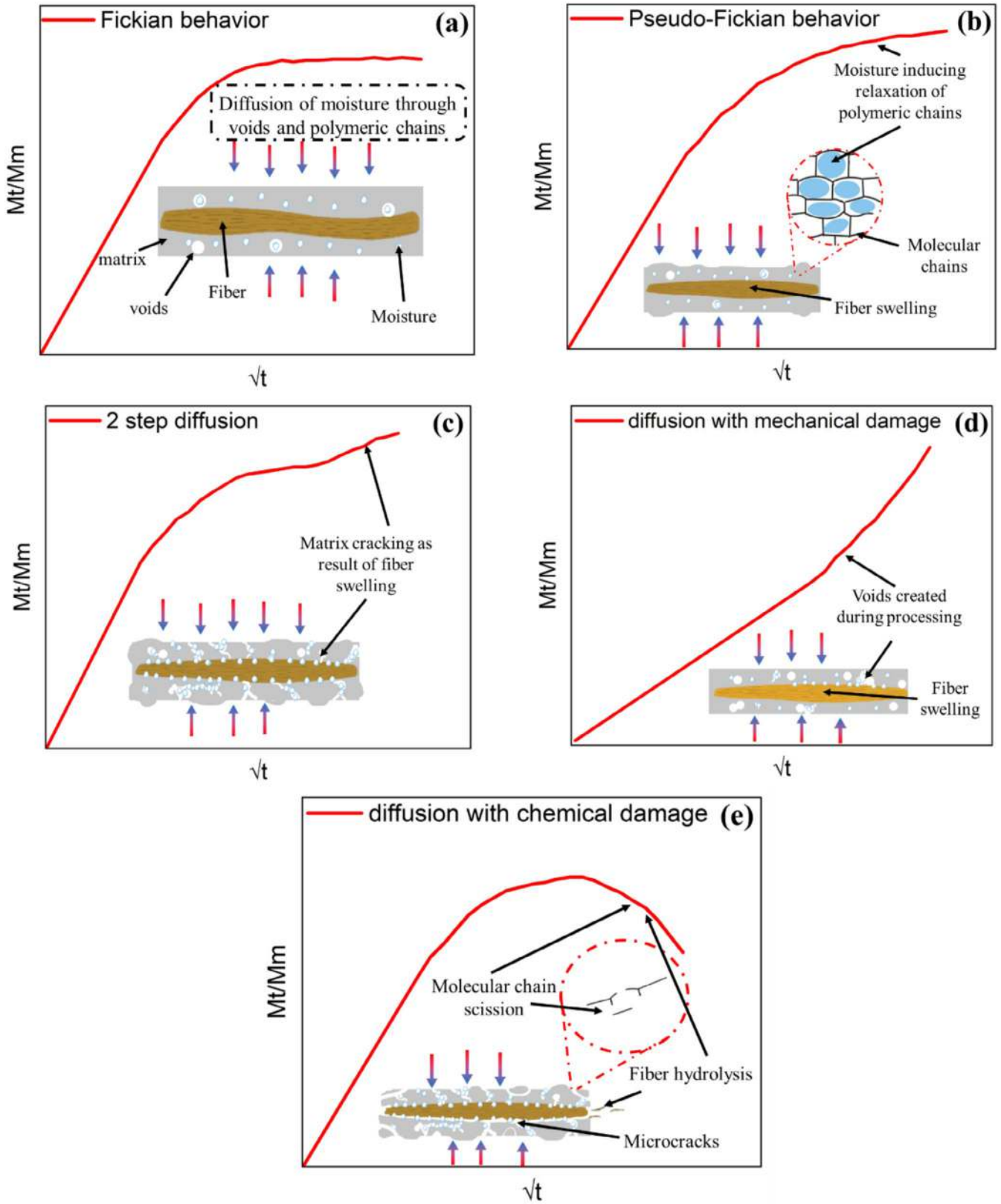

FIGURE 11 | Mechanisms of moisture diffusion of PFRCs in hygro and hydrothermal conditions; (a) Fickian diffusion, (b) diffusion with relaxation of polymeric chains, (c) two-step diffusion, (d) diffusion with mechanical damage, and (e) diffusion with chemical damage.

decrease in water uptake with the occurrence of chemical damage. In fact, in both studies above, a high temperature of 60°C affected the water uptake at the later stages due to the hydrolysis of the matrix, deterioration of the fiber-matrix interface, and the loss of the main components of fibers. Eventually, Habibi et al. [130] found also a decrease in water uptake after aging of a flax/epoxy composite for 25 days in a water bath maintained at 45°C. However, not only temperature can lead to chemical damage in

plant-fiber reinforced composites, but also the medium of aging. For instance, Ma et al. [31] investigated the hydrothermal aging behavior of bi-directional plain woven jute fabric/epoxy composites immersed in tap water at 20°C and 40°C for 180 days. A rapid moisture uptake was observed during the first 2 weeks [32, 137], followed by a plateau between 30 and 45 days, indicating water absorption in accordance with Fick's law. The corrosive nature of the tap water induced hydrolysis of both fibers and epoxy matrix, leading to a decline in weight gain after reaching saturation.

Other factors such as the architecture of the reinforcement and the quality of the resin might also affect the behavior of moisture uptake during aging. As observed by Shi et al. [28], the moisture uptake of twisted bamboo fibers/epoxy composites aged for 30 days in different conditions (at 70°C/85 RH%, and at (20°C and 70°C)/100 RH%) exhibited two-step or many step diffusion during aging. Hence, defects in the epoxy matrix (i.e., voids and cracks) facilitated the diffusion of water which bonded with its free amine and hydroxyl groups in its molecular chains. Afterward, a consecutive phenomenon occurred, beginning with the retention of water at the interface, then sorbed with the help of the twisted architecture, the lumen, and the free adsorption sites of fibers [138–140]. Interestingly, such diffusion behavior (two-step diffusion) was also reported for flax/bio-epoxy aged for 30 days at 45°C/75RH% in Moudood et al. [24] work, as well as in Jiang et al. [29] work, where they have aged an injected molded jute/PLA composite for 56 days in a test chamber filled with deionized water maintained at 50°C after pre-conditioning in air for 24 h at 40°C. Water uptake showed a rapid increase after 7 days due to the diffusion mechanism [141, 142], without reaching saturation between 7 and 28 days. Herein, the nucleating effect of pores caused a notable increase once again in the absorption rate.

Many authors based their conclusions on determining the diffusion mechanism and the kinetic parameters in composites based on Fick's law prediction. The logarithmic fitting of Equation (2) allowed determining the value of n, which permits inferring the mode of water uptake.

$$\frac{M_t}{M_m} = k.t^n \tag{2}$$

Where M_t represents moisture uptake at time t, M_m maximum moisture uptake, k and n represent the kinetic parameters. The value of n determines the diffusion mechanism. Values close to 0.5 indicate Fickian diffusion, while those between 0.5 and 1 reflect non-Fickian behavior. Consequently, n values equal to or greater than 1 correspond to a relaxation-controlled mechanism. Nevertheless, the 1D mathematical representation of Fick's law (Equations 3 and 4) was applied to approximate the water diffusion in the composites.

$$\frac{M_t}{M_m} = 1 - \frac{8}{\pi^2}\sum_{n=0}^{\infty}\frac{1}{(2n+1)^2}\exp\left[-\left(\frac{D\times t}{h^2}\right)\pi^2\times(2n+1)^2\right] \tag{3}$$

$$D = \frac{\pi}{(4M_m)^2}\times\left(\frac{M_t\times h}{\sqrt{t}}\right)^2 = \frac{\pi.k'^2}{(4.M_m)^2} \tag{4}$$

where h is the initial specimen's thickness (mm), D is the diffusion coefficient through thickness (mm^2/s) and could be obtained from the slope of the initial part of the curve or calculated using Equation (4), and k' represents a constant obtained from the slope of $M_t = f(\sqrt{t}/h)$.

Interestingly, the determination of diffusion coefficient and maximum moisture uptake established a conclusion about the effect of temperature on water absorption kinetic parameters. As demonstrated in Table 3 representing the obtained maximum moisture uptake and diffusion coefficient in several study cases that performed accelerated aging tests on composites in a hygro and hydrothermal environment. It was inferred that an increase in aging temperature impacts the diffusion coefficient and the saturation value of moisture uptake. In most of studies [26–28, 31, 50, 144], temperature accelerated diffusion and increased maximum water uptake because of the development of cracks and interfaces inside composites, promoting more pronounced water uptake. Figure 12a illustrates this tendency for flax/epoxy composites aged in hydrothermal conditions at 23°C, 37.8°C, and 60°C. Otherwise, in the study case of Gil-Castell [30], maximum water uptake fluctuated when aging composites at different temperatures (from 65°C to 85°C), which might be due to temperature-induced viscoelastic effects to the thermoplastic matrix (PLA) in composites. This is explained by the fact that with an increase in the immersion temperature, a softening of the matrix may occur, especially near the glass-transition temperature. That leads to increased chain mobility and facilitates moisture diffusion. Otherwise, the elastic response to this behavior causes structural adjustments, leading to variations in moisture absorption.

Besides, Jiang et al. [29] have analyzed the water absorption behavior of injected molded jute/PLA composite specimens when aged for 56 days in a test chamber filled with deionized water maintained at 50°C after pre-conditioning in air for 24 h at 40°C. The water absorption test during that aging time exhibited three different stages of weight gain. The first stage (7 days) showed a rapid increase in water absorption in agreement with Fickian prediction [141, 142], indicating that water penetrated the internal structure of jute/PLA through a diffusion mechanism. Thereby, at the second stage (between 7 and 28 days), the water absorption curve deviated from Fickian behavior without reaching saturation. In the third stage, the absorption rate exhibited a notable increase once again, which was attributed to the nucleating effect of pores. Besides, an increase in temperature was reported to alter the diffusion behavior and invoke more than three stages of diffusion for plant fiber-reinforced PLA composites. That was explained by the development of surface microcracks through which water seeps into fibers and induces their swelling, resulting in a capillarity phenomenon. Though, with a rise in temperature, such mechanisms are accelerated. Similarly, Gil-Castell et al. [30, 122] have reported such a phenomenon during the aging of sisal fiber-reinforced PLA composites in distilled water at temperatures between 75°C and 85°C.

Considering the medium of aging, it was shown that high humidity levels allow high moisture uptake in composites. Such observation was asserted in the study of Xian et al. [32], where they conducted aging tests in three different relative humidity conditions (50 RH%, 85 RH%, and 98 RH%). This was also

TABLE 3 | Water absorption kinetics (diffusion coefficient and maximum moisture uptake) of different PFRCs.

Case study	Composites	Weight (wt%) or volume (V%) fraction of fibers	Aging conditions	Maximum moisture uptake (%)	The kinetic parameter (n)	Diffusion coefficient ($\times 10^{-6}$ mm^2/s)
Li and Xue [27].	Flax/Epoxy	37 V%	23°C/100 RH%	7.245	0.5450	1.414
			37.8°C/100 RH%	8.652	0.4750	3.525
			60°C/100 RH%	9.365	0.5710	11.924
Cai et al. [26]	Flax/phenolic resin	65 V%	23°C/100 RH%	15.9	0.3542	1.09
			37.8°C/100 RH%	16.6	0.2676	2.73
			60°C/100 RH%	18.3	0.1531	7.30
Mejri et al. [127]	Wood/HDPE	40 wt%	60°C/100 RH%	9.95	—	—
Gil-Castell et al. [30, 122]	Sisal/PLA	30 wt%	60°C/100 RH%	9.4	—	—
			65°C/100 RH%	8.7	—	16
			70°C/100 RH%	10.4	—	—
			75°C/100 RH%	9.3	—	21
			80°C/100 RH%	6.3	—	—
			85°C/100 RH%	10.3	—	22
Ma et al. [31]	Jute/Epoxy	—	20°C/100 RH%	6.43	—	—
			40°C/100 RH%	6.48	—	—
Habibi et al. [130]	Flax/Epoxy	40 V% ± 1.8%	45°C/100 RH%	12.8	—	2.06
Shi et al. [28]	Bamboo/Epoxy	—	20°C/100 RH%	12.4	0.4460	4.083
			70°C/100 RH%	21.2	0.3030	6.246
			70°C/85 RH%	5.65	0.3590	4.227
Moudood et al. [24]	Flax/Bio-epoxy	37 wt%	45°C/75 RH%	2.57	—	2.17
Xian et al. [32]	Ramie/ Phenolic resin	40.4 wt%	Ambient/50 RH%	0.73	—	5.50
			Ambient/85 RH%	2.09	—	2.08
			Ambient/98 RH%	4.40	—	0.83
Depuydt et al. [140]	Bamboo/Epoxy	40 V%	30°C/32 RH%	1.8	—	—
			30°C/75 RH%	6.6	—	—
			30°C/84 RH%	6.8	—	—
Sanjeevi et al. [143]	*Calotropis gigantea* and *Areca* fine/ Phenol-formaldehyde	25 wt%	Ambient/100 RH%	3.6	0.5584	9.41
		35 wt%		4.1	0.5300	11.26
		45 wt%		4.3	0.5688	11.47

confirmed by Depuydt et al. [140] for bamboo/epoxy composites aged in different humidity levels (32 RH%, 75 RH%, and 84 RH%) at 30°C. Herein, it is worth also mentioning that the weight fraction of plant fibers inside composites plays also a key role in the retainment of water. A high amount of fibers leads to high moisture uptake [30, 122], thus accelerating the diffusion process. Figure 12b illustrates this behavior for hybrid *Calotropis gigantea* and *Areca* fine fibers reinforced phenol-formaldehyde composites aged for 10 days at room temperature. The maximum moisture uptake increased from 3.6% at 25 wt% of fibers to 4.1% at 35 wt% of fibers. However, it increased to 4.3% with 45 wt% of the reinforcement. Additionally, the diffusion coefficient increased with fiber content from a minimum of 9.41 mm^2/s to 11.47 mm^2/s.

2.2.2 | Crystallinity

The effect of temperature and humidity on PFRC's crystallinity can vary significantly depending on whether the matrix is

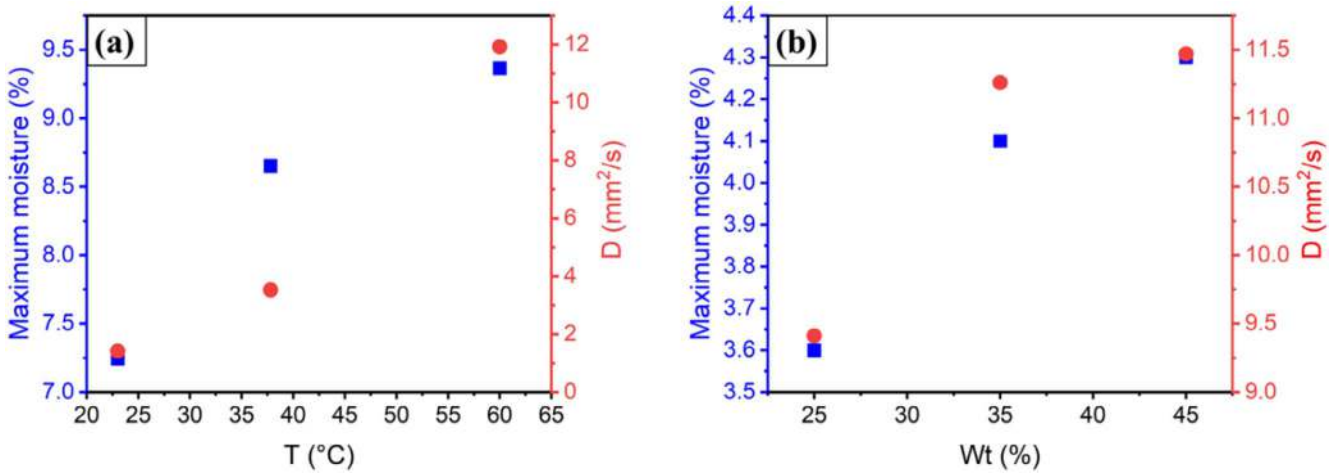

FIGURE 12 | Maximum moisture and diffusion coefficient versus (a) hydrothermal aging temperatures (23°C, 37.8°C, and 60°C) of flax/epoxy composites [27]; (b) weight fractions (wt%) of *Calotropis gigantea* and *Areca* fine fibers (25 wt%, 35 wt%, and 45 wt%) in Phenol-formaldehyde composites [143].

semi-crystalline or amorphous. For those with semi-crystalline matrices such as PLA, PP, PA, and HDPE, temperature and humidity result in crystallinity changes. Exposure to hot and humid conditions enhances their crystallinity. This is because heat can facilitate the reorganization of polymer chains into more ordered structures [145], while humidity acts as a plasticizer, reducing the glass transition temperature and allowing more mobility of the polymer molecular chains. For instance, Gil-Castell et al. [30] experienced an increase in the crystallinity of sisal fiber/PLA composites after exposure to humid conditions (aging at 85°C above the glass transition temperature of PLA) when evaluated through XRD analysis. Sisal fibers acted as nucleating agents, promoting the formation of larger crystalline domains in the amorphous region of the PLA matrix. However, that was observed for PLA composites reinforced with a less weight fraction of fibers. Moreover, Neat PLA showed a similar trend. Such results were confirmed by the XRD patterns that depicted for the aged specimens intensified peaks corresponding to lattice planes of crystalline domains of PLA (200)/(110), (203), and (210) for 2θ values 16.8°, 19.1°, and 22.6°, respectively. They also depicted a reduced signal (halo) corresponding to the amorphous region in PLA.

Differently, using another technical method (Differential Scanning Calorimetry (DSC)), Gil-Castell et al. [122] evaluated crystallinity in a previous work on sisal/PLA composites aged under the same conditions and showed a similar trend. Yu et al. [128] also used DSC to evaluate the crystallinity of short ramie fiber reinforced PLA composites after aging at a temperature of 60°C in a water bath. Interestingly, crystallinity increased after aging. An increase was related to a reduction in molecular weight and plasticization of PLA by water through chain scissions in the molecular chains of the amorphous region.

In addition to other degradation mechanisms, hygrothermal and hydrothermal aging at high temperatures contribute to the demolition and reduction of the amorphous areas in semi-crystalline polymer matrices [146–148]. This degradation primarily occurs through chain scission and hydrolysis reactions, which paradoxically can lead to an increase in crystallinity. Falkenreck et al. [146] observed this phenomenon in polyamide (PA) aged under hydrothermal conditions for 168 h at temperatures of 23°C, 50°C, 70°C, and 90°C. DSC results revealed an increase in crystallinity from an initial value of 27.3% to 31% at 90°C. Similarly, in PP-based composites, Marquard et al. [148] demonstrated that hydrolysis reactions occurring predominantly in the amorphous regions contribute to an increase in crystallinity following exposure to UV and hygrothermal aging at 80 RH% for over a month. Furthermore, Bazan et al. [149] reported that high aging temperatures facilitate molecular chain rearrangement in HDPE matrices, resulting in enhanced crystallinity. This increase in crystallinity, although initially counterintuitive, often leads to changes in the mechanical performance of these materials, potentially enhancing stiffness while reducing ductility due to the diminished amorphous phase content.

Apparently, composites with amorphous matrices respond differently to temperature and humidity. Amorphous resins do not have a melting point and lack a crystalline structure. However, a change in the crystallinity of their composites may engage a change in crystallinity at the scale of the plant fiber. In fact, there is a lack of knowledge concerning the variations in crystallinity for plant fiber-reinforced amorphous matrix composites [11].

2.2.3 | Chemical Composition

The structural properties of the polymeric matrices and their based composites are highly affected by temperature and the hygro or hydrothermal conditions. Based on FTIR analysis, these properties were examined in many studies. Besides, an increase in temperature was shown to result in degradation of the polymeric matrix and the plant fibers embedded into it in composite materials, involving a change in the chemical structure, such as the breakdown of cellulose and hemicellulose in fibers, and the oxidation or thermal degradation of the polymeric matrix [150–154]. Rousseau et al. [126] have ascertained through FTIR the effect induced by thermal aging on flax/PP composites' structural properties. The PP matrix lost its stabilizers due to the evaporation of ester groups [155] after 50 days of aging.

Meanwhile, aging for 252 days resulted in a thermo-oxidation reaction initiated in a small number of sites in the amorphous region of the PP matrix [151, 152, 156]. As demonstrated by FTIR, the fibers were exposed after such damage. The peaks corresponding to peresters or lactones, carbonyl function, and ketones appeared at 1775 cm^{-1}, 1730 cm^{-1}, and 1715 cm^{-1}, respectively, and eventually the intensity of the peak corresponding to lignin at 1640 cm^{-1} increased.

Temperature and humid environments have more pronounced effects on composites' structural properties and their constitutive materials. FTIR analysis has shown that these conditions can cause alterations in functional groups of both the polymeric matrix and fibers, leading to oxidation and hydrolysis reactions. Rousseau et al. [126] have also investigated the changes in structural properties of the thermally compressed flax/PP composites during aging in distilled water at 70°C. Hydrothermal aging caused the degradation of PP and its oxidation [157, 158], revealed by FTIR analysis that showed a decrease in the band corresponding to the carbonyl function (C=O) at 1730 cm^{-1} over aging time. As a consequence of matrix degradation, flax fibers were exposed. Thus, a peak corresponding to lignin appeared and its intensity increased after 30 days of aging [159].

Differently, Jiang et al. [29] used the approach of analyzing the soaking solution to get valuable insights into the changes in structural properties occurring when exposing PFRC to completely humid conditions. They compared the FTIR spectrum of deionized water used as a soaking solution before and after aging jute/PLA composites at 50°C. They observed no changes after 7 days. Herein, after 42 days, a chemical degradation occurred in the composite material, and hemicellulose was hydrolyzed as several peaks corresponding to jute fibers and PLA were depicted. At a wavenumber of 1186 cm^{-1}, the band corresponding to C-O stretching revealed that PLA oligomer diffused into the solution. Eventually, the peaks corresponding to cellulose and hemicellulose (C-O-C and C-O stretching) were at 1100 cm^{-1} and 1062 cm^{-1}, respectively.

Eventually, Cai et al. [26] analyzed the soaking solution used for the aging of flax/phenolic composites at 60°C. After 16 months of aging, the phenolic resin began to deteriorate, as demonstrated by the peaks observed in FTIR spectra at 1505 cm^{-1}, 1364 cm^{-1}, 1150 cm^{-1}, and 1004 cm^{-1}, corresponding to the vibration of aromatic rings. Indeed, after 36 months, flax fibers were altered since the intensity of the peak at 3408 cm,$^{-1}$ corresponding to water, was intensified, and peaks corresponding to fibers appeared at 1046 cm^{-1} and 1654 cm^{-1}. Obviously, the hydrothermal conditions caused the deterioration of the phenolic resin and the leaching of the amorphous constituents such as hemicelluloses, pectins, and some poorly crystallized cellulose into the solution.

Differently, Mejri et al. [127] showed that no chemical degradation occurred in birch fibers/HDPE composite when hydrothermally aged at 60°C and dried at 65°C, inferring that HDPE composites undergo just a fatigue mechanism [160, 161].

Although there are limited studies investigating the impact of high temperature and hot/wet conditions on the chemical properties of PFRCs, it could be inferred from the existing research that chemical degradation primarily depends on the polymeric matrix used, as it serves as a crucial barrier, determining the extent to which the composite material can resist chemical changes under such conditions. Besides, the matrix's ability to prevent moisture ingress and withstand thermal stress plays a critical role in maintaining composites' structural integrity. Hence, the selection of an appropriate polymeric matrix is essential for enhancing the durability and performance of PFRCs when exposed to harsh environmental conditions.

2.2.4 | Morphology

The high temperatures significantly impact the morphology of PFRCs, particularly affecting the matrix. Techniques such as Scanning Electron Microscopy (SEM) and x-ray tomography reveal that high temperatures can cause void formation and fiber-matrix debonding. Using SEM, Oliveira et al. [102] observed some of these microstructural changes in fique fabric-reinforced epoxy composites induced by accelerated aging at 170°C. The findings revealed fiber breakage and pullout, tearing, debris, and matrix collapsing, as well as fiber-matrix debonding as a result of thermal oxidation [129].

The synergetic effect of temperature and humidity exacerbates morphological degradation in PFRCs leading to interfacial debonding and matrix cracking. Such observation was evidenced in many studies [5, 27–29, 127, 129]. A great example of the effect induced by the hydrothermal environment on the microstructure of a composite was shown by Jiang et al. [29] through x-ray tomography and SEM observations (Figure 13). PLA and jute fibers showed great compatibility at the interface (Figure 13a) with negligible porosity (0.05%) before aging. However, after exposure to humid conditions at 50°C, the microstructural changes were obvious by the formation of gaps at the fiber-matrix interface (Figure 13b) and an increase in porosity revealing matrix cracking (Figure 13c).

Eventually, through SEM, Gil-Castell et al. [30] observed that aging in water at a high temperature of 85°C induces changes in the cryo-fractured surface of sisal fibers reinforced PLA composites, with the same observation of the weakening of the fiber-matrix interface. In fact, PLA texture changed from smooth to rough due to the crystallization induced after exposure to humid conditions. Mejri et al. [127] also highlighted the weakening of the interface and collapsing of the matrix and pullout of fibers in HDPE thermoplastic composite reinforced with short birch fibers after aging at a high temperature (60°C) in distilled water when observing the fractured surface after fatigue test. The same damage was also observed by SEM in plant-fiber composites with a thermoset matrix, in the fractured surfaces of twisted bamboo fibers and jute fibers reinforced epoxy composite aged in distilled water at different temperatures (20°C and 70°C) as observed by Shi et al. [28] (Figure 13d,e), as well in jute, kenaf, and hemp fiber-reinforced epoxy composites after aging at (95°C and 97% RH) [129]. Li and al. [27] also observed interface weakening and matrix cracking when comparing SEM micrographs of unaged (Figure 13f) and aged flax/epoxy composites aged for 17 weeks in hydrothermal conditions at 23°C (Figure 13g), 37.8°C (Figure 13h), and 60°C (Figure 13i). Indeed, in the same conditions of aging but for a long period (2 years), Cai et al.

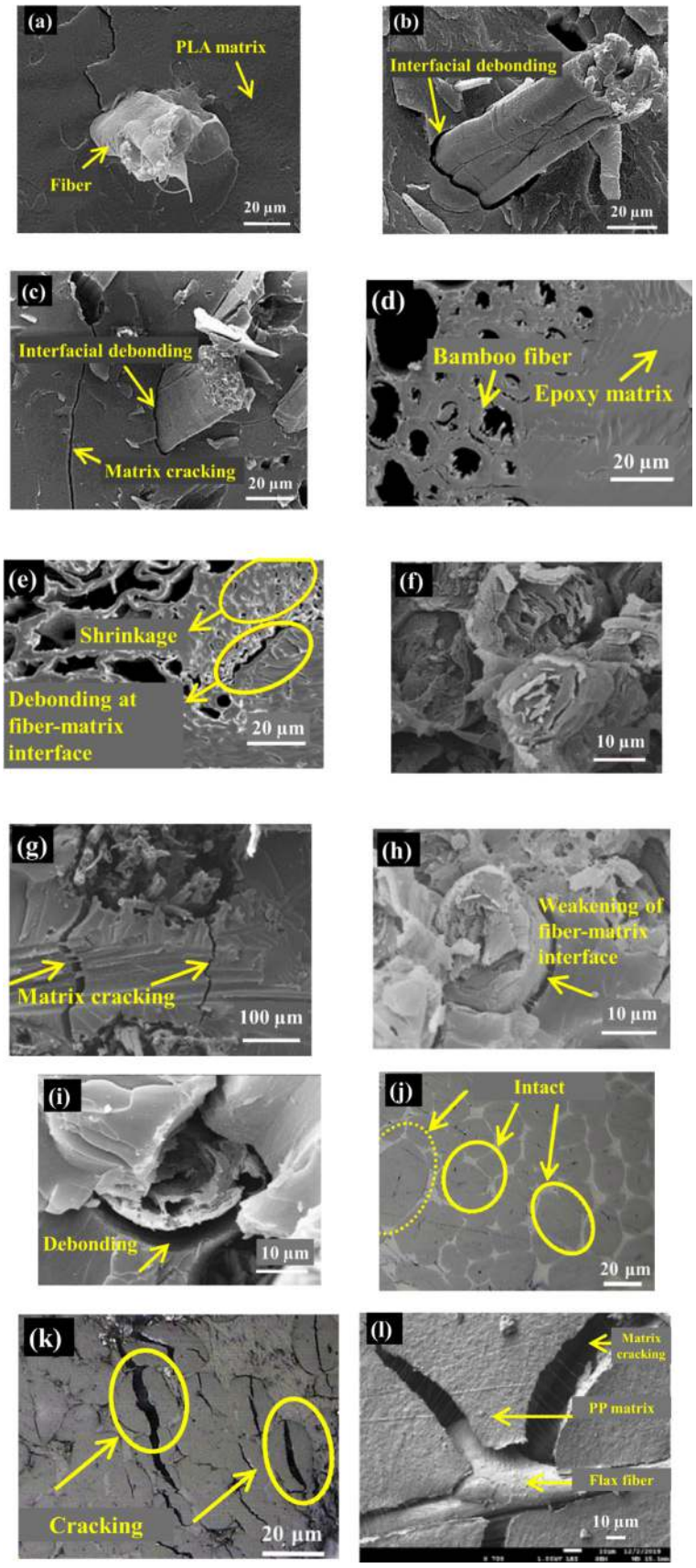

FIGURE 13 | SEM observations of impact fracture surfaces of unaged (a), aged for 21 days at 50°C/100 RH% (b), and aged for 42 days at 50°C/100 RH% (c) [29]; unaged bamboo/epoxy composite (e), and hydrothermally aged (f) [28]; unaged flax/epoxy composite (f), hydrothermally aged for 17 weeks at 23°C (g), at 37.8°C (h), and at 60°C (i) [27]; unaged flax/phenolic composite (j), and hydrothermally aged for 2 years at 60°C (k) [26]; flax/polypropylene composite thermally aged for 78 days at 120°C (l) [126].

highlighted the deterioration of fibers, interface debonding, and matrix cracking in a phenolic composite reinforced with flax fibers (Figure 13j,k). Otherwise, high temperatures were shown to induce the same damage to PFRCs with the weakening of the interface and matrix cracking, as demonstrated by Rousseau et al. [126] when performing thermal aging of flax/polypropylene composite at 120°C (Figure 13l).

2.2.5 | Mechanical Properties

The mechanical properties of PFRCs are significantly influenced by hygro and hydrothermal environments. Exposure to high temperatures can lead to the degradation of the matrix, fibers, and their interfacial regions, leading to a reduction in the composite's overall strength and stiffness. In hot/wet conditions, water molecules act as plasticizers when infiltrated through the molecular chains of the polymeric matrices and reach the fibers [13, 127, 159, 162], causing a differential swelling. Additionally, high temperatures cause differences in thermal expansion between the polymeric matrices and fibers, weakening their interfacial adhesion [13, 163–165]. In fact, the thermal and hygroscopic mismatches develop stresses at the interface during the service life of composites. For instance, Le Duigou et al. [163] investigated the contribution of flax fiber hygroscopic expansion to interfacial stresses in Maleic Anhydride grafted polypropylene (MAPP)/flax composites conditioned in different hygrothermal conditions and demonstrated that hygroscopic stress notably exceeds thermal-induced stresses. The hygroscopic radial expansion coefficient (defined as the strain ε induced by variation of 1% of moisture content) was measured at 1.14 ε/Δm, considerably higher than the thermal expansion coefficient of 78×10^{-6} ε/°C. Furthermore, in another study, Le Duigou et al. [164] showed that thermal stresses generated by differential thermal expansion and polymer shrinkage during polymerization induce radial pressure that prestresses the fibers. This prestress can damage fiber surface components, weakening interfacial adhesion between fiber cell wall layers and even the fiber/matrix interface. Their results showed that the friction strength decreases with the loss of interfacial interactions. However, even though the hygroscopic stress overtakes the thermal stress, the hygroscopic stress highlighted in that study was very low as fibers were prestressed by temperature.

Besides, many studies reported the reduction of the mechanical properties with changes in the response to mechanical load. Depuydt et al. [140] examined the mechanical performance of unidirectional bamboo fiber-reinforced epoxy composites aged for 6 weeks in different hygrothermal conditions (32 RH%, 75 RH%, and 84 RH%) at 30°C. Figure 14a shows the stress–strain curves obtained for the unaged and aged composites. Their findings revealed an enhancement of the tensile strength with the flexibilization effect induced in bamboo fibers by moisture increase. They suggested that the reduction in stiffness and the increased strain were involved in such a phenomenon rather than the swelling of fibers. Furthermore, Xian et al. [32] revealed that the mechanical response of the thermally compressed ramie fiber-reinforced phenolic composite changed after 6 months of aging in various relative humidities (50 RH%, 85 RH%, and 98 RH%) (see Figure 14b). The stress–strain curves presented an elastoplastic behavior for the different RHs, with increased strain at break, and reduced strength and stiffness upon RH. Interestingly, several studies have ascertained that the turning point in PFRCs' mechanical performance (tensile, flexural, fatigue, and impact properties) is the weakening of the fiber-matrix interface [5, 64, 126, 130, 166–168]. As reported by Rousseau et al. [126], the weakening of the fiber-matrix interface and matrix cracking caused a decrease in bending and impact properties of thermally-compressed flax/PP composites aged in severe conditions (70°C/100 RH%). Both strength and elastic modulus decreased from the first stages of aging (10 days). The plasticization phenomenon was also evidenced in the flax/PP composites as demonstrated by the increase of the strain at failure. Mejri et al. [127] evaluated flexural properties of short wood fibers reinforced HDPE composites at different stages of aging at 60°C/100 RH%. Eventually, the rise of the flexural strain demonstrated that the HDPE composites were plasticized. Herein, both flexural strength and modulus of the composites decreased by 50.81% and 47.24%, respectively, after aging.

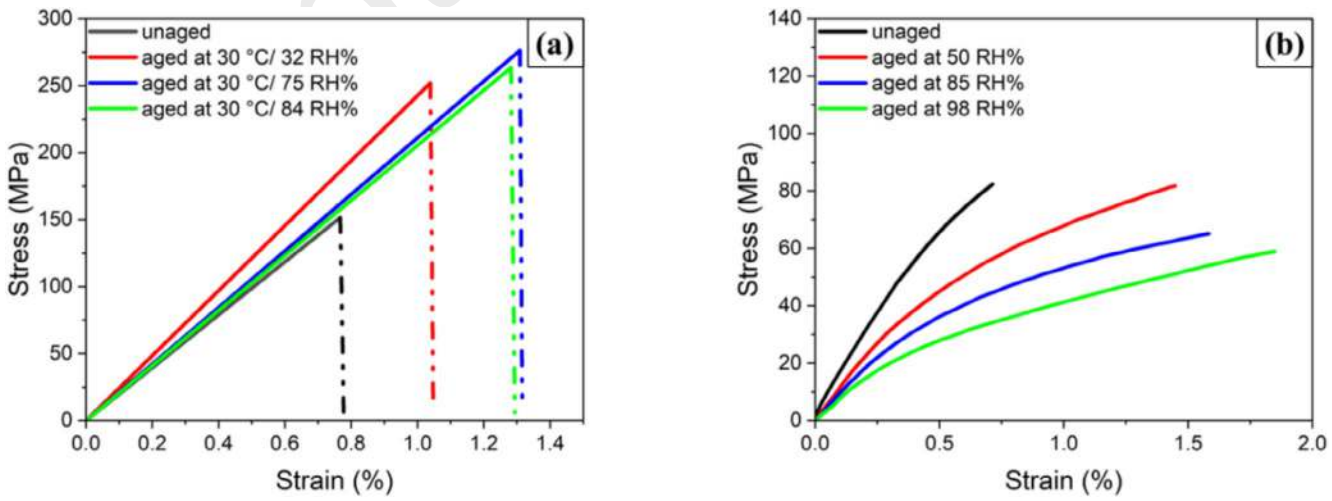

FIGURE 14 | Stress–strain curves of (a) unaged and aged bamboo/epoxy composites for 6 weeks in different hygrothermal conditions (32 RH%, 75 RH%, and 84 RH%) at 30°C [140]; (b) unaged and aged ramie/phenolic composites for 6 months in different hygrothermal conditions (50 RH%, 85 RH%, and 98 RH%) at ambient temperature [32].

The plasticization effect observed in these composites, based on PP and HDPE matrices, is primarily attributed to moisture absorption at the fiber scale. Although PP and HDPE are inherently hydrophobic, water infiltrates the fiber structure through capillary action facilitated by cracks in the matrix, defects, and the sensitivity of plant fibers to water. This leads to fiber swelling and plasticization. Furthermore, Jiang et al. [29] have stated the plasticization of PLA matrix when investigated the evolution of the tensile properties of jute fibers reinforced PLA composites under a hydrothermal environment (50°C/100 RH%). Thus, during the first week of aging, strain at failure increased from 1.4% to 2.3%. Herein, tensile strength and elastic modulus decreased by 12% and 14.6% respectively, but as long as composites were exposed for a prolonged time (28 days) to such conditions, strength, stiffness, and strain at failure depleted drastically. Again, because of the weakening of the interfacial adhesion between jute fibers and PLA matrix, and the collapsing of the matrix by the nucleated cracks resulting from the swelling of fibers and their propagation after the fiber's shrinkage.

From what concerns, plant fiber-reinforced thermoset polymeric composites. Hydric conditions were shown to induce the same effect (plasticization). Ma et al. [31] have found that the epoxy matrix in the jute/epoxy composite was plasticized for the first period of immersion in water at temperatures of 20°C and 40°C. Herein, tensile strength and elastic modulus leveled off over aging time. Besides, increasing temperature exacerbated composite degradation as differential stresses were generated at both the matrix and fibers after swelling, and with the development of osmotic pressure inside fibers, the soluble substances were leached over time until the 180th day of aging. Despite this, the tensile stress–strain response remained non-linear and similar for aged and unaged samples [32, 169, 170]. Though, aged samples exhibited a softer behavior due to accumulated damage.

In another study case, Habibi et al. [130] evaluated the tensile properties of non-woven flax mats/epoxy composites at different temperatures (50°C and 75°C) after aging at 45°C/100 RH%. Indeed, during aging in a hydrothermal environment, tensile strength and modulus decreased during the rapid increase in water uptake and then remained stable. However, evaluating tensile properties (strain at failure) at higher temperatures revealed the plasticization phenomenon induced by temperature on the epoxy matrix. Besides, temperature drastically affected tensile strength and modulus. They dropped by 45% and 35% at 50°C and by 75% and 53% at 75°C, respectively.

Cai et al. [26] asserted a combination of phenomena occurring during the aging of unidirectional flax/phenolic composites for 3 years in hydrothermal conditions at different temperatures of 23°C, 37.8°C, and 60°C. During the first linear increase of water uptake (8 weeks), tensile strength and modulus decreased by 37% and 38.5% after aging at 23°C, by 27% and 47% after aging at 37.8°C, and 27.7% and 57% after aging at 60°C, respectively. Such a drop in mechanical performances during that period was explained by the deterioration of the fiber-matrix interface as a result of water molecules infiltrating through the composite, which caused the swelling of flax fibers, induced localized stresses at fiber cell walls, and changed their microfibrillar angle. Indeed, after the water uptake in the composite approached saturation, the tensile properties were enhanced slightly as water seeped through the capillaries and the spaces between fibrils, resulting in the reorientation of flax microfibrils [164], though the plasticization of fibers. Meanwhile, after saturation, amorphous constituents of fibers deteriorated, and the phenolic matrix was degraded. That resulted in the stabilization of tensile strength and modulus after aging for 3 years at 23°C and 37°C. In another way, after aging at 60°C, another mechanism was involved. The fiber network structure was destroyed with the molecular chain stretches induced by moisture absorption, which caused a depletion in tensile strength and modulus of about 76.7% and 47%, respectively.

Otherwise, Li and Xue [27] have observed an increased tensile strength of the unidirectional flax-reinforced epoxy composites within the first weeks of aging in hydrothermal conditions at 23°C, and its stabilization after reaching moisture equilibrium. An increase was ascribed to the high mobility of epoxy macromolecular chains that induced post-crosslinking reactions [171]. Contrary to those aged at high temperatures (37.8°C and 60°C), tensile strength degraded slightly without stabilization, and drastically at a temperature of 60°C.

Other research studies have confirmed that exposure to high temperatures and humidity conditions induces the degradation of plant fiber composites. As reported by Shi et al. [28], the mechanical properties of twisted bamboo fibers/epoxy composites were sensitive to temperature more than relative humidity, affirming that the fiber-matrix interfacial bonding is significantly affected by temperature rather than humidity, as demonstrated by the decrease in the shear properties. Moreover, the epoxy matrix was more sensitive to the harsh hydrothermal environment. Herein, the drop in the mechanical properties was more prominent when specimens were immersed in water at 70°C. The tensile strength of twisted bamboo fibers/epoxy composites decreased by 13.2%, 38.7%, and 29.0% when immersed in water at 20°C, at 70°C, and in thermostatic and hydrostatic environments (70°C/85%), respectively. Similarly, the flexural strength decreased by 23.1%, 40.8%, and 29.0% under the same conditions.

Cadu et al. [16] also examined tensile properties of a thermally-compressed flax/epoxy composite after humidification (90 RH% for 3.5 days)/drying (40 RH% for 3.5 days) cycles at a moderated temperature of 55°C. The findings revealed stable tensile strength and strain at break for up to 26 weeks. Thereafter, tensile strength decreased slightly by 12%. Otherwise, elastic modulus decreased from the 1st week (1st cycle) until the 4th week by 8%, then stabilized. Despite that, a slight decrease in tensile modulus, it was proven that no damage occurred at the fiber scale.

The evaluation of the frictional properties of jute, hemp, and kenaf fiber-reinforced epoxy composites after aging at 90°C and 97% (RH) for 30 days revealed a decrease in the critical normal load for all the varieties [129]. It decreased by 14.39%, 57.84%, and 37.3% for jute, kenaf, and hemp-reinforced epoxy composites, respectively. Such a difference in behavior was ascribed to the chemical composition of fibers that differs from one to another. Furthermore, the hemp fiber-reinforced epoxy composite exhibited better scratch resistance after hygrothermal aging as the penetration depth of the indenter was lower. In fact, the

high temperature of aging caused a decrease in the resistance of penetration, which is related to the matrix cracking and the weakening of the fiber-matrix interface [172]. Otherwise, the fracture toughness of all the bio-composites was depleted over aging time.

Additionally, one can note that the plasticization induced by hygro and hydrothermal conditions in PFRCs is initially reversible. Early exposure leads to water absorption, causing temporary softening and swelling, which subside upon drying, restoring mechanical properties [17, 27]. However, prolonged exposure triggers irreversible changes, such as fiber/matrix debonding, microstructural damage, and the leaching of fibers' amorphous components. At this stage, the composites' properties cannot fully recover, marking a transition from reversible to permanent degradation.

Another point to mention is that the high temperature of aging could lead the thermoset matrix in composites to degradation in 2 steps [173]. The first step involves a post-curing reaction which could consolidate resin and improve the mechanical properties. Meanwhile, the second step engenders prominently a degradation and loss of the mechanical properties. Furthermore, in certain severe conditions, the synergetic effect of temperature and oxygen is encountered. Generally, the thermal-oxidative aging results in three stages of degradation for thermoset resin. The dominance of polymer viscoelastic behavior and stress relaxation at high temperatures is prominent in the first stage, but within the second stage, the matrix shrinks (decrease in free volume), and its elastic modulus changes with exposure to the thermo-oxidative environment [174]. Thereafter, some microcracks are developed on it [175].

Oliveira et al. [102] have evidenced the effect induced by thermal aging on the thermo-mechanical properties of a fique fabric-reinforced epoxy composite at 170°C for different durations (0, 72, 120, and 140 h). Using DMA analysis, it was proven that the mobility of molecular chains of the polymeric matrix and for the composites depended on the time of exposure and temperature. The chain mobility increased during the glassy/rubbery transition when composites were aged for 72 h at 170°C, and that was marked by the highest storage modulus (E') observed [176]. The latter decreased after 240 h of aging which marks the decrease in composite's viscoelastic stiffness, and that was ascribed to the degradation of the fiber-matrix interface, as confirmed by SEM observations. Furthermore, the glass transition temperature (T_g) of both the epoxy matrix and composites was affected. It increased by 45°C after aging for 120 h.

In a study evaluating the compressive properties (strength and elastic modulus) of epoxy matrix exposed to thermal aging at different temperatures (90°C, 110°C, 120°C, 130°C, and 180°C) for different durations (1 to 16 days) [177], it was inferred that a low aging temperature such as 90°C enhances the mechanical properties by contributing to the curing of the resin. Meanwhile, its free volume might decrease (physical aging). Differently, at higher temperatures, degradation overcomes the post-curing stiffening. Epoxy specimens aged at 110°C exhibited an increase in elastic modulus after 1 day, then decreased as oxidation occurs. While above the temperature of glass transition, the mechanical properties were significantly depleted.

Furthermore, in real-life applications, PFRCs are often subjected to both hygro or hydrothermal conditions and mechanical loading simultaneously, which can significantly influence their properties. While factors such as temperature, moisture, radiation, and mechanical stress individually contribute to material aging and potential degradation, their combined action can intensify these effects. Studies investigating the coupled influence of water and mechanical stress primarily on thermoset composites have highlighted that applied mechanical loads accelerate water diffusion within the polymer matrix, thereby hastening physicochemical aging mechanisms and potentially initiating additional degradation processes [22, 178, 179]. To illustrate this effect for thermoplastic composites, Regazzi et al. [178] investigated the thermo-hydro-mechanical aging of twin-screw extruded PLA composites reinforced with varying fiber contents (10 wt% and 30 wt%) through creep tests at 20°C and 35°C. Their results showed that aging temperature led to a loss in elastic properties, particularly with high fiber content. They demonstrated a strong synergetic effect between mechanical load and water immersion, which significantly reduced the composites' lifetime, but limited defect development (such as crazes) within the PLA matrix. Otherwise, higher immersion temperatures promoted material ductility. Moreover, the presence of fibers was found to mitigate environmental stress cracking mechanisms and extend the time to failure.

Indeed, studies investigating the property changes of natural fibers reinforced composites to temperature are very scarce. However, for most, it was shown that above the glass transition temperature (T_g) of the polymeric matrix, composite strength and stiffness reduced [180]. Meanwhile, the interface between fiber and matrix could undergo various aggressive reaction changes when subjected to high temperatures [181], by generating differential thermal expansion between fibers and the polymer matrix. Indeed, the effect of temperature on tensile strength and modulus is more intense for unreinforced materials than for composites [182, 183]. Generally, those tensile properties were also shown to decrease with temperature for thermoplastic composites, especially near the glass transition temperature (T_g) [184, 185], while the strain at fracture increases above that temperature because of the rise in the mobility of the molecular chains of the polymeric matrix.

2.2.6 | Thermal Stability

The thermal stability of PFRCs is significantly influenced by exposure to high temperatures and hot/wet conditions. Despite the limited research in this area, thermogravimetric analysis (TGA) has provided valuable insights. TGA typically reveals a five-stage degradation process in PFRCs: Evaporation of water in the matrix or fibers, degradation of hemicellulose in fibers, degradation of cellulose and lignin, degradation of the polymeric matrix, and degradation of char. Insights from TGA after aging indicate that the onset temperature for a 5% weight loss is a critical parameter for evaluating the influence of aging on thermal stability. Gil-Castell et al. [30] have examined the thermal stability of sisal fibers reinforced PLA composites before and after aging at 85°C based on TGA. Eventually, the degradation of composites occurred in five stages, with evaporation of water retained by the matrix and fibers in the first stage, then

degradation of hemicellulose between temperatures 222°C and 315°C in the second stage [186]. From that latter temperature to 400°C, the third and fourth stages occurred with decomposition of both cellulose and PLA matrix. In the later stage from 380°C to 500°C, the char formed during previous decomposition degraded. Indeed, a comparison of the onset degradation temperature ($T_{5\%}$) between composites and PLA matrix revealed that the presence of fibers results in a decrease in the onset degradation temperature because of hemicellulose degradation and the small molecular weight of PLA matrix present in composites [122]. Aside from this, the onset degradation temperature of those composites decreased after hydrothermal aging since hydrolytic reactions occurred at the fiber-matrix interface and resulted in peeling, delamination, and exposure of fibers.

Mejri et al. have also investigated the thermal behavior through TGA of thermally compressed HDPE composites reinforced by 40 wt% short birch fibers being hydrothermally aged at 60°C and dried at 65°C. Eventually, findings have revealed the degradation of composites following the five stages. However, after aging, an insignificant change was observed when comparing the temperature at which there is a 5% weight loss ($T_{5\%}$) in TGA. Though, it leveled off from 266°C to 261°C.

The resistance of PFRCs to thermal conditions is significantly influenced by aging in hygro and hydrothermal environments. This is evident as the onset degradation temperature demonstrates sensitivity and a marked decrease post-aging. Consequently, there is a critical need to optimize these composites by enhancing their stability and durability under varying environmental conditions. Gil-Castell et al. [30] have proposed the use of a coupling agent in the formulation of PLA composites reinforced by sisal fibers, and they achieved improved thermal stability after hydrothermal aging because the coupling agent aided in the formation of crystals around fibers and acted as a barrier [187], and even improved the adhesion along the fiber-matrix interface. Despite that, further research is essential to develop strategies that mitigate these impacts, ensuring thermal stability and performance of PFRCs for a long service life.

2.2.7 | Degradation Mechanisms of Composites: A Summary

In summary, the degradation mechanism of PFRCs seems to be complex. Herein, based on the findings above concerning the changes in the global properties of composites (mechanical, structural, or morphological) when aging composites in a simulated aging environment, a degradation mechanism is proposed and illustrated in Figure 15. From the first stages of aging, moisture of the surrounding environment seeps into composites through voids and molecular chains of the polymeric matrix, which could lead in many cases to plasticization and breakdown of intramolecular hydrogen bonds, resulting in the addition of free volume where moisture could be held. However, when moisture is driven into plant fibers, a difference in swelling between fibers and matrix occurs, leading to localized stress in the interface. Hence, fiber swelling promotes the nucleation of cracks and more pathways for moisture absorption. Indeed, at that stage, temperature could induce thermal stress to matrices and fibers and provoke shrinkages and crack propagation, which alters mechanical properties. Again, with the synergetic effect of temperature and humidity, as well as prolonged exposure, matrix hydrolysis occurs because of the molecular chain's scission; meanwhile, temperature exacerbates degradation by developing cracks inside fibers and removing their binding materials.

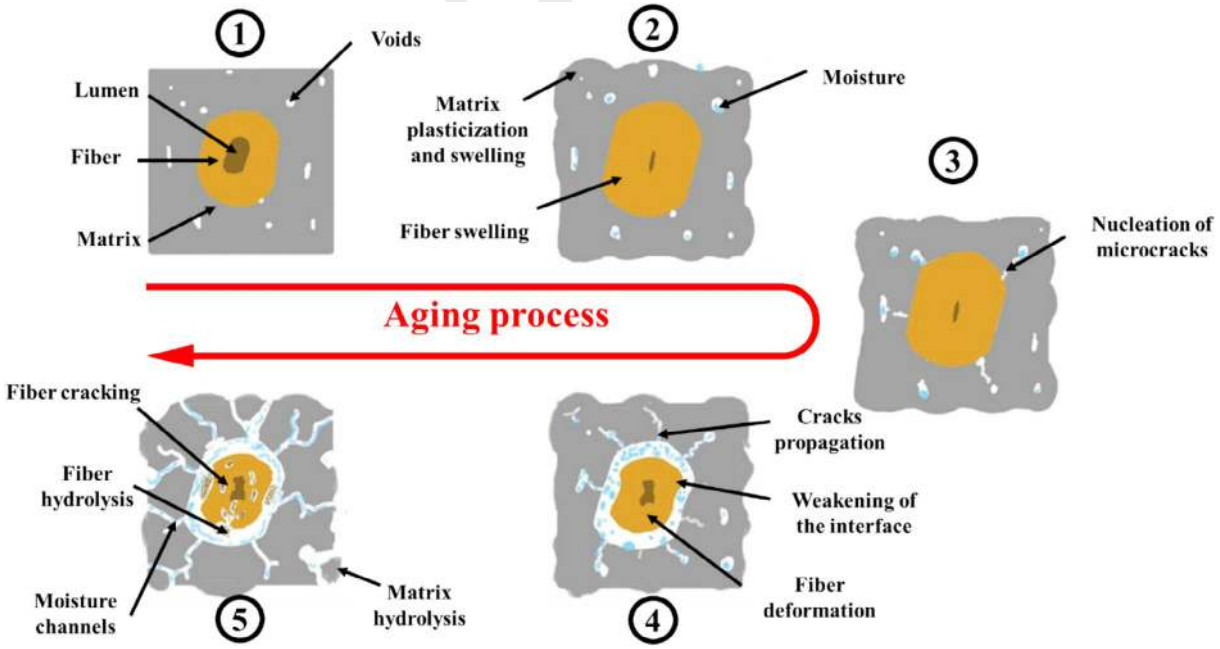

FIGURE 15 | Schematic illustration of the degradation mechanism of PFRCs under hygro and hydrothermal conditions. (1) Diffusion of moisture through the voids and polymeric chains of the matrix. (2) Matrix plasticization and diffusion of moisture through interfaces by capillaries inducing fiber swelling. (3) Nucleation of cracks as result of differential swelling. (4) Weakening of fiber-matrix interface and crack propagation. (5) Matrix and fiber hydrolysis.

3 | Service-Life Prediction Using Analytical Models

The development of plant fiber-reinforced composites for applications that require lightweight and durable materials is quite challenging. The understanding of the mechanical behavior of these during their operation would be of great interest. However, compared to composites reinforced with synthetic fibers like carbon and glass, there is limited knowledge about the durability of plant fiber-reinforced materials. The assessment of the degradation mechanisms of composites during their service life is required. Hence, it is essential to adopt accelerated protocols that are suitable for understanding the progressive damage that attends to composites and induces a failure or a loss in their performance and links between them and the service environment exposure time for the long term via analytical models. In fact, the prediction of the property changes of the plant fiber-reinforced composites is relevant in terms of the technical application of the material and providing a shred of evidence to rely on it during its period of usage. In this section, the analytical models used to predict the mechanical behavior of composite materials are scrutinized.

3.1 | Mechanistic Model

It uses continuum mechanics and the non-equilibrium thermodynamic concept to methodologically investigate the effect of different degradation modes on materials' mechanical behavior [188]. However, the durability response of PFRCs in their life service typically depends on several parameters, mainly moisture and temperature. It is identified based on the chemical composition changes, physical and mechanical aging, either by their combination [189]. As described by Mulenga et al. [190], in humid conditions, there is an interaction between the elastic and inelastic deformation, water diffusion, and propagating damage. With the variety of constitutive models introduced by continuum damage mechanics, it is possible to get more insights into the mechanical damage occurring for fiber-reinforced composites. Helmholtz free energy formulation of a material for isothermal deformation and water absorption processes can be assumed as in Equation (5).

$$\Psi = \Psi\acute{C}, C_\alpha, \alpha_1, \alpha_2 \tag{5}$$

Where $\acute{C}$ represents the modified right Cauchy-Green deformation tensor, the C_α is the molar concentration of water molecules in the composite and could be obtained using Equation (6). However, α_1 and α_2 are introduced to describe respectively the effect of damages induced by water absorption and external loading, and ν represents a parameter of the material (i.e., curing degree of the thermoset matrix).

$$C_\alpha = \frac{J-1}{\nu} \tag{6}$$

For the formulation of the constitutive equations, Helmholtz's free energy function is decomposed into two parts, one considering the mechanical energy caused by deformation and one considering the chemical energy by water diffusion [188], as shown in Equation (7).

$$\psi = \psi\acute{C}, C_\alpha, \alpha_1, \alpha_2 = \varphi_{\text{mech}}\acute{C}, C_\alpha, \alpha_1, \alpha_2 + \varphi_{\text{diff}}C_\alpha \tag{7}$$

φ_{mech} represents the mechanical energy caused by deformation while φ_{diff} represents the chemical energy driving the water diffusion. However, based on the continuum theory, it is possible to report degradation caused by water absorption in short or long PFRCs by establishing an internal parameter and introducing its kinetics. The internal parameters are determined based on the water absorption behavior obtained when aging composites in hygro or hydrothermal environment. The kinetic parameters are obtained by fitting the experimental data using theoretical models.

Tian et al. [191] integrated two internal variables into the Helmholtz free energy and energy dissipations with a non-equilibrium thermodynamic framework reflecting respectively the effect of moisture absorption and hydrolysis reaction to study the constitutive behaviors of composites and to develop a model for the long-term hydrothermal aging of an unidirectional natural fiber reinforced composite. The elastic responses were analyzed based on the theoretical model, and the results obtained agreed with experimental observations of the elastic modulus responses for long-term aging (Figure 16). Furthermore, in their recent studies [38], a nonlinear constitutive model for natural fiber-reinforced composites under hygrothermal aging was established considering the elastic and inelastic strains, dimensional instability due to swelling, and hydrolysis reaction. Changes in composite properties like matrix cracking, interfacial debonding, and the microstructural properties of plant fibers were pointed out in the model. Meanwhile, the influence of aging temperature on composites' elastic response was a point of focus. Besides, the theoretical model described well the evolution of elastic modulus with dependency on temperature and corroborated well with experimental data.

3.2 | Empirical Models

3.2.1 | Gunyaev Model

Gunyaev model is one of the main models used to predict the mechanical degradation of plant-fiber reinforced composites during long-term aging based on short trials [28, 192, 193]. It

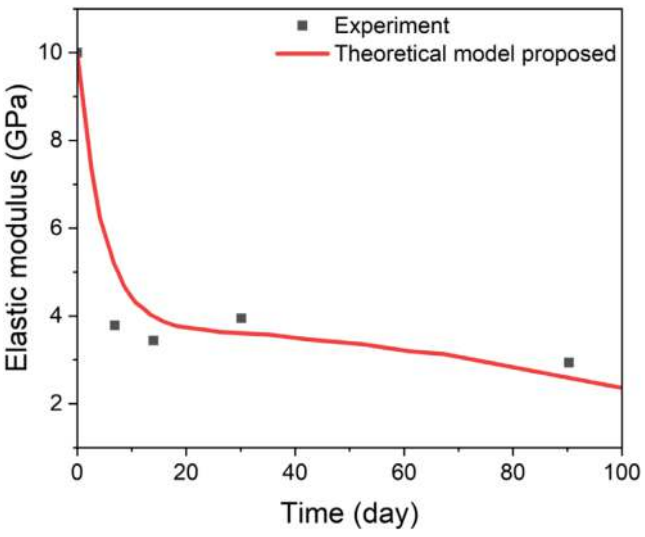

FIGURE 16 | Theoretical model and experimental result of ramie/phenolic composites aged at 60°C and 85 RH% [191].

considers both material properties and environmental factors. In this model (Equation 8), the composite's strength (S) after aging for t hours is expressed as a function of the initial strength (S_0), aging time (t), curing degree of composite (η), material and environmental parameter (λ), crack propagation resistance (β), and external environmental corrosion (θ). The prediction of composites' service life by this model requires conducting an accelerated aging test. The residual strength obtained through the experiments can be described thereafter with the Gunyaev semi-empirical mathematical model.

$$S = S_0 + \eta\left(1 - e^{-\lambda t}\right) - \beta \ln(1 + \theta t) \tag{8}$$

Shi et al. [28] applied this model to evaluate the evolution of bending properties of twisted bamboo fiber/epoxy composites and jute fiber composites undergoing accelerated hygrothermal (70°C/85 RH%) and hydrothermal (20°C and 70°C) aging over periods ranging from 1 to 90 days. Herein, composites were assumed to be completely cured ($\eta = 1$), and their critical residual bending strength was set at 70% and 50%. Their findings are presented in Table 4. This model allowed inferring that the bending strength of those composites will be reduced progressively over time, retaining about 40%–50% of their initial properties over time (in 5 and 10 years) when exposed to harsh environmental conditions. However, composites subjected to hydrothermal aging at low temperatures exhibit long service life. In fact, the projected service duration has not been contrasted with the performance of composites exposed to genuine hydrothermal environments.

Differently, Wang et al. [192] extended this model to consider various environmental factors encountered in the environment rather than temperature and humidity, as the Gunyaev model failed to predict the long-term performance of a flax/epoxy composite based on an accelerated aging test.

TABLE 4 | Results of service life prediction of the filament wound composites based on bending strength [23].

	Residual strength 50%		Residual strength 70%	
Samples	**Bending strength (MPa)**	**Time (days)**	**Bending strength (MPa)**	**Time (days)**
TBF/EP—20	52.71	1269	73.79	96
TBF/EP—70	52.71	101	73.79	15
TBF/EP—70/85	52.71	514	73.79	46
JF/EP—20	57.17	185,050	80.03	2171
JF/EP—70	57.17	118	80.03	69
JF/EP—70/85	57.17	1514	80.03	187

3.2.2 | Arrhenius Model

The Arrhenius theoretical model is one of the primary models used for predicting the long-term behavior of fiber-reinforced composites, based on short-term data from accelerated aging tests. This model assumes that a single dominant degradation mechanism remains constant over time and temperature during the aging process [34–36]. Nevertheless, the temperature is known to accelerate degradation; meanwhile, PFRCs were shown to undergo various degradation mechanisms. Hence, in many cases, the Arrhenius equation is often combined with other theoretical models, such as the linear model, to predict the durability of composites. Besides, the linear model is a phenomenological representation of test data but lacks assumptions regarding degradation mechanisms. In this model (Equation 9), a parameter (Y) representing the property retention versus aging time (t) at different temperatures (T) is linearly regressed. In fact, an acceptable regression value (R^2 of at least 0.80) allows combining the linear model with Arrhenius. However, at this stage, the Arrhenius plot may be constructed as a function of inverse absolute temperature for various percentages of property retention. Hence, determining the time to reach given levels of property retention at each of the aging temperatures could be ascertained by substituting various property retention values into the plotted regression equations (Equation 9).

$$Y = at + b \tag{9}$$

However, the time shift factor (TSF) which measures the acceleration factor between two temperatures, can also be used to assess the degradation process. It is given by the relation (Equation 10).

$$TSF = \exp\left[\frac{E_a}{R}\left(\frac{1}{T_0} - \frac{1}{T_1}\right)\right] \tag{10}$$

Where E_a is the activation energy, R is the gas constant, T_0 and T_1 are the absolute temperatures that can be obtained from Arrhenius plots. Wang et al. [189] found that the Arrhenius-based predictions were reliable for short conditioning.

Eventually, various researchers employed such models mainly in synthetic fibers-reinforced composites being aged at high temperatures and humid conditions over extended periods. For instance, Ghabezi and Harrison [36] investigated the long-term durability of glass fiber-reinforced epoxy composites and carbon-reinforced epoxy composites in artificial seawater (3.5% salinity) for 6 months at low and high temperatures using both experimental and analytical models. They applied the Arrhenius equation in conjunction with the linear model to predict tensile strength retention following accelerated aging. For glass-epoxy composites, tensile strength retention after aging at 60°C for 45, 90, and 180 days was 78.67%, 74.3%, and 72.42%, respectively, corresponding to a lifetime of 792, 1584, and 3167 days at 12°C. Similarly, carbon/epoxy composites retained 89.32%, 86.17%, and 80.35% of their tensile strength over a real lifetime period of 831, 1662, and 3323 days at 12°C. It is important to note that the performance of these composites has not been tested over such an extended real lifetime period. In fact, the linear model's prediction accuracy decreased over time, leading researchers to consider non-linear models.

A non-linear model was proposed, accounting for the observation that the degradation rates are initially high but decrease as exposure time increases. This model assumes that debonding at the interface is the primary cause of composites degradation. The non-linear relationship for tensile strength retention is given by Equation (11) or alternatively by Equation (12):

$$Y = 100 \exp\left(-\frac{t}{\tau}\right) \tag{11}$$

$$Y = \left(100 - Y_\infty\right) \exp\left(-\frac{t}{\tau}\right) + Y_\infty \tag{12}$$

where τ represents the fitted parameter, and Y_∞ represents the tensile strength retention (%) at infinite exposure time. By assuming $Y_\infty = 72\%$ for glass/epoxy composite and 80% for carbon/epoxy composites, the non-linear model better fitted experimental data. The estimated acceleration factor for carbon/epoxy composites at 12°C was 20.3, predicting tensile strength retention of 89.32%, 86.17%, and 80.35% over aging periods of 913, 1827, and 3654 days at 12°C. For glass/epoxy composites, the time-shift factor was 67.26, corresponding to tensile strength retention of 78.68%, 74.3%, and 72.42% over 3027, 6054, and 12,107 days, respectively. Again, the relevance of the predicted lifespan of composites was not confirmed by actual aging time.

Thus, in a comparison between the three models, Arrhenius with the linear model and the two non-linear models, it was found that the linear model and the first non-linear model were inadequate for predicting composite lifetime beyond 2 years. In contrast, the second non-linear model provided accurate predictions, converging on realistic values of Y_∞ consistent with experimental results at 22°C over 180 days.

3.2.3 | Time–Temperature Superposition Principle (TTSP)

The time–temperature superposition principle (TTSP) is an empirical method used to predict the long-term behavior of polymeric composite materials under extreme temperatures based on short-term test data. This method is suitable for thermorheologically simple materials, where temperature is used to shift isothermal segments of a response function, such as creep compliance, along the time scale to construct a master curve recorded at a reference temperature T_{ref}. TTSP enables the extension of the time scale beyond the practical limits of conventional testing, providing an accelerated testing methodology [194]. The response function such as creep compliance is expressed by Equation (13).

$$S\left(T_{ref}, t\right) = S\left(T_{elev}, \frac{t}{\alpha_t}\right) \tag{13}$$

Yang et al. [195] applied TTSP to predict the creep behavior of bamboo fiber-reinforced PLA composites using a short-term accelerated creep test and DMA, which enabled testing over a wide temperature range. Creep compliance curves were generated for the duration of the test at different temperatures and were then shifted along the time scale using a shift factor (α_t) derived from TTSP. The determination of this shift factor can be performed using either the Williams–Landel–Ferry (WLF) equation or the Arrhenius equation, depending on the temperature range. The WLF equation is suitable for polymers at temperatures near and above their glass-transition temperature (T_g), typically when tested in the range from T_g to $T_g + 100$°C. Conversely, the Arrhenius equation is used for polymers tested at temperatures below T_g.

In Yang et al.'s study [195], the WLF equation was not appropriate due to the melting behavior of the PLA matrix in the temperature range of 60°C to 160°C. Therefore, the shift factor (α_t) was calculated using the Arrhenius equation (Equation 14):

$$log\,\alpha_T = \frac{E_a}{R}\left(\frac{1}{T} - \frac{1}{T_{ref}}\right) \times \log e \tag{14}$$

where α_T represents the horizontal shift factor, E_a the activation energy of the glass transition relaxation (KJ/mol), T_{ref} represents the reference temperature (K). T_g at different frequencies was determined from the peak of tan δ curves obtained by mean of DMA, whereas E_a was calculated from the slop of ln(f) versus $1/T_g$ according to Equation (15).

$$E_a = -R\frac{d(\ln(f))}{d\left(\frac{1}{T_g}\right)} \tag{15}$$

where f is the frequency (Hz), and T_g is the glass transition temperature. A linear regression was then used to determine E_a. Using the estimated shift factors, the creep compliance master curves of the composites were modeled with the Findley power law (Equation 16).

$$S(t) = S_0^{'} + at^b \tag{16}$$

where $S(t)$ is the time-dependent compliance, (S_0') represents the instantaneous elastic compliance, a and b are material-specific constants, and t represents the elapsed time.

Although TTSP is a useful method, it has some limitations in terms of prediction accuracy, as small variations in shift factors can lead to discrepancies in long-term predictions at room temperature.

In another way, Cui et al. [196] investigated the service life of ethylene propylene diene monomer (EPDM) rubber using accelerated aging tests at temperatures ranging from 70°C to 130°C. The tensile strength was evaluated, and they evidenced the non-Arrhenius behavior of this material by combining Arrhenius and TTSF extrapolations, indicating that the activation energy of the material is not constant across temperature ranges. This highlighted the inadequacy of the Arrhenius equation for predicting the aging of EPDM. To better capture the material's behavior, the Mooney-Rivlin equation was employed to analyze the effects of aging temperature and time on the crosslinking density of the elastomer. This approach allowed for the identification of temperature points where activation energy shifts, providing more accurate insights into the long-term aging process of EPDM.

3.3 | Finite Element Analysis (FEA)

The FEA is one of the main modeling and simulation tools that have been used to predict the multi-physical properties of PFRCs. It can mathematically compute specific properties of the resulting composite material and conduct virtual experiments. However, most of the research focused on predicting the mechanical properties, while few investigated moisture absorption and thermal properties [37, 197–200]. Multiple simulation tools were utilized, such as ABAQUS, COMSOL, ANSYS, and so on. Each of these platforms was suitable for a function. ABAQUS seemed advantageous from what concerns geometry modeling, englobing a wide range of materials, and has reasonable control in meshing [40]. Furthermore, ANSYS has a very flexible workbench and automatic meshing. Its material library consists of reactive material, creep, viscosity, viscoelasticity, elasticity, plasticity, etc. [37]. Indeed, these tools require parameters such as the material properties (elastic modulus, Poisson's ratio), fiber size, volume fraction, mesh size and type as inputs to define a representative volume element (RVE). For the analysis of the multi-physical properties, many theoretical theories were involved. Among them, the rule of mixture (ROM) was used to predict the elastic properties of unidirectional fiber-reinforced composites [201, 202], Halpin and Tsai-based models were mainly used to predict the tensile strength [198, 203]. Hirsch's model promoted the best prediction of Young's modulus. However, Fourier's heat conduction equation was suitable for predicting the thermal behavior of composites, and Fick's law for moisture absorption. Nevertheless, Hashin's model was convenient for predicting damage or failure criteria.

However, to the best of the author's knowledge, there have been only a few studies focusing on predicting the aging behavior of PFRCs because of the complexity of the physicochemical changes encountered during aging in hygro or hydrothermal environments [39, 197, 198, 204]. For instance, Jain et al. [197] investigated the moisture diffusion in agave fiber-reinforced epoxy composites under various hygrothermal conditions. In the pre-processing step, they considered the length of fibers and diameter, which were assumed to be homogeneous and isotropic. However, the Fickian FEA used matched the experimental results perfectly, and the 3D model created in ABAQUS software effectively verified the model.

Regazzi et al. [198] developed a thermo-hygro-mechanical model to describe the evolutionary behavior of short flax fiber-reinforced PLA composite under service conditions using the finite element analysis software COMSOL Multiphysics. This model accounted only for the irreversible mechanisms encountered during hygro or hydrothermal aging, such as swelling and plasticization. The simulated results aligned with experimental data from hydrothermal aging tests conducted at 20°C but deviated from the experimental outcomes at higher temperatures of 35°C and 50°C. The researchers applied the Halpin-Kardos homogenization model to predict the influence of moisture on the local elastic modulus. Figure 17 presents a schematic representation of the model's construction. Moisture diffusion was modeled using a two-stage diffusion process, incorporating the content of free water molecules (n), bound water molecules (N), the probability per unit time of free molecules becoming bound (γ), and the probability per unit time of bound molecules

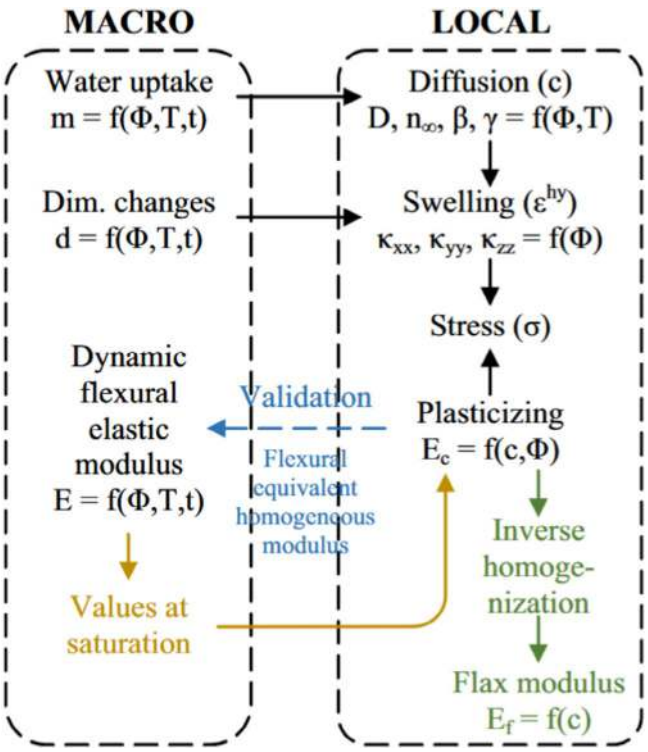

FIGURE 17 | Schematic representation of the model construction in Regazzi et al. [198] work.

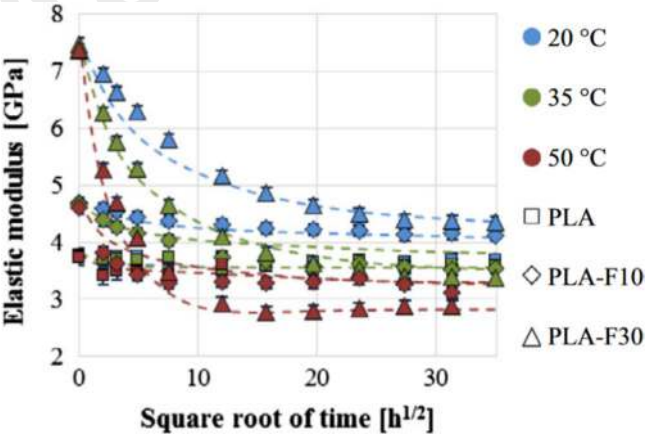

FIGURE 18 | Experimental dynamic elastic modulus (markers) and simulated flexural modulus (dashed lines) of PLA and flax/PLA composites with different fiber content (10wt% and 30wt%) during immersion in water at different temperatures (20°C, 35°C, and 50°C) in Regazzi et al. [198] work.

becoming mobile (β). Swelling was modeled by relating local strain variations to moisture content, with an orthotropic swelling tensor defined by three swelling coefficients (K_{xx}), (K_{yy}), and (K_{zz}), representing swelling along the x, y, and z directions, respectively. Additionally, plasticization was assessed by analyzing the dependency of the local elastic modulus on composites' moisture content. Figure 18 illustrates the predicted results compared with experimental data based on this model.

This type of model showed accuracy in predicting the short-term behavior of PFRCs in service conditions, but as a matter

of fact, there is a need to develop new models that are capable of simulating the behavior of composites even when multiple damages occur. Recently, Gholami et al. [39] developed a finite element model to predict the hygrothermal degradation of composite material properties using ABAQUS software. The approach coupled Python scripts with a FORTRAN-coded UMAT subroutine. Model validation was achieved by comparing results with existing experimental and analytical data. Moisture distribution was predicted using a finite difference solution of Fick's law, considering the temperature-dependent coefficient of diffusion. Changes in elastic and hygrothermal properties across the composite thickness were analyzed based on temperature and humidity effects on the glass-transition temperature. The model studied stress, moisture distribution, and property variations in symmetric cross-ply [0/90/90/0] and asymmetric angle-ply [20/−20/45/−45] laminated composites under transient and steady-state hygrothermal conditions.

3.4 | Artificial Intelligence (AI)

In recent decades, machine learning-based artificial intelligence (AI) methods have emerged as powerful tools for predictive modeling, offering the ability to make decisions without explicit programming. These methods have increasingly been applied to enhance predictive models in the manufacturing and durability analysis of composite materials, especially for complex applications. Among the various AI techniques, neural networks have shown high accuracy in solving non-linear and dynamic problems. Michel and Marcos-Meson [205] applied the neural network for service life prediction of a concrete composite reinforced with synthetic steel fibers. The study demonstrated that the integration of physics-based models with data-driven approaches can optimize and predict the performance of complex physical systems. However, despite their effectiveness, neural networks are often trained with high accuracy on specific datasets (achieving over 99% classification accuracy), yet they remain limited by their inability to incorporate fundamental physical principles such as material history, physical invariance, and conservation laws. These limitations are particularly critical when predicting degradation mechanisms such as fiber degradation or hydrolysis in PFRCs.

Despite these challenges, several studies have utilized artificial neural networks (ANNs) to predict water absorption behavior in PFRCs without considering the evolution of physical properties during aging. For instance, Belaadi et al. [206] predicted the water diffusion behavior in epoxy composites reinforced with different fractions of Washingtonia fibers using the response surface methodology (RSM) and ANN. They refined the numerical model with a genetic algorithm to estimate water uptake, addressing Fick's law behavior. Their approach employed a multilayer perceptron (MLP) with backpropagation, optimizing the hidden layer neurons using the lowest root mean square error (RMSE) and correlation coefficient to enhance accuracy and mitigate overfitting or slow convergence. The dataset was partitioned into 70% for training, 15% for testing, and 15% for validation, ensuring model reliability. Similarly, Saaidia et al. [207] applied ANN models to predict the water absorption behavior of sisal and jute biocomposites, while Ighalo et al. [208] employed ANN modeling to predict water absorption behavior in polystyrene (PS) reinforced by bamboo fibers. Beyond standalone predictive modeling, AI has also been integrated with other analytical techniques to enhance the assessment of aging effects on the multi-physical properties of PFRCS. Drouhet et al. [204] combined AI with micro-computed tomography (micro-CT) to study water-aged and cyclically wet/dried hemp/Elium biocomposites (39.7% ± 1.6% fiber volume fraction). Using the Trainable Weka Segmentation 3D plugin, AI improved composite visualization after the micro-CT scan, enabling damage quantification.

4 | Future Trends and Prospects

PFRCs are increasingly recognized as the materials of the future. They have emerged as versatile materials spanning different industrial applications demanding performance and eco-friendly materials. However, a significant barrier to their broader adoption lies in their durability. Hygro and hydrothermal stress triggers several degradation mechanisms in plant fibers, driven by swelling and shrinkage, plasticization, and leaching of amorphous constituents. When embedded in composite, these mechanisms pose a critical issue and emerge in debonding between fibers and matrix, causing ultimate structural damage and impacting composites' load-bearing capacity.

In response to these challenges, researchers tested various treatments to enhance the adhesion between the hydrophilic plant fibers and the hydrophobic polymers. Among these, alkali treatments [209, 210], the acetylation process [2, 9], coupling agent incorporation [211, 212], coatings [213], and grafting techniques [2, 9], have substantially improved fiber-matrix chemical and physical bonding, dimensional and thermal stability [30, 122], and reduced moisture absorption of composites. Although these treatments could have beneficial effects, suitable use of green solvents or enzymatic treatments speeding biological reactions and targeting components such as lignin, hemicellulose, and pectins is recommended to achieve a reduced usage of chemicals, energy, and water, as well as promoting sustainability and circular tenets [214]. Additionally, recent studies have demonstrated that radiation-based treatments, such as electron beam and gamma irradiation, offer promising alternatives by enhancing fiber-matrix adhesion through radical-induced crosslinking without the need for additional chemicals, thus supporting eco-friendly and scalable industrial applications [215–218].

Plant fibers exhibit variability in their physical properties due to factors such as extraction methods, plant origin, and more. In this context, breakthrough technologies involving genetic transforming techniques could be developed to standardize and optimize these properties, thereby enabling plants with improved fiber output, with capabilities including resistance to UV, temperature, and even antibacterial characteristics [214, 219].

The degradation of PFRCs during aging frequently involves the collapse of the matrix by plasticization and hydrolysis reactions. Neglecting this issue could severely undermine the performance of PFRCs. Additionally, sustainability remains a critical concern. Therefore, relying on bio-based polymers must provide a more sustainable alternative for the development of

PFRCs [214, 215]. Bio-based polymers derived from natural resources are considered a greener substitute for petroleum-based polymers. Indeed, cellulose, starch, and PLA have garnered attention due to the important properties that they can provide to composites [214, 220, 221].

To support the sustainable development and broader adoption of PFRCs, it is essential to integrate life cycle assessment (LCA) with techno-economic analysis (TEA), particularly concerning the end-of-life phase after material aging. These combined approaches allow for a holistic evaluation of long-term performance, energy consumption, environmental impact, and resource use. By assessing how PFRCs degrade over time and the implications for disposal, recycling, or repurposing, LCA and TEA help identify viable end-of-life strategies while ensuring responsible management of natural resources and minimizing environmental burdens [222].

Otherwise, creating high-performance composites that fulfill the needs of the industry and can endure an aggressive operational environment necessitates the advancement of manufacturing technologies tailored to plant fibers, enabling improvement of surface quality, mitigating moisture absorption, and promoting good interfacial adhesion with the polymeric matrices [215]. Differently, integrating nanomaterials such as nanocrystalline cellulose (NCC) [216, 219, 223–226], or graphene-based materials offers exciting potential to strengthen composites, improve fiber/matrix adhesion and adsorption capabilities, promoting their use in emerging technologies including hydrogen storage or transportation [227].

Eventually, the exploration of such applications represents an exciting frontier in PFRC research. Applications in automotive, aerospace, renewable energies, or marine environments [228], and even in health products require composites that are not only resistant to environmental factors but also to more extreme conditions such as radiation, corrosive media, and thermal cycling. Therefore, understanding the influence of these conditions on the multi-physical properties of PFRCs is critical for developing advanced materials meeting the stringent demands of high-performance applications [24, 123, 229, 230].

The recyclability of biocomposites remains a challenge, especially as the hygro and the hydrothermal aging alter fiber and matrix properties, complicating end-of-life processing [222, 231]. Fully bio-based composites offer a sustainable alternative, but effective recycling requires understanding degradation effects on methods like composting and pyrolysis [232]. While these processes enable material recovery, they may also generate toxic byproducts. Thus, further research is needed to optimize recycling strategies that balance environmental impact and sustainability.

Aside from that, looking ahead, developing sophisticated analytical models that simulate the long-term behavior of PFRCs under various environmental stressors is a promising avenue for future research. Such models will enable more precise predictions of composite durability by accounting for factors like moisture diffusion, mechanical fatigue, thermal cycling, and UV exposure. These advancements will provide engineers with the tools needed to design PFRCs that are not only robust but also tailored to specific operational environments [36]. By facilitating the creation of highly durable, high-performance composites, these models will play a pivotal role in securing the confidence of industries in PFRCs, thereby accelerating their transition from niche materials to mainstream industrial applications.

5 | Conclusion

The scope of the current review is to gain new insights into the degradation mechanisms of PFRCs and to shed light on the empirical models used to predict their service life. Exposure to harsh environments may inevitably influence the durability of PFRCs when used in demanding and structural applications. In this context, the multi-physical properties of plant fibers and their reinforced composites in outdoor environments are exhaustively discussed. Herein, the correlation between the microstructural, physicochemical, and mechanical properties of fibers and composites is scrutinized to shed light on their degradation pathways. Consequently, changes in internal structure and crystallinity drive the evolution of the overall properties of plant fibers after being subjected to hygro and hydrothermal aging. Interestingly, the fiber swelling and matrix plasticization reversibly decrease the mechanical properties of PFRCs, leading to significant fiber pull-out and debonding. Microstructural damage is developed in both fibers and matrix when the internal stresses are big enough. More importantly, the leaching of amorphous components at the fiber-matrix interfaces becomes active, resulting in reduced shear strength. In fact, the development of cracks modifies the water vapor diffusion kinetic from Fick to anomalous diffusion. The current paper also discusses the analytical models (i.e., mechanistic models, time–temperature superposition principle...) combined with accelerated aging data, intending to gain an in-depth knowledge of the expected service life of composite materials. Nevertheless, limited attention has been devoted to understanding the influence of low and cryogenic temperatures on the durability of PFRCs. Similarly, research studies into freeze–thaw aging cycles remain limited. This would be of great interest for assessing their potential for aeronautic applications and hydrogen storage. This highlights the need for future research to be directed towards the aforementioned gaps.

Although various research surveys have been carried out on PFRCs, there are still some unsolved technological and scientific questions. This paper highlights the critical need for more targeted research to bridge the different knowledge gaps. As the environmental issues of PFRCs are not the primary focus of this paper, they nevertheless represent crucial dimensions that must be considered. Herein, further research studies are required to explore eco-friendly alternatives to traditional polymers. A thorough understanding of the durability of plant fiber-reinforced bio-resin composites is required. It is therefore of the utmost importance to strike a balance between maintaining long-term durability and promoting eco-sustainability. Consequently, adapting research to the specific requirements of industries must catalyze relevant breakthroughs in material science, addressing other specific challenges in this field.

However, this study highlights the critical need for more targeted research to fill the knowledge gaps identified, particularly concerning the behavior of each plant fiber's constitutive layers when exposed to hygro-and hydrothermal stress, and eventually, there is a need for research investigating the aging of plant-fiber composites in real conditions during years. Indeed, more research needs to focus on developing a model describing the durability of PFRCs, which would consider the different degradation mechanisms faced in particular by PFRCs.

Nomenclature

$\acute{C}$	the modified right Cauchy-Green deformation tensor
C_{∞}	molar concentration of water molecules in the composites
φ_{diff}	chemical energy driving the water diffusion
φ_{mech}	mechanical energy caused by deformation
AI	artificial intelligence
ANN	artificial neural network
D	diffusion coefficient through thickness (mm^2/s)
DFT	density functional theory
DTG	differential thermogravimetric analysis
E'	storage modulus
E_a	activation energy
EP	epoxy
EPDM	ethylene propylene diene monomer
f	frequency
FEA	finite element analysis
FTIR	Fourier-transform infrared spectroscopy
h	initial thickness (mm)
HDPE	high-density polyethylene
HPLC	high-performance liquid chromatography
JF	jute fibers
K_{xx}	the swelling coefficient characterizing swelling in the x direction
K_{zz}	the swelling coefficient characterizing swelling in the y direction
K_{zz}	the swelling coefficient characterizing swelling in the z direction
LCA	life cycle assessment
LCC	lignin carbohydrate complexes
LDPE	low-density polyethylene
MAPP	maleic anhydride grafted polypropylene
MFA	microfibrillar angle
MLP	multilayer perceptron
M_m	maximum moisture uptake
MSE	mean square error
M_t	moisture uptake at time t
n	the content of free water molecules
N	the content of bound water molecules
NCC	nanocrystalline cellulose
OPEFB	oil palm empty fruit bunch
PA	polyamide
PFRC	plant fiber-reinforced composites
PLA	polylactic acid
PP	polypropylene
PS	polystyrene
R	gas constant
RH	relative humidity
RMSE	root mean square error
ROM	rule of mixture
RSM	response surface methodology
RVE	representative volume element
S	composite strength
$S(t)$	time-dependent compliance
S_0	initial composite's strength
S_0'	instantaneous elastic compliance
SEM	scanning electronic microscope
t	aging time
TAPPI	Technical Association of the Paper and Pulp Industry
TBF	twisted bamboo fibers
TEA	techno-economic analysis
T_g	glass-transition temperature
TGA	thermogravimetric analysis
T_{ref}	reference temperature
TSF	time shift factor
TTSP	time–temperature superposition principle
WLF	William–Landel–Ferry
WRV	water retention value
XRD	x-ray diffraction
Y	property retention
α_t	shift factor
β	crack propagation resistance
β	the probability per unit time of bound water molecules becoming mobile
γ	the probability per unit time of free water molecules becoming bound
η	curing degree of composite
θ	external environment corrosion
λ	material and environmental parameter
ν	material parameter
τ	fitted parameter

Author Contributions

Conceptualization: Amine Fourari, Mohamed Ould Moussa, Mouad Chakkour, Ismail Khay, and Tarak Ben Zineb. Methodology: Amine Fourari, Mohamed Ould Moussa, Mouad Chakkour, Ismail Khay, and Tarak Ben Zineb. Data curation: Amine Fourari. Writing original draft: Amine Fourari. Writing review: Mohamed Ould Moussa, Mouad Chakkour, Ismail Khay, and Tarak Ben Zineb. Visualization: Amine Fourari, Mohamed Ould Moussa, Mouad Chakkour, Ismail Khay, and

Tarak Ben Zineb. Supervision: Mohamed Ould Moussa, Ismail Khay, Mouad Chakkour, and Tarak Ben Zineb.

Acknowledgments

The authors acknowledge funding from the International University of Rabat.

Conflicts of Interest

The authors declare no conflicts of interest.

Data Availability Statement

The data that support the findings of this study are available from the corresponding author upon reasonable request.

References

1. I. Elfaleh, F. Abbassi, M. Habibi, et al., "A Comprehensive Review of Natural Fibers and Their Composites: An Eco-Friendly Alternative to Conventional Materials," *Results in Engineering* 19 (2023): 101271, https://doi.org/10.1016/j.rineng.2023.101271.

2. M. Chakkour, M. Ould Moussa, I. Khay, M. Balli, and T. Ben Zineb, "Towards Widespread Properties of Cellulosic Fibers Composites: A Comprehensive Review," *Journal of Reinforced Plastics and Composites* 42, no. 5–6 (2023): 222–263, https://doi.org/10.1177/07316844221112974.

3. T. Cadu, M. Berges, O. Sicot, et al., "What Are the Key Parameters to Produce a High-Grade Bio-Based Composite? Application to Flax/Epoxy UD Laminates Produced by Thermocompression," *Composites Part B: Engineering* 150 (2018): 36–46, https://doi.org/10.1016/j.compositesb.2018.04.059.

4. M. R. Sanjay, P. Madhu, M. Jawaid, P. Senthamaraikannan, S. Senthil, and S. Pradeep, "Characterization and Properties of Natural Fiber Polymer Composites: A Comprehensive Review," *Journal of Cleaner Production* 172 (2018): 566–581, https://doi.org/10.1016/j.jclepro.2017.10.101.

5. Z. N. Azwa, B. F. Yousif, A. C. Manalo, and W. Karunasena, "A Review on the Degradability of Polymeric Composites Based on Natural Fibres," *Materials and Design* 47 (2013): 424–442, https://doi.org/10.1016/j.matdes.2012.11.025.

6. A. Gholampour and T. Ozbakkaloglu, "A Review of Natural Fiber Composites: Properties, Modification and Processing Techniques, Characterization, Applications," *Journal of Materials Science* 55, no. 3 (2020): 829–892, https://doi.org/10.1007/s10853-019-03990-y.

7. A. Stamboulis, C. A. Baillie, and T. Peijs, "Effects of Environmental Conditions on Mechanical and Physical Properties of Flax Fibers," *Composites Part A, Applied Science and Manufacturing* 32, no. 8 (2001): 1105–1115, https://doi.org/10.1016/S1359-835X(01)00032-X.

8. A. Bourmaud, D. U. Shah, J. Beaugrand, and H. N. Dhakal, "Property Changes in Plant Fibres During the Processing of Bio-Based Composites," *Industrial Crops and Products* 154 (2020): 112705, https://doi.org/10.1016/j.indcrop.2020.112705.

9. M. Li, Y. Pu, V. M. Thomas, et al., "Recent Advancements of Plant-Based Natural Fiber–Reinforced Composites and Their Applications," *Composites Part B: Engineering* 200 (2020): 108254, https://doi.org/10.1016/j.compositesb.2020.108254.

10. W. Garat, N. Le Moigne, S. Corn, J. Beaugrand, and A. Bergeret, "Swelling of Natural Fibre Bundles Under Hygro- and Hydrothermal Conditions: Determination of Hydric Expansion Coefficients by Automated Laser Scanning," *Composites Part A: Applied Science and Manufacturing* 131 (2020): 105803, https://doi.org/10.1016/j.compositesa.2020.105803.

11. M. Chakkour, M. O. Moussa, I. Khay, M. Balli, and T. Ben Zineb, "Hygroscopic Aging Cycles of Bamboo Fiber/Epoxy Composites: Comparative Study Between Distilled Water and Sea Water," *Industrial Crops and Products* 209 (2024): 117957, https://doi.org/10.1016/j.indcrop.2023.117957.

12. C. Baley, A. Le Duigou, A. Bourmaud, and P. Davies, "Influence of Drying on the Mechanical Behaviour of Flax Fibres and Their Unidirectional Composites," *Composites Part A: Applied Science and Manufacturing* 43, no. 8 (2012): 1226–1233, https://doi.org/10.1016/j.compositesa.2012.03.005.

13. A. Le Duigou, A. Bourmaud, and C. Baley, "In-Situ Evaluation of Flax Fibre Degradation During Water Ageing," *Industrial Crops and Products* 70 (2015): 204–210, https://doi.org/10.1016/j.indcrop.2015.03.049.

14. A. Bourmaud, C. Morvan, A. Bouali, V. Placet, P. Perré, and C. Baley, "Relationships Between Micro-Fibrillar Angle, Mechanical Properties and Biochemical Composition of Flax Fibers," *Industrial Crops and Products* 44 (2013): 343–351, https://doi.org/10.1016/j.indcrop.2012.11.031.

15. J. Cui, L. Mi, L. Li, et al., "Stepwise Failure Behavior of Thermal-Treated Bamboo Under Uniaxial Tensile Load," *Industrial Crops and Products* 204 (2023): 117313, https://doi.org/10.1016/j.indcrop.2023.117313.

16. T. Cadu, L. Van Schoors, O. Sicot, S. Moscardelli, L. Divet, and S. Fontaine, "Cyclic Hygrothermal Ageing of Flax Fibers' Bundles and Unidirectional Flax/Epoxy Composite. Are Bio-Based Reinforced Composites So Sensitive?," *Industrial Crops and Products* 141 (2019): 111730, https://doi.org/10.1016/j.indcrop.2019.111730.

17. A. Thuault, S. Eve, D. Blond, J. Bréard, and M. Gomina, "Effects of the Hygrothermal Environment on the Mechanical Properties of Flax Fibres," *Journal of Composite Materials* 48, no. 14 (2014): 1699–1707, https://doi.org/10.1177/0021998313490217.

18. H. Elmoudnia, P. Faria, R. Jalal, M. Waqif, and L. Saadi, "Effectiveness of Alkaline and Hydrothermal Treatments on Cellulosic Fibers Extracted From the Moroccan *Pennisetum alopecuroides* Plant: Chemical and Morphological Characterization," *Carbohydrate Polymer Technologies and Applications* 5 (2023): 100276, https://doi.org/10.1016/j.carpta.2022.100276.

19. R. Crespo Gutiérrez, M. T. Uribe, and H. P. Wilson, "Hygrothermal Treatment of Tepa (*Laureliopsis philippiana* Looser) Fibers: Effects on Chemical and Physical Properties," *Drvna Industrija* 71, no. 1 (2020): 69–77, https://doi.org/10.5552/drvind.2020.1905.

20. E. H. Saidane, D. Scida, and R. Ayad, "Thermo-Mechanical Behaviour of Flax/Green Epoxy Composites: Evaluation of Thermal Expansion Coefficients and Application to Internal Stress Calculation," *Industrial Crops and Products* 170 (2021): 113786, https://doi.org/10.1016/j.indcrop.2021.113786.

21. K. L. Pickering, M. G. A. Efendy, and T. M. Le, "A Review of Recent Developments in Natural Fibre Composites and Their Mechanical Performance," *Composites Part A: Applied Science and Manufacturing* 83 (2016): 98–112, https://doi.org/10.1016/j.compositesa.2015.08.038.

22. A. Joseph, V. Mahesh, V. Mahesh, D. Harursampath, and M. A. R. Loja, "Effects of Hygrothermal Aging on the Mechanical Properties of the Biocomposites," in *Aging Effects on Natural Fiber-Reinforced Polymer Composites: Durability and Life Prediction*, ed. C. Muthukumar, S. Krishnasamy, S. M. K. Thiagamani, and S. Siengchin (Springer Nature, 2022), 63–83, https://doi.org/10.1007/978-981-16-8360-2_5.

23. D. U. Shah, P. J. Schubel, and M. J. Clifford, "Can Flax Replace E-Glass in Structural Composites? A Small Wind Turbine Blade Case Study," *Composites Part B: Engineering* 52 (2013): 172–181, https://doi.org/10.1016/j.compositesb.2013.04.027.

24. A. Moudood, A. Rahman, H. M. Khanlou, W. Hall, A. Öchsner, and G. Francucci, "Environmental Effects on the Durability and the Mechanical Performance of Flax Fiber/Bio-Epoxy Composites," *Composites Part B: Engineering* 171 (2019): 284–293, https://doi.org/10.1016/j.compositesb.2019.05.032.

25. P. Aceti, L. Carminati, P. Bettini, and G. Sala, "Hygrothermal Ageing of Composite Structures. Part 1: Technical Review," *Composite Structures* 319 (2023): 117076, https://doi.org/10.1016/j.compstruct.2023.117076.

26. M. Cai, X. Zhang, B. Sun, H. Takagi, G. I. N. Waterhouse, and Y. Li, "Durable Mechanical Properties of Unidirectional Flax Fiber/Phenolic Composites Under Hydrothermal Aging," *Composites Science and Technology* 220 (2022): 109264, https://doi.org/10.1016/j.compscitech.2022.109264.

27. Y. Li and B. Xue, "Hydrothermal Ageing Mechanisms of Unidirectional Flax Fabric Reinforced Epoxy Composites," *Polymer Degradation and Stability* 126 (2016): 144–158, https://doi.org/10.1016/j.polymdegradstab.2016.02.004.

28. J. Shi, S. Yuan, W. Zhang, J. Zhang, and H. Chen, "Hydrothermal Aging Mechanisms and Service Life Prediction of Twisted Bamboo Fiber Wound Composites," *Materials & Design* 227 (2023): 111716, https://doi.org/10.1016/j.matdes.2023.111716.

29. N. Jiang, T. Yu, Y. Li, T. J. Pirzada, and T. J. Marrow, "Hygrothermal Aging and Structural Damage of a Jute/Poly (Lactic Acid) (PLA) Composite Observed by X-Ray Tomography," *Composites Science and Technology* 173 (2019): 15–23, https://doi.org/10.1016/j.compscitech.2019.01.018.

30. O. Gil-Castell, J. D. Badia, T. Kittikorn, et al., "Impact of Hydrothermal Ageing on the Thermal Stability, Morphology and Viscoelastic Performance of PLA/Sisal Biocomposites," *Polymer Degradation and Stability* 132 (2016): 87–96, https://doi.org/10.1016/j.polymdegradstab.2016.03.038.

31. G. Ma, L. Yan, W. Shen, D. Zhu, L. Huang, and B. Kasal, "Effects of Water, Alkali Solution and Temperature Ageing on Water Absorption, Morphology and Mechanical Properties of Natural FRP Composites: Plant-Based Jute vs. Mineral-Based Basalt," *Composites Part B: Engineering* 153 (2018): 398–412, https://doi.org/10.1016/j.compositesb.2018.09.015.

32. G. Xian, P. Yin, I. Kafodya, H. Li, and W. Wang, "Durability Study of Ramie Fiber Fabric Reinforced Phenolic Plates Under Humidity Conditions," *Science and Engineering of Composite Materials* 23, no. 1 (2016): 45–52, https://doi.org/10.1515/secm-2014-0018.

33. C. Muthukumar, S. Krishnasamy, S. M. K. Thiagamani, and S. Siengchin, eds., *Aging Effects on Natural Fiber-Reinforced Polymer Composites: Durability and Life Prediction* (Springer Nature, 2022), https://doi.org/10.1007/978-981-16-8360-2.

34. P. Marru, V. Latane, C. Puja, K. Vikas, P. Kumar, and S. Neogi, "Lifetime Estimation of Glass Reinforced Epoxy Pipes in Acidic and Alkaline Environment Using Accelerated Test Methodology," *Fibers and Polymers* 15, no. 9 (2014): 1935–1940, https://doi.org/10.1007/s12221-014-1935-8.

35. J. Zhou, X. Chen, and S. Chen, "Durability and Service Life Prediction of GFRP Bars Embedded in Concrete Under Acid Environment," *Nuclear Engineering and Design* 241, no. 10 (2011): 4095–4102, https://doi.org/10.1016/j.nucengdes.2011.08.038.

36. P. Ghabezi and N. M. Harrison, "Multi-Scale Modelling and Life Prediction of Aged Composite Materials in Salt Water," *Journal of Reinforced Plastics and Composites* 43, no. 3–4 (2024): 205–219, https://doi.org/10.1177/07316844231160189.

37. M. Alhijazi, Q. Zeeshan, Z. Qin, B. Safaei, and M. Asmael, "Finite Element Analysis of Natural Fibers Composites: A Review," *Nanotechnology Reviews* 9, no. 1 (2020): 853–875, https://doi.org/10.1515/ntrev-2020-0069.

38. F. Tian, Z. Zhong, and Y. Pan, "Modeling of Natural Fiber Reinforced Composites Under Hygrothermal Ageing," *Composite Structures* 200 (2018): 144–152, https://doi.org/10.1016/j.compstruct.2018.05.083.

39. M. Gholami, H. Afrasiab, A. M. Baghestani, and A. Fathi, "A Novel Multiscale Parallel Finite Element Method for the Study of the Hygrothermal Aging Effect on the Composite Materials," *Composites Science and Technology* 217 (2022): 109120, https://doi.org/10.1016/j.compscitech.2021.109120.

40. M. Cai, Y. Guo, L. Wang, Q. Ma, B. Sun, and G. I. N. Waterhouse, "Recent Advances in Hygrothermal Aging of Plant Fiber Reinforced Composites," *Applied Composite Materials* (2024), https://doi.org/10.1007/s10443-024-10275-4.

41. S. Ajouguim, K. Abdelouahdi, M. Waqif, M. Stefanidou, and L. Saâdi, "Modifications of Alfa Fibers by Alkali and Hydrothermal Treatment," *Cellulose* 26, no. 3 (2019): 1503–1516, https://doi.org/10.1007/s10570-018-2181-9.

42. J. Cui, D. Fu, L. Mi, et al., "Effects of Thermal Treatment on the Mechanical Properties of Bamboo Fiber Bundles," *Materials* 16, no. 3 (2023): 1239, https://doi.org/10.3390/ma16031239.

43. J. Wu, T. Zhong, W. Zhang, J. Shi, B. Fei, and H. Chen, "Comparison of Colors, Microstructure, Chemical Composition and Thermal Properties of Bamboo Fibers and Parenchyma Cells With Heat Treatment," *Journal of Wood Science* 67, no. 1 (2021): 56, https://doi.org/10.1186/s10086-021-01988-2.

44. H. Yun, K. Li, D. Tu, and C. Hu, "Effect of Heat Treatment on Bamboo Fiber Morphology Crystallinity and Mechanical Properties," *Wood Research* 61, no. 2 (2016): 227–234.

45. A. Azadeh, K. Ghavami, and J. J. García, "The Influence of Heat on Mechanical Properties of *Dendrocalamus giganteus* Bamboo," *Journal of Building Engineering* 43 (2021): 102613, https://doi.org/10.1016/j.jobe.2021.102613.

46. M. Bao, S. Zhao, R. Tang, et al., "Effect of Hygro-Mechanical Treatment Combined With Saturated Steam on Bamboo Cell Wall: Structural, Chemical, and Hygroscopic Properties," *Industrial Crops and Products* 219 (2024): 119085, https://doi.org/10.1016/j.indcrop.2024.119085.

47. J. Yin, T. Yuan, Y. Lu, et al., "Effect of Compression Combined With Steam Treatment on the Porosity, Chemical Compositon and Cellulose Crystalline Structure of Wood Cell Walls," *Carbohydrate Polymers* 155 (2017): 163–172, https://doi.org/10.1016/j.carbpol.2016.08.013.

48. E. K. Ezugwu, J. Calabria-Holley, and K. Paine, "Physico-Mechanical and Morphological Behavior of Hydrothermally Treated Plant Fibers in Cementitious Composites," *Industrial Crops and Products* 200 (2023): 116832, https://doi.org/10.1016/j.indcrop.2023.116832.

49. Y. Zouaoui, F. Benmahiddine, A. Yahia, and R. Belarbi, "Hygrothermal and Mechanical Behaviors of Fiber Mortar: Comparative Study Between Palm and Hemp Fibers," *Energies* 14, no. 21 (2021): 7110, https://doi.org/10.3390/en14217110.

50. H. Dhakal, Z. Zhang, and M. Richardson, "Effect of Water Absorption on the Mechanical Properties of Hemp Fibre Reinforced Unsaturated Polyester Composites," *Composites Science and Technology* 67, no. 7–8 (2007): 1674–1683, https://doi.org/10.1016/j.compscitech.2006.06.019.

51. P. P. Das and V. Chaudhary, "Environmental Impact and Effect of Chemical Treatment on Bio Fiber Based Polymer Composites," *Materials Today Proceedings* 49 (2022): 3418–3422, https://doi.org/10.1016/j.matpr.2021.03.097.

52. L. Toubal, C. J. Cuillière, K. Bensalem, V. Francois, and P. B. Gning, "Hygrothermal Effect on Moisture Kinetics and Mechanical Properties of Hemp/Polypropylene Composite: Experimental and Numerical Studies," *Polymer Composites* 37, no. 8 (2016): 2342–2352, https://doi.org/10.1002/pc.23414.

53. Q. C. P. Bourgogne, M. Abida, O. Perroud, and V. Bouchart, "Influence of Different Long and Short Ageing Protocols on the Mechanical Behaviour and Damage Mechanisms of a Hemp Fibre Reinforced Polypropylene," *Next Materials* 4 (2024): 100096, https://doi.org/10.1016/j.nxmate.2023.100096.

54. C. Gourier, A. L. Duigou, A. Bourmaud, and C. Baley, "Mechanical Analysis of Elementary Flax Fibre Tensile Properties After Different Thermal Cycles," *Composites Part A: Applied Science and Manufacturing* 64 (2014): 159–166, https://doi.org/10.1016/j.compositesa.2014.05.006.

55. A. Langhorst, M. Ravandi, D. Mielewski, and M. Banu, "Technical Agave Fiber Tensile Performance: The Effects of Fiber Heat-Treatment," *Industrial Crops and Products* 171 (2021): 113832, https://doi.org/10.1016/j.indcrop.2021.113832.

56. A. Langhorst, W. Paxton, S. Bollin, et al., "Heat-Treated Blue Agave Fiber Composites," *Composites Part B: Engineering* 165 (2019): 712–724, https://doi.org/10.1016/j.compositesb.2019.02.035.

57. Y. Pathan and V. K. Gb, "Potential of *Agave angustifolia* Marginata for Composite and Textile Applications—A New Source of Natural Fibre," *Industrial Crops and Products* 203 (2023): 117213, https://doi.org/10.1016/j.indcrop.2023.117213.

58. A. Gutierrez, I. M. Rodrıguez, and J. C. del Río, "Chemical Composition of Lipophilic Extractives From Sisal (*Agave sisalana*) Fibers," *Industrial Crops and Products* 28, no. 1 (2008): 81–87, https://doi.org/10.1016/j.indcrop.2008.01.008.

59. S. R. Ferreira, L. E. Silva, Z. McCaffrey, C. Ballschmiede, and E. Koenders, "Effect of Elevated Temperature on Sisal Fibers Degradation and Its Interface to Cement Based Systems," *Construction and Building Materials* 272 (2021): 121613, https://doi.org/10.1016/j.conbuildmat.2020.121613.

60. F. P. Teixeira, O. D. F. M. Gomes, and F. D. A. Silva, "Degradation Mechanisms of Curaua, Hemp, and Sisal Fibers Exposed to Elevated Temperatures," *BioRes* 14, no. 1 (2019): 1494–1511, https://doi.org/10.15376/biores.14.1.1494-1511.

61. S. R. Ferreira, P. R. L. Lima, F. A. Silva, and R. D. Toledo Filho, "Effect of Sisal Fiber Hornification on the Fiber-Matrix Bonding Characteristics and Bending Behavior of Cement Based Composites," *Key Engineering Materials* 600 (2014): 421–432, https://doi.org/10.4028/www.scientific.net/KEM.600.421.

62. D. Ariawan, M. S. Salim, R. M. Taib, M. Z. A. Thirmizir, and Z. A. M. Ishak, "Interfacial Characterisation and Mechanical Properties of Heat Treated Non-Woven Kenaf Fibre and Its Reinforced Composites," *Composite Interfaces* 25, no. 2 (2018): 187–203, https://doi.org/10.1080/09276440.2017.1354562.

63. Y. Cao, S. Sakamoto, and K. Goda, "Effects of Heat and Alkali Treatments on Mechanical Properties of Kenaf Fibers," in *16th International Conference on Composite Materials* (2007).

64. I. Tharazi, F. A. Abdul Azam, N. Muhamad, D. Hui, A. B. Sulong, and M. Gaff, "Effect of Fiber Orientation and Elevated Temperature on the Mechanical Properties of Unidirectional Continuous Kenaf Reinforced PLA Composites," *Reviews on Advanced Materials Science* 62, no. 1 (2023): 20220275, https://doi.org/10.1515/rams-2022-0275.

65. P. T. D. L. Carada, T. Fujii, and K. Okubo, "Effects of Heat Treatment on the Mechanical Properties of Kenaf Fiber," *AIP Conference Proceedings* 1736 (2016): 020029, https://doi.org/10.1063/1.4949604.

66. A. Solikhin, Y. S. Hadi, M. Y. Massijaya, and S. Nikmatin, "Morphological and Chemo-Thermal Changes of Oven-Heat Treated Oil Palm Empty Fruit Bunch Fibers During Dry Disk Milling," *Journal of the Indian Academy of Wood Science* 14, no. 1 (2017): 9–17, https://doi.org/10.1007/s13196-016-0182-6.

67. A. Solikhin, Y. S. Hadi, M. Y. Massijaya, and S. Nikmatin, "Basic Properties of Oven-Heat Treated Oil Palm Empty Fruit Bunch Stalk Fibers," *BioResources* 11, no. 1 (2016): 2224–2237, https://doi.org/10.15376/biores.11.1.2224-2237.

68. E. Kamal Bahrin, A. Samsu Baharuddin, M. F. Ibrahim, et al., "Physicochemical Property Changes and Enzymatic Hydrolysis Enhancement of Oil Palm Empty Fruit Bunches Treated With Superheated Steam," *BioResources* 7, no. 2 (2012): 1784–1801, https://doi.org/10.15376/biores.7.2.1784-1801.

69. M. Rahim, O. Douzane, A. D. Tran Le, et al., "Characterization of Flax Lime and Hemp Lime Concretes: Hygric Properties and Moisture Buffer Capacity," *Energy and Buildings* 88 (2015): 91–99, https://doi.org/10.1016/j.enbuild.2014.11.043.

70. A. Célino, S. Fréour, F. Jacquemin, and P. Casari, "The Hygroscopic Behavior of Plant Fibers: A Review," *Frontiers in Chemistry* 1 (2013): 43, https://doi.org/10.3389/fchem.2013.00043.

71. A. Célino, S. Fréour, F. Jacquemin, and P. Casari, "Characterization and Modeling of the Moisture Diffusion Behavior of Natural Fibers," *Journal of Applied Polymer Science* 130, no. 1 (2013): 297–306, https://doi.org/10.1002/app.39148.

72. Y. Jiang, M. Lawrence, A. Hussain, M. Ansell, and P. Walker, "Comparative Moisture and Heat Sorption Properties of Fibre and Shiv Derived From Hemp and Flax," *Cellulose* 26, no. 2 (2019): 823–843, https://doi.org/10.1007/s10570-018-2145-0.

73. T. Joffre, P. Isaksson, P. J. J. Dumont, et al., "A Method to Measure Moisture Induced Swelling Properties of a Single Wood Cell," *Experimental Mechanics* 56, no. 5 (2016): 723–733, https://doi.org/10.1007/s11340-015-0119-9.

74. K. S. Salem, N. K. Kasera, M. A. Rahman, et al., "Comparison and Assessment of Methods for Cellulose Crystallinity Determination," *Chemical Society Reviews* 52, no. 18 (2023): 6417–6446, https://doi.org/10.1039/D2CS00569G.

75. İ. Uzun, "Methods of Determining the Degree of Crystallinity of Polymers With X-Ray Diffraction: A Review," *Journal of Polymer Research* 30, no. 10 (2023): 394, https://doi.org/10.1007/s10965-023-03744-0.

76. P. Zugenmaier, *Crystalline Cellulose and Cellulose Derivatives: Characterization and Structures* (Springer, 2008).

77. L. Segal, J. J. Creely, A. E. Martin, and C. M. Conrad, "An Empirical Method for Estimating the Degree of Crystallinity of Native Cellulose Using the X-Ray Diffractometer," *Textile Research Journal* 29, no. 10 (1959): 786–794, https://doi.org/10.1177/004051755902901003.

78. E. Guillou, L. Dumazert, C. Caër, et al., "In-Situ Monitoring of Changes in Ultrastructure and Mechanical Properties of Flax Cell Walls During Controlled Heat Treatment," *Carbohydrate Polymers* 321 (2023): 121253, https://doi.org/10.1016/j.carbpol.2023.121253.

79. F. L. Dri, S. Shang, L. G. Hector, et al., "Anisotropy and Temperature Dependence of Structural, Thermodynamic, and Elastic Properties of Crystalline Cellulose Iβ: A First-Principles Investigation," *Modelling and Simulation in Materials Science and Engineering* 22, no. 8 (2014): 085012, https://doi.org/10.1088/0965-0393/22/8/085012.

80. M. Wada, R. Hori, U. J. Kim, and S. Sasaki, "X-Ray Diffraction Study on the Thermal Expansion Behavior of Cellulose Iβ and Its High-Temperature Phase," *Polymer Degradation and Stability* 95, no. 8 (2010): 1330–1334, https://doi.org/10.1016/j.polymdegradstab.2010.01.034.

81. T. C. Yang, Y. H. Yang, and C. H. Yeh, "Thermal Decomposition Behavior of Thin Makino Bamboo (*Phyllostachys makinoi*) Slivers Under Nitrogen Atmosphere," *Materials Today Communications* 26 (2021): 102054, https://doi.org/10.1016/j.mtcomm.2021.102054.

82. K. E. Okon, F. Lin, Y. Chen, and B. Huang, "Effect of Silicone Oil Heat Treatment on the Chemical Composition, Cellulose Crystalline Structure and Contact Angle of Chinese Parasol Wood," *Carbohydrate Polymers* 164 (2017): 179–185, https://doi.org/10.1016/j.carbpol.2017.01.076.

83. W. Zhu, Y. Yao, Y. Zhang, et al., "Preparation of an Amine-Modified Cellulose Nanocrystal Aerogel by Chemical Vapor Deposition and Its Application in CO_2 Capture," *Industrial and Engineering Chemistry Research* 59, no. 38 (2020): 16660–16668, https://doi.org/10.1021/acs.iecr.0c02687.

84. M. Z. Rong, M. Q. Zhang, Y. Liu, G. C. Yang, and H. M. Zeng, "The Effect of Fiber Treatment on the Mechanical Properties of Unidirectional Sisal-Reinforced Epoxy Composites," *Composites Science and Technology* 61, no. 10 (2001): 1437–1447, https://doi.org/10.1016/S0266-3538(01)00046-X.

85. M. Akgül, E. Gümüşkaya, and S. Korkut, "Crystalline Structure of Heat-Treated Scots Pine [*Pinus sylvestris* L.] and Uludağ Fir [*Abies nordmanniana* (Stev.) Subsp. *bornmuelleriana* (Mattf.)] Wood," *Wood Science and Technology* 41, no. 3 (2007): 281, https://doi.org/10.1007/s00226-006-0110-9.

86. M. Wada, J. Sugiyama, and T. Okano, "Native Celluloses on the Basis of Two Crystalline Phase (Iα/Iβ) System," *Journal of Applied Polymer Science* 49, no. 8 (1993): 1491–1496, https://doi.org/10.1002/app.1993.070490817.

87. A. Bourmaud, J. Beaugrand, D. U. Shah, V. Placet, and C. Baley, "Towards the Design of High-Performance Plant Fibre Composites," *Progress in Materials Science* 97 (2018): 347–408, https://doi.org/10.1016/j.pmatsci.2018.05.005.

88. S. Garriba and S. H. Jailani, "Extraction and Characterization of Natural Cellulosic Fiber From *Mariscus ligularis* Plant as Potential Reinforcement in Composites," *International Journal of Biological Macromolecules* 253 (2023): 127609, https://doi.org/10.1016/j.ijbiomac.2023.127609.

89. E. Terpáková, L. Kidalová, A. Eštoková, J. Čigášová, and N. Števulová, "Chemical Modification of Hemp Shives and Their Characterization," *Procedia Engineering* 42 (2012): 931–941, https://doi.org/10.1016/j.proeng.2012.07.486.

90. Q. Lin, Y. Huang, and W. Yu, "An In-Depth Study of Molecular and Supramolecular Structures of Bamboo Cellulose Upon Heat Treatment," *Carbohydrate Polymers* 241 (2020): 116412, https://doi.org/10.1016/j.carbpol.2020.116412.

91. A. Bezazi, A. Belaadi, M. Bourchak, F. Scarpa, and K. Boba, "Novel Extraction Techniques, Chemical and Mechanical Characterisation of *Agave americana* L," *Natural Fibres. Part B* 66 (2014): 194–203, https://doi.org/10.1016/j.compositesb.2014.05.014.

92. K. S. Prado and M. A. S. Spinacé, "Isolation and Characterization of Cellulose Nanocrystals From Pineapple Crown Waste and Their Potential Uses," *International Journal of Biological Macromolecules* 122 (2019): 410–416, https://doi.org/10.1016/j.ijbiomac.2018.10.187.

93. X. Piao, M. Xie, X. Duan, C. Jin, and Z. Wang, "Novel High-Performance Bamboo Modification Through Nature Rosin-Based Benzoxazine," *Construction and Building Materials* 319 (2022): 126123, https://doi.org/10.1016/j.conbuildmat.2021.126123.

94. R. Javier-Astete, J. Jimenez-Davalos, and G. Zolla, "Determination of Hemicellulose, Cellulose, Holocellulose and Lignin Content Using FTIR in *Calycophyllum spruceanum* (Benth.) K. Schum. and *Guazuma crinita* Lam," *PLoS One* 16, no. 10 (2021): e0256559, https://doi.org/10.1371/journal.pone.0256559.

95. N. H. Sari, E. Syafri, Suteja, et al., "Evaluation of Moisture Content, Chemical, and Functional Groups of *Paederia foetida* Fibers: Effects of Time Soaking in Chemical Solutions," in *Proceedings of the First Mandalika International Multi-Conference on Science and Engineering 2022, MIMSE 2022 (Mechanical and Electrical)*, ed. S. Sugiman, Y. P. Asmara, P. K. Ray, and A. T. Wijayanta (Atlantis Press International BV, 2023), 299–307, https://doi.org/10.2991/978-94-6463-078-7_28.

96. C. H. Lee, T. H. Yang, Y. W. Cheng, and C. J. Lee, "Effects of Thermal Modification on the Surface and Chemical Properties of Moso Bamboo," *Construction and Building Materials* 178 (2018): 59–71, https://doi.org/10.1016/j.conbuildmat.2018.05.099.

97. S. R. Ferreira, F. d. A. Silva, P. R. L. Lima, and R. D. T. Filho, "Effect of Fiber Treatments on the Sisal Fiber Properties and Fiber–Matrix Bond in Cement Based Systems," *Construction and Building Materials* 101 (2015): 730–740, https://doi.org/10.1016/j.conbuildmat.2015.10.120.

98. Y. Zhang, Y. Yu, Y. Lu, W. Yu, and S. Wang, "Effects of Heat Treatment on Surface Physicochemical Properties and Sorption Behavior of Bamboo (*Phyllostachys edulis*)," *Construction and Building Materials* 282 (2021): 122683, https://doi.org/10.1016/j.conbuildmat.2021.122683.

99. X. Yin, A. Huang, S. Zhang, R. Liu, and F. Ma, "Identification of Three Dalbergia Species Based on Differences in Extractive Components," *Molecules* 23, no. 9 (2018): 2163, https://doi.org/10.3390/molecules23092163.

100. Y. Huang, F. Meng, R. Liu, Y. Yu, and W. Yu, "Morphology and Supramolecular Structure Characterization of Cellulose Isolated From Heat-Treated Moso Bamboo," *Cellulose* 26, no. 12 (2019): 7067–7078, https://doi.org/10.1007/s10570-019-02614-7.

101. S. Youssefian and N. Rahbar, "Molecular Origin of Strength and Stiffness in Bamboo Fibrils," *Scientific Reports* 5, no. 1 (2015): 11116, https://doi.org/10.1038/srep11116.

102. M. Oliveira, F. Da Luz, F. Da Costa Garcia Filho, et al., "Dynamic Mechanical Analysis of Thermally Aged Fique Fabric-Reinforced Epoxy Composites," *Polymers* 13, no. 22 (2021): 4037, https://doi.org/10.3390/polym13224037.

103. M. Hughes, "Defects in Natural Fibres: Their Origin, Characteristics and Implications for Natural Fibre-Reinforced Composites," *Journal of Materials Science* 47, no. 2 (2012): 599–609, https://doi.org/10.1007/s10853-011-6025-3.

104. W. Garat, S. Corn, N. Moigne, J. Beaugrand, P. Ienny, and A. Bergeret, "Dimensional Variations and Mechanical Behavior of Various Plant Fibre Species Under Controlled Hydro/Hygrothermal Conditions," *RCMA* 29, no. 5 (2019): 299–304, https://doi.org/10.18280/rcma.290504.

105. E. Huguet, S. Corn, N. L. Moigne, and P. Ienny, "Mechanical Behavior of Flax Fibers During Cyclic Tensile Tests in a Controlled Humid Environment," in *Twenty-Third International Conference on Composite Materials (ICCM23)* (2023).

106. V. Placet, O. Cisse, and M. L. Boubakar, "Influence of Environmental Relative Humidity on the Tensile and Rotational Behaviour of Hemp Fibres," *Journal of Materials Science* 47, no. 7 (2012): 3435–3446, https://doi.org/10.1007/s10853-011-6191-3.

107. V. Guicheret-Retel, O. Cisse, V. Placet, J. Beaugrand, M. Pernes, and M. L. Boubakar, "Creep Behaviour of Single Hemp Fibres. Part II: Influence of Loading Level, Moisture Content and Moisture Variation," *Journal of Materials Science* 50, no. 5 (2015): 2061–2072, https://doi.org/10.1007/s10853-014-8768-0.

108. I. Burgert, "Exploring the Micromechanical Design of Plant Cell Walls," *American Journal of Botany* 93, no. 10 (2006): 1391–1401, https://doi.org/10.3732/ajb.93.10.1391.

109. V. Placet, O. Cissé, and M. Lamine Boubakar, "Nonlinear Tensile Behaviour of Elementary Hemp Fibres. Part I: Investigation of the Possible Origins Using Repeated Progressive Loading With In Situ Microscopic Observations," *Composites Part A: Applied Science and Manufacturing* 56 (2014): 319–327, https://doi.org/10.1016/j.compositesa.2012.11.019.

110. V. Placet, J. Passard, and P. Perré, "Viscoelastic Properties of Wood Across the Grain Measured Under Water-Saturated Conditions up to 135°C: Evidence of Thermal Degradation," *Journal of Materials Science* 43, no. 9 (2008): 3210–3217, https://doi.org/10.1007/s10853-008-2546-9.

111. B. van Voorn, H. H. G. Smit, R. J. Sinke, and B. de Klerk, "Natural Fibre Reinforced Sheet Moulding Compound," *Composites Part A, Applied Science and Manufacturing* 32, no. 9 (2001): 1271–1279, https://doi.org/10.1016/S1359-835X(01)00085-9.

112. G. C. Davies and D. M. Bruce, "Effect of Environmental Relative Humidity and Damage on the Tensile Properties of Flax and Nettle Fibers," *Textile Research Journal* 68, no. 9 (1998): 623–629, https://doi.org/10.1177/004051759806800901.

113. L. Salmin, "Viscoelastic Properties of In Situ Lignin Under Water-Saturated Conditions," *Journal of Materials Science* 19 (1984): 3090–3096, https://doi.org/10.1007/BF01026988.

114. A. Ebringerová, Z. Hromádková, and T. Heinze, "Hemicellulose," in *Polysaccharides I. Advances in Polymer Science*, vol. 186, ed. T. Heinze (Springer-Verlag, 2005), 1–67, https://doi.org/10.1007/b136816.

115. I. M. AI-Ruqaie, S. Kasapis, R. K. Richardson, and G. Mitchell, "The Glass Transition Zone in High Solids Pectin and Gellan Preparations," *Polymer* 38, no. 22 (1997): 5685–5694, https://doi.org/10.1016/S0032-3861(97)00119-5.

116. S. Basu, U. S. Shivhare, and S. Muley, "Moisture Adsorption Isotherms and Glass Transition Temperature of Pectin," *Journal of Food Science and Technology* 50, no. 3 (2013): 585–589, https://doi.org/10.1007/s13197-011-0327-y.

117. A. Tejado and T. G. M. Van De Ven, "Why Does Paper Get Stronger as It Dries?," *Materials Today* 13, no. 9 (2010): 42–49, https://doi.org/10.1016/S1369-7021(10)70164-4.

118. M. N. K. Chowdhury, M. D. H. Beg, M. R. Khan, and M. F. Mina, "Modification of Oil Palm Empty Fruit Bunch Fibers by Nanoparticle Impregnation and Alkali Treatment," *Cellulose* 20, no. 3 (2013): 1477–1490, https://doi.org/10.1007/s10570-013-9921-7.

119. E. Trujillo, M. Moesen, L. Osorio, A. W. Van Vuure, J. Ivens, and I. Verpoest, "Bamboo Fibres for Reinforcement in Composite Materials: Strength Weibull Analysis," *Composites Part A: Applied Science and Manufacturing* 61 (2014): 115–125, https://doi.org/10.1016/j.compositesa.2014.02.003.

120. J. Song, C. Chen, S. Zhu, et al., "Processing Bulk Natural Wood Into a High-Performance Structural Material," *Nature* 554, no. 7691 (2018): 224–228, https://doi.org/10.1038/nature25476.

121. M. Ramesh, M. T. Selvan, and K. Niranjana, "Thermal Characterization and Hygrothermal Aging of Lignocellulosic *Agave cantala* Fiber Reinforced Polylactide Composites," *Polymer Composites* 43, no. 9 (2022): 6453–6463, https://doi.org/10.1002/pc.26958.

122. O. Gil-Castell, J. D. Badia, T. Kittikorn, et al., "Hydrothermal Ageing of Polylactide/Sisal Biocomposites. Studies of Water Absorption Behaviour and Physico-Chemical Performance," *Polymer Degradation and Stability* 108 (2014): 212–222, https://doi.org/10.1016/j.polymdegradstab.2014.06.010.

123. I. Spiridon, K. Leluk, A. M. Resmerita, and R. N. Darie, "Evaluation of PLA–Lignin Bioplastics Properties Before and After Accelerated Weathering," *Composites Part B: Engineering* 69 (2015): 342–349, https://doi.org/10.1016/j.compositesb.2014.10.006.

124. M. Berges, R. Léger, V. Placet, et al., "Influence of Moisture Uptake on the Static, Cyclic and Dynamic Behaviour of Unidirectional Flax Fibre-Reinforced Epoxy Laminates," *Composites Part A: Applied Science and Manufacturing* 88 (2016): 165–177, https://doi.org/10.1016/j.compositesa.2016.05.029.

125. A. Bourmaud, C. Morvan, and C. Baley, "Importance of Fiber Preparation to Optimize the Surface and Mechanical Properties of Unitary Flax Fiber," *Industrial Crops and Products* 32, no. 3 (2010): 662–667, https://doi.org/10.1016/j.indcrop.2010.08.002.

126. J. Rousseau, N. E. N. Donkeng, F. Farcas, S. Chevalier, and V. Placet, "Thermal and Hydrothermal Ageing of Flax/Polypropylene Composites and Their Stainless Steel Hybrid Laminates," *Composites Part A: Applied Science and Manufacturing* 171 (2023): 107582, https://doi.org/10.1016/j.compositesa.2023.107582.

127. M. Mejri, L. Toubal, J. C. Cuillière, and V. François, "Hygrothermal Aging Effects on Mechanical and Fatigue Behaviors of a Short-Natural-Fiber-Reinforced Composite," *International Journal of Fatigue* 108 (2018): 96–108, https://doi.org/10.1016/j.ijfatigue.2017.11.004.

128. T. Yu, F. Sun, M. Lu, and Y. Li, "Water Absorption and Hygrothermal Aging Behavior of Short Ramie Fiber Reinforced Poly(Lactic Acid) Composites," *Polymer Composites* 39 (2016): 1098–1104, https://doi.org/10.1002/pc.24038.

129. S. Ugochukwu, M. J. M. Ridzuan, M. S. Abdul Majid, E. M. Cheng, Z. M. Razlan, and N. Marsi, "Effect of Thermal Ageing on the Scratch Resistance of Natural-Fibre-Reinforced Epoxy Composites," *Composite Structures* 261 (2021): 113586, https://doi.org/10.1016/j.compstruct.2021.113586.

130. M. Habibi, L. Laperrière, and H. M. Hassanabadi, "Effect of Moisture Absorption and Temperature on Quasi-Static and Fatigue Behavior of Nonwoven Flax Epoxy Composite," *Composites Part B: Engineering* 166 (2019): 31–40, https://doi.org/10.1016/j.compositesb.2018.11.131.

131. W. Wang, M. Sain, and P. Cooper, "Study of Moisture Absorption in Natural Fiber Plastic Composites," *Composites Science and Technology* 66, no. 3–4 (2006): 379–386, https://doi.org/10.1016/j.compscitech.2005.07.027.

132. N. Mustapha and T. Mahfoud, "Hydro/Hygrothermal Behavior of Plant Fibers and Its Influence on Bio-Composite Properties," in *Natural Fiber*, ed. H. Y. Jeon (IntechOpen, 2022), https://doi.org/10.5772/intechopen.102580.

133. D. Valentin, F. Paray, and B. Guetta, "The Hygrothermal Behaviour of Glass Fibre Reinforced Pa66 Composites: A Study of the Effect of Water Absorption on Their Mechanical Properties," *Journal of Materials Science* 22, no. 1 (1987): 46–56, https://doi.org/10.1007/BF01160550.

134. T. Illing, M. Schoßig, C. Bierögel, and W. Grellmann, "Influence of Hygrothermal Aging on Dimensional Stability of Thin Injection-Molded Short Glass Fiber Reinforced PA6 Materials," *Journal of Applied Polymer Science* 132, no. 28 (2015): app.42245, https://doi.org/10.1002/app.42245.

135. M. P. Foulc, A. Bergeret, L. Ferry, P. Ienny, and A. Crespy, "Study of Hygrothermal Ageing of Glass Fibre Reinforced PET Composites," *Polymer Degradation and Stability* 89, no. 3 (2005): 461–470, https://doi.org/10.1016/j.polymdegradstab.2005.01.025.

136. M. Ramesh, M. Tamil Selvan, and K. Niranjana, "Hygrothermal Aging, Kinetics of Moisture Absorption, Degradation Mechanism and Their Influence on Performance of the Natural Fibre Reinforced Composites," in *Aging Effects on Natural Fiber-Reinforced Polymer Composites: Durability and Life Prediction*, ed. C. Muthukumar, S. Krishnasamy, S. M. K. Thiagamani, and S. Siengchin (Springer Nature, 2022), 257–277, https://doi.org/10.1007/978-981-16-8360-2_14.

137. H. Wang, G. Xian, H. Li, and L. Sui, "Durability Study of a Ramie-Fiber Reinforced Phenolic Composite Subjected to Water Immersion," *Fibers and Polymers* 15, no. 5 (2014): 1029–1034, https://doi.org/10.1007/s12221-014-1029-7.

138. B. K. Venkatesha, R. Saravanan, and K. Anand Babu, "Effect of Moisture Absorption on Woven Bamboo/Glass Fiber Reinforced Epoxy Hybrid Composites," *Materials Today Proceedings* 45 (2021): 216–221, https://doi.org/10.1016/j.matpr.2020.10.421.

139. W. Chunhong, L. Shengkai, and Y. Zhanglong, "Mechanical, Hygrothermal Ageing and Moisture Absorption Properties of Bamboo Fibers Reinforced With Polypropylene Composites," *Journal of Reinforced Plastics and Composites* 35, no. 13 (2016): 1062–1074, https://doi.org/10.1177/0731684416637681.

140. D. E. C. Depuydt, J. Soete, Y. D. Asfaw, M. Wevers, J. Ivens, and A. W. van Vuure, "Sorption Behaviour of Bamboo Fibre Reinforced Composites, Why Do They Retain Their Properties?," *Composites Part A Applied Science and Manufacturing* 119 (2019): 48–60, https://doi.org/10.1016/j.compositesa.2019.01.020.

141. N. Jiang, T. Yu, and Y. Li, "Effect of Hydrothermal Aging on Injection Molded Short Jute Fiber Reinforced Poly(Lactic Acid) (PLA)

Composites," *Journal of Polymers and the Environment* 26, no. 8 (2018): 3176–3186, https://doi.org/10.1007/s10924-018-1205-8.

142. A. Regazzi, S. Corn, P. Ienny, J. C. Bénézet, and A. Bergeret, "Reversible and Irreversible Changes in Physical and Mechanical Properties of Biocomposites During Hydrothermal Aging," *Industrial Crops and Products* 84 (2016): 358–365, https://doi.org/10.1016/j.indcrop.2016.01.052.

143. S. Sanjeevi, V. Shanmugam, S. Kumar, et al., "Effects of Water Absorption on the Mechanical Properties of Hybrid Natural Fibre/Phenol Formaldehyde Composites," *Scientific Reports* 11, no. 1 (2021): 13385, https://doi.org/10.1038/s41598-021-92457-9.

144. H. Deng, C. T. Reynolds, N. O. Cabrera, N. M. Barkoula, B. Alcock, and T. Peijs, "The Water Absorption Behaviour of All-Polypropylene Composites and Its Effect on Mechanical Properties," *Composites Part B: Engineering* 41, no. 4 (2010): 268–275, https://doi.org/10.1016/j.compositesb.2010.02.007.

145. J. D. Badia, L. Santonja-Blasco, A. Martínez-Felipe, and A. Ribes-Greus, "Hygrothermal Ageing of Reprocessed Polylactide," *Polymer Degradation and Stability* 97, no. 10 (2012): 1881–1890, https://doi.org/10.1016/j.polymdegradstab.2012.06.001.

146. C. K. Falkenreck, J. C. Zarges, H. P. Heim, M. Seitz, and C. Bonten, "Degradation of Regenerated Cellulose Fiber-Reinforced Bio-Polyamide in Hydrothermal Environment," *Composites Part A: Applied Science and Manufacturing* 188 (2025): 108584, https://doi.org/10.1016/j.compositesa.2024.108584.

147. Q. Deshoulles, M. Le Gall, C. Dreanno, et al., "Origin of Embrittlement in Polyamide 6 Induced by Chemical Degradations: Mechanisms and Governing Factors," *Polymer Degradation and Stability* 191 (2021): 109657, https://doi.org/10.1016/j.polymdegradstab.2021.109657.

148. H. Marquard, A. M. Deshpande, S. Aditya, S. Doshi, and S. Pilla, "Effect of Environmental Aging on the Thermal and Chemical Properties of Flax Fiber-Polypropylene Natural Fiber Reinforced Thermoplastic Composites," in *2024 ASC Technical Conference*.

149. P. Bazan, D. Mierzwiński, R. Bogucki, and S. Kuciel, "Bio-Based Polyethylene Composites With Natural Fiber: Mechanical, Thermal, and Ageing Properties," *Materials* 13, no. 11 (2020): 2595, https://doi.org/10.3390/ma13112595.

150. S. Tompkins, D. Tenney, and J. Unnam, "Prediction of Moisture and Temperature Changes in Composites During Atmospheric Exposure," in *Fifth Conference on Composite Materials: Testing and Design*, ed. S. Tsai (ASTM International, 1979), 368–380, https://doi.org/10.1520/STP36919S.

151. B. Fayolle, L. Audouin, G. A. George, and J. Verdu, "Macroscopic Heterogeneity in Stabilized Polypropylene Thermal Oxidation," *Polymer Degradation and Stability* 77, no. 3 (2002): 515–522, https://doi.org/10.1016/S0141-3910(02)00110-6.

152. B. Fayolle, E. Richaud, J. Verdu, and F. Farcas, "Embrittlement of Polypropylene Fibre During Thermal Oxidation," *Journal of Materials Science* 43, no. 3 (2008): 1026–1032, https://doi.org/10.1007/s10853-007-2242-1.

153. M. Asim, M. T. Paridah, M. Chandrasekar, et al., "Thermal Stability of Natural Fibers and Their Polymer Composites," *Iranian Polymer Journal* 29, no. 7 (2020): 625–648, https://doi.org/10.1007/s13726-020-00824-6.

154. M. Poletto, H. L. O. Júnior, and A. J. Zattera, "Thermal Decomposition of Natural Fibers: Kinetics and Degradation Mechanisms," in *Reactions and Mechanisms in Thermal Analysis of Advanced Materials*, 1st ed., ed. A. Tiwari and B. Raj (Wiley, 2015), 515–545, https://doi.org/10.1002/9781119117711.ch21.

155. E. Richaud, C. Monchy-Leroy, X. Colin, L. Audouin, and J. Verdu, "Kinetic Modelling of Stabilization Coupled With Stabilizer Loss by Evaporation. Case of Dithioester Stabilized Polyethylene," *Polymer Degradation and Stability* 94 (2009): 2004–2014, https://doi.org/10.1016/j.polymdegradstab.2009.07.017.

156. A. Niemczyk, K. Dziubek, M. Grzymek, and K. Czaja, "Accelerated Laboratory Weathering of Polypropylene Composites Filled With Synthetic Silicon-Based Compounds," *Polymer Degradation and Stability* 161 (2019): 30–38, https://doi.org/10.1016/j.polymdegradstab.2019.01.005.

157. J. Huang, P. Yves Le Gac, and E. Richaud, "Thermal Oxidation of Poly(Dicyclopentadiene)—Effect of Phenolic and Hindered Amine Stabilizers," *Polymer Degradation and Stability* 183 (2021): 109267, https://doi.org/10.1016/j.polymdegradstab.2020.109267.

158. G. M. Marielle, C. Durrieu, A. Guenne, et al., "Impact of Polyethylene and Polypropylene Geomembranes in Sensitive Aquatic Environment," *Ecotoxicology and Environmental Safety* 148 (2018): 884–891, https://doi.org/10.1016/j.ecoenv.2017.11.015.

159. I. Papa, A. Formisano, V. Lopresto, F. Cimino, L. Vitiello, and P. Russo, "Water Ageing Effects on the Mechanical Properties of Flax Fibre Fabric/Polypropylene Composite Laminates," *Journal of Composite Materials* 54, no. 24 (2020): 3481–3489, https://doi.org/10.1177/0021998320916546.

160. S. Migneault, A. Koubaa, P. Perré, and B. Riedl, "Effects of Wood Fiber Surface Chemistry on Strength of Wood–Plastic Composites," *Applied Surface Science* 343 (2015): 11–18, https://doi.org/10.1016/j.apsusc.2015.03.010.

161. A. Kumar, K. Staněk, P. Ryparová, P. Hajek, and J. Tywoniak, "Hydrophobic Treatment of Wood Fibrous Thermal Insulator by Octadecyltrichlorosilane and Its Influence on Hygric Properties and Resistance Against Moulds," *Composites Part B: Engineering* 106 (2016): 285–293, https://doi.org/10.1016/j.compositesb.2016.09.034.

162. N. Hamour, A. Boukerrou, H. Djidjelli, J. E. Maigret, and J. Beaugrand, "Effects of MAPP Compatibilization and Acetylation Treatment Followed by Hydrothermal Aging on Polypropylene Alfa Fiber Composites," *International Journal of Polymer Science* 2015, no. 1 (2015): 451691, https://doi.org/10.1155/2015/451691.

163. A. Le Duigou, J. Merotte, A. Bourmaud, P. Davies, K. Belhouli, and C. Baley, "Hygroscopic Expansion: A Key Point to Describe Natural Fibre/Polymer Matrix Interface Bond Strength," *Composites Science and Technology* 151 (2017): 228–233, https://doi.org/10.1016/j.compscitech.2017.08.028.

164. A. Le Duigou, P. Davies, and C. Baley, "Exploring Durability of Interfaces in Flax Fibre/Epoxy Micro-Composites," *Composites Part A: Applied Science and Manufacturing* 48 (2013): 121–128, https://doi.org/10.1016/j.compositesa.2013.01.010.

165. M. Péron, A. Célino, M. Castro, F. Jacquemin, and A. Le Duigou, "Study of Hygroscopic Stresses in Asymmetric Biocomposite Laminates," *Composites Science and Technology* 169 (2019): 7–15, https://doi.org/10.1016/j.compscitech.2018.10.027.

166. H. Chen, M. Miao, and X. Ding, "Influence of Moisture Absorption on the Interfacial Strength of Bamboo/Vinyl Ester Composites," *Composites Part A: Applied Science and Manufacturing* 40, no. 12 (2009): 2013–2019, https://doi.org/10.1016/j.compositesa.2009.09.003.

167. C. Cerbu, H. Wang, M. F. Botis, Z. Huang, and C. Plescan, "Temperature Effects on the Mechanical Properties of Hybrid Composites Reinforced With Vegetable and Glass Fibers," *Mechanics of Materials* 149 (2020): 103538, https://doi.org/10.1016/j.mechmat.2020.103538.

168. S. Liu, P. Rawat, Z. Chen, S. Guo, C. Shi, and D. Zhu, "Pullout Behaviors of Single Yarn and Textile in Cement Matrix at Elevated Temperatures With Varying Loading Speeds," *Composites Part B: Engineering* 199 (2020): 108251, https://doi.org/10.1016/j.compositesb.2020.108251.

169. D. Hristozov, L. Wroblewski, and P. Sadeghian, "Long-Term Tensile Properties of Natural Fibre-Reinforced Polymer Composites:

Comparison of Flax and Glass Fibres," *Composites Part B: Engineering* 95 (2016): 82–95, https://doi.org/10.1016/j.compositesb.2016.03.079.

170. L. Yan and N. Chouw, "Effect of Water, Seawater and Alkaline Solution Ageing on Mechanical Properties of Flax Fabric/Epoxy Composites Used for Civil Engineering Applications," *Construction and Building Materials* 99 (2015): 118–127, https://doi.org/10.1016/j.conbuildmat.2015.09.025.

171. G. Apolinario, P. Ienny, S. Corn, R. Léger, A. Bergeret, and J. M. Haudin, "Effects of Water Ageing on the Mechanical Properties of Flax and Glass Fibre Composites: Degradation and Reversibility," in *Natural Fibres: Advances in Science and Technology Towards Industrial Applications*, vol. 12, eds. R. Fangueiro and S. Rana (Springer, 2016), 183–196, http://link.springer.com/10.1007/978-94-017-7515-1_14.

172. S. N. A. B. Safri, M. T. H. Sultan, and M. Jawaid, "Damage Analysis of Glass Fiber Reinforced Composites," in *Durability and Life Prediction in Biocomposites, Fibre-Reinforced Composites and Hybrid Composites* (Elsevier, 2019), 133–147, https://doi.org/10.1016/B978-0-08-102290-0.00007-6.

173. L. Sorrentino, D. S. De Vasconcellos, M. D'Auria, F. Sarasini, and J. Tirillò, "Effect of Temperature on Static and Low Velocity Impact Properties of Thermoplastic Composites," *Composites Part B: Engineering* 113 (2017): 100–110, https://doi.org/10.1016/j.compositesb.2017.01.010.

174. D. Q. Vu, M. Gigliotti, and M. C. Lafarie-Frenot, "Experimental Characterization of Thermo-Oxidation-Induced Shrinkage and Damage in Polymer–Matrix Composites," *Composites Part A: Applied Science and Manufacturing* 43, no. 4 (2012): 577–586, https://doi.org/10.1016/j.compositesa.2011.12.018.

175. M. Gigliotti, Y. Pannier, M. Minervino, M. C. Lafarie-Frenot, and P. Corigliano, "The Effect of a Thermo-Oxidative Environment on the Behaviour of Multistable [0/90] Unsymmetric Composite Plates," *Composite Structures* 106 (2013): 863–872, https://doi.org/10.1016/j.compstruct.2013.07.016.

176. J. L. Oliveira, A. W. B. Skilbred, A. Loken, R. R. Henriques, and B. G. Soares, "Effect of Accelerated Ageing Procedures and Flash Rust Inhibitors on the Anti-Corrosive Performance of Epoxy Coatings: EIS and Dynamic-Mechanical Analysis," *Progress in Organic Coatings* 159 (2021): 106387, https://doi.org/10.1016/j.porgcoat.2021.106387.

177. M. Zhang, B. Sun, and B. Gu, "Accelerated Thermal Ageing of Epoxy Resin and 3-D Carbon Fiber/Epoxy Braided Composites," *Composites Part A: Applied Science and Manufacturing* 85 (2016): 163–171, https://doi.org/10.1016/j.compositesa.2016.03.028.

178. A. Regazzi, S. Corn, P. Ienny, and A. Bergeret, "Coupled Hydro-Mechanical Aging of Short Flax Fiber Reinforced Composites," *Polymer Degradation and Stability* 130 (2016): 300–306, https://doi.org/10.1016/j.polymdegradstab.2016.06.016.

179. F. K. Sodoke, L. Toubal, and L. Laperrière, "Hygrothermal Effects on Fatigue Behavior of Quasi-Isotropic Flax/Epoxy Composites Using Principal Component Analysis," *Journal of Materials Science* 51, no. 24 (2016): 10793–10805, https://doi.org/10.1007/s10853-016-0291-z.

180. Z. Lu, G. Xian, and H. Li, "Effects of Elevated Temperatures on the Mechanical Properties of Basalt Fibers and BFRP Plates," *Construction and Building Materials* 127 (2016): 1029–1036, https://doi.org/10.1016/j.conbuildmat.2015.10.207.

181. B. C. Ray and D. Rathore, "Durability and Integrity Studies of Environmentally Conditioned Interfaces in Fibrous Polymeric Composites: Critical Concepts and Comments," *Advances in Colloid and Interface Science* 209 (2014): 68–83, https://doi.org/10.1016/j.cis.2013.12.014.

182. M. Eftekhari and A. Fatemi, "Tensile Behavior of Thermoplastic Composites Including Temperature, Moisture, and Hygrothermal Effects," *Polymer Testing* 51 (2016): 151–164, https://doi.org/10.1016/j.polymertesting.2016.03.011.

183. B. Mouhmid, A. Imad, N. Benseddiq, S. Benmedakhène, and A. Maazouz, "A Study of the Mechanical Behaviour of a Glass Fibre Reinforced Polyamide 6,6: Experimental Investigation," *Polymer Testing* 25, no. 4 (2006): 544–552, https://doi.org/10.1016/j.polymertesting.2006.03.008.

184. M. De Monte, E. Moosbrugger, and M. Quaresimin, "Influence of Temperature and Thickness on the Off-Axis Behaviour of Short Glass Fibre Reinforced Polyamide 6.6—Quasi-Static Loading," *Composites Part A: Applied Science and Manufacturing* 41, no. 7 (2010): 859–871, https://doi.org/10.1016/j.compositesa.2010.02.018.

185. S. Mortazavian and A. Fatemi, "Tensile and Fatigue Behaviors of Polymers for Automotive Applications: Zähigkeits- Und Ermüdungsverhalten von Polymeren für Automobilanwendungen," *Materialwissenschaft und Werkstofftechnik* 46, no. 2 (2015): 204–213, https://doi.org/10.1002/mawe.201400376.

186. A. R. Martin, M. A. Martins, O. R. R. F. Da Silva, and L. H. C. Mattoso, "Studies on the Thermal Properties of Sisal Fiber and Its Constituents," *Thermochimica Acta* 506, no. 1–2 (2010): 14–19, https://doi.org/10.1016/j.tca.2010.04.008.

187. A. Le Duigou, P. Davies, and C. Baley, "Interfacial Bonding of Flax Fibre/Poly(l-Lactide) Bio-Composites," *Composites Science and Technology* 70, no. 2 (2010): 231–239, https://doi.org/10.1016/j.compscitech.2009.10.009.

188. F. Tian and Z. Zhong, "Modeling of Load Responses for Natural Fiber Reinforced Composites Under Water Absorption," *Composites Part A: Applied Science and Manufacturing* 125 (2019): 105564, https://doi.org/10.1016/j.compositesa.2019.105564.

189. J. Wang, H. GangaRao, R. Liang, and W. Liu, "Durability and Prediction Models of Fiber-Reinforced Polymer Composites Under Various Environmental Conditions: A Critical Review," *Journal of Reinforced Plastics and Composites* 35, no. 3 (2016): 179–211, https://doi.org/10.1177/0731684415610920.

190. T. K. Mulenga, A. U. Ude, and C. Vivekanandhan, "Techniques for Modelling and Optimizing the Mechanical Properties of Natural Fiber Composites: A Review," *Fibers* 9, no. 1 (2021): 6, https://doi.org/10.3390/fib9010006.

191. F. Tian, Y. Pan, and Z. Zhong, "A Long-Term Mechanical Degradation Model of Unidirectional Natural Fiber Reinforced Composites Under Hydrothermal Ageing," *Composites Science and Technology* 142 (2017): 156–162, https://doi.org/10.1016/j.compscitech.2017.01.021.

192. X. Wang and M. Petrů, "Degradation of Bending Properties of Flax Fiber Reinforced Polymer After Natural Aging and Accelerated Aging," *Construction and Building Materials* 240 (2020): 117909, https://doi.org/10.1016/j.conbuildmat.2019.117909.

193. V. N. Bulmanis, G. M. Gunyaev, V. V. Krivonos, et al., "Atmospheric Durability of Polymer-Fiber Composites in Cold Climates," *Mechanics of Composite Materials* 27, no. 6 (1992): 698–705, https://doi.org/10.1007/BF00808081.

194. A. E. Krauklis, A. G. Akulichev, A. I. Gagani, and A. T. Echtermeyer, "Time–Temperature–Plasticization Superposition Principle: Predicting Creep of a Plasticized Epoxy," *Polymers* 11, no. 11 (2019): 1848, https://doi.org/10.3390/polym11111848.

195. T. C. Yang, T. L. Wu, K. C. Hung, Y. L. Chen, and J. H. Wu, "Mechanical Properties and Extended Creep Behavior of Bamboo Fiber Reinforced Recycled Poly(Lactic Acid) Composites Using the Time–Temperature Superposition Principle," *Construction and Building Materials* 93 (2015): 558–563, https://doi.org/10.1016/j.conbuildmat.2015.06.038.

196. Z. Cui, W. Liu, L. Tan, G. Sun, and X. Hu, "Evidence for Non-Arrhenius Behavior of EPDM Rubber by Combining Arrhenius and Time–Temperature Superposition (TTS) Extrapolations," *RSC Advances* 14, no. 8 (2024): 5216–5221, https://doi.org/10.1039/D3RA07159F.

197. D. Jain, I. Kamboj, T. K. Bera, A. S. Kang, and R. K. Singla, "Experimental and Numerical Investigations on the Effect of Alkaline Hornification on the Hydrothermal Ageing of Agave Natural Fiber Composites," *International Journal of Heat and Mass Transfer* 130 (2019): 431–439, https://doi.org/10.1016/j.ijheatmasstransfer.2018.10.106.

198. A. Regazzi, R. Léger, S. Corn, and P. Ienny, "Modeling of Hydrothermal Aging of Short Flax Fiber Reinforced Composites," *Composites Part A: Applied Science and Manufacturing* 90 (2016): 559–566, https://doi.org/10.1016/j.compositesa.2016.08.011.

199. N. Jiang, Y. Li, D. Li, et al., "3D Finite Element Modeling of Water Diffusion Behavior of Jute/PLA Composite Based on X-Ray Computed Tomography," *Composites Science and Technology* 199 (2020): 108313, https://doi.org/10.1016/j.compscitech.2020.108313.

200. P. Prasanthi Parvathaneni, V. V. V. Madhav, C. S. Chaitanya, et al., "Prediction of Impact Behaviour for Natural Fiber-Reinforced Composites Using the Finite Element Method," *Composites and Advanced Materials* 31 (2022): 263498332211450, https://doi.org/10.1177/26349833221145016.

201. Z. J. Li, Z. W. Huang, H. L. Dai, Y. Yao, and Y. S. Li, "Hygrothermal Coupled Modeling and Behavior Analysis of Natural Fiber-Reinforced Tubular Composites," *Construction and Building Materials* 411 (2024): 134384, https://doi.org/10.1016/j.conbuildmat.2023.134384.

202. R. Potluri, V. Diwakar, K. Venkatesh, and B. Srinivasa Reddy, "Analytical Model Application for Prediction of Mechanical Properties of Natural Fiber Reinforced Composites," *Materials Today Proceedings* 5, no. 2 (2018): 5809–5818, https://doi.org/10.1016/j.matpr.2017.12.178.

203. G. Kalaprasad, K. Joseph, S. Thomas, and C. Pavithran, "Theoretical Modelling of Tensile Properties of Short Sisal Fibre-Reinforced Low-Density Polyethylene Composites," *Journal of Materials Science* 32, no. 16 (1997): 4261–4267, https://doi.org/10.1023/A:1018651218515.

204. Q. Drouhet, F. Touchard, and L. Chocinski-Arnault, "Tensile Behavior of [0/90]7 Hemp/Elium Biocomposites After Water Aging: In-Situ Micro-CT Testing and Numerical Analysis," *Micro* 3, no. 2 (2023): 496–509, https://doi.org/10.3390/micro3020033.

205. A. Michel and V. Marcos-Meson, "On the Application of Neural Networks for Service Life Prediction of Steel Fibre-Reinforced Concrete," *Journal of Building Engineering* 76 (2023): 107286, https://doi.org/10.1016/j.jobe.2023.107286.

206. A. Belaadi, A. Lekrine, M. Boumaaza, et al., "Water Uptake of HDPE Reinforced With *Washingtonia* Fibre Biocomposites: Mathematical Modelling Using Artificial Neural Network, Response Surface Methodology and Genetic Algorithm," *Advances in Materials and Processing Technologies* 10, no. 3 (2024): 1627–1650, https://doi.org/10.1080/2374068X.2023.2198828.

207. A. Saaidia, A. Belaadi, M. Boumaaza, H. Alshahrani, and M. Bourchak, "Effect of Water Absorption on the Behavior of Jute and Sisal Fiber Biocomposites at Different Lengths: ANN and RSM Modeling," *Journal of Natural Fibers* 20, no. 1 (2023): 2140326, https://doi.org/10.1080/15440478.2022.2140326.

208. J. O. Ighalo, C. A. Igwegbe, A. G. Adeniyi, and S. A. Abdulkareem, "Artificial Neural Network Modeling of the Water Absorption Behavior of Plantain Peel and Bamboo Fibers Reinforced Polystyrene Composites," *Journal of Macromolecular Science, Part B* 60, no. 7 (2021): 472–484, https://doi.org/10.1080/00222348.2020.1866282.

209. M. Chakkour, M. Ould Moussa, I. Khay, M. Balli, and T. Ben Zineb, "Long-Term Water Aging Effects on the Durability of Alkali-Treated Bamboo Fiber Reinforced Composite," *Cellulose* 30, no. 18 (2023): 11589–11604, https://doi.org/10.1007/s10570-023-05598-7.

210. E. S. Rodriguez, P. M. Stefani, and A. Vazquez, "Effects of Fibers' Alkali Treatment on the Resin Transfer Molding Processing and Mechanical Properties of Jute—Vinylester Composites," *Journal of Composite Materials* 41, no. 14 (2007): 1729–1741, https://doi.org/10.1177/0021998306069889.

211. K. L. Pickering, A. Abdalla, C. Ji, A. G. McDonald, and R. A. Franich, "The Effect of Silane Coupling Agents on Radiata Pine Fibre for Use in Thermoplastic Matrix Composites," *Composites Part A, Applied Science and Manufacturing* 34, no. 10 (2003): 915–926, https://doi.org/10.1016/S1359-835X(03)00234-3.

212. X. Li, L. G. Tabil, and S. Panigrahi, "Chemical Treatments of Natural Fiber for Use in Natural Fiber-Reinforced Composites: A Review," *Journal of Polymers and the Environment* 15, no. 1 (2007): 25–33, https://doi.org/10.1007/s10924-006-0042-3.

213. T. H. Mokhothu and M. J. John, "Bio-Based Coatings for Reducing Water Sorption in Natural Fibre Reinforced Composites," *Scientific Reports* 7, no. 1 (2017): 13335, https://doi.org/10.1038/s41598-017-13859-2.

214. M. Sathish, N. Radhika, N. Venuvanka, and L. Rajeshkumar, "A Review on Sustainable Properties of Plant Fiber-Reinforced Polymer Composites: Characteristics and Properties," *Polymer International* 73, no. 11 (2024): 887–943, https://doi.org/10.1002/pi.6686.

215. M. R. Sanjay, S. Siengchin, J. Parameswaranpillai, M. Jawaid, C. I. Pruncu, and A. Khan, "A Comprehensive Review of Techniques for Natural Fibers as Reinforcement in Composites: Preparation, Processing and Characterization," *Carbohydrate Polymers* 207 (2019): 108–121, https://doi.org/10.1016/j.carbpol.2018.11.083.

216. N. Le Moigne, B. Otazaghine, S. Corn, H. Angellier-Coussy, and A. Bergeret, *Surfaces and Interfaces in Natural Fibre Reinforced Composites* (Springer International Publishing, 2018), https://doi.org/10.1007/978-3-319-71410-3.

217. T. Huber, U. Biedermann, and J. Müssig, "Enhancing the Fibre Matrix Adhesion of Natural Fibre Reinforced Polypropylene by Electron Radiation Analyzed With the Single Fibre Fragmentation Test," *Composite Interfaces* 17, no. 4 (2010): 371–381, https://doi.org/10.1163/092764410X495270.

218. N. Le Moigne, R. Sonnier, R. El Hage, and S. Rouif, "Radiation-Induced Modifications in Natural Fibres and Their Biocomposites: Opportunities for Controlled Physico-Chemical Modification Pathways?," *Industrial Crops and Products* 109 (2017): 199–213, https://doi.org/10.1016/j.indcrop.2017.08.027.

219. M. Ramesh, K. Palanikumar, and K. H. Reddy, "Plant Fibre Based Bio-Composites: Sustainable and Renewable Green Materials," *Renewable and Sustainable Energy Reviews* 79 (2017): 558–584, https://doi.org/10.1016/j.rser.2017.05.094.

220. H. Sharma, A. Kumar, S. Rana, et al., "Critical Review on Advancements on the Fiber-Reinforced Composites: Role of Fiber/Matrix Modification on the Performance of the Fibrous Composites," *Journal of Materials Research and Technology* 26 (2023): 2975–3002, https://doi.org/10.1016/j.jmrt.2023.08.036.

221. G. F. Schutz, S. De Ávila Gonçalves, R. M. V. Alves, and R. P. Vieira, "A Review of Starch-Based Biocomposites Reinforced With Plant Fibers," *International Journal of Biological Macromolecules* 261 (2024): 129916, https://doi.org/10.1016/j.ijbiomac.2024.129916.

222. M. Ramesh, C. Deepa, L. R. Kumar, M. Sanjay, and S. Siengchin, "Life-Cycle and Environmental Impact Assessments on Processing of Plant Fibres and Its Bio-Composites: A Critical Review," *Journal of Industrial Textiles* 51, no. 4_suppl (2022): 5518S–5542S, https://doi.org/10.1177/1528083720924730.

223. R. Shen, S. Xue, Y. Xu, et al., "Research Progress and Development Demand of Nanocellulose Reinforced Polymer Composites," *Polymers* 12, no. 9 (2020): 2113, https://doi.org/10.3390/polym12092113.

224. D. Liang, W. Liu, T. Zhong, et al., "Nanocellulose Reinforced Lightweight Composites Produced From Cotton Waste via Integrated

Nanofibrillation and Compounding," *Scientific Reports* 13, no. 1 (2023): 2144, https://doi.org/10.1038/s41598-023-29335-z.

225. Z. Kassab, H. Daoudi, M. H. Salim, C. El Idrissi Hassani, Y. Abdellaoui, and M. El Achaby, "Process-Structure-Property Relationships of Cellulose Nanocrystals Derived From *Juncus effusus* Stems on κ-Carrageenan-Based Bio-Nanocomposite Films," *International Journal of Biological Macromolecules* 265 (2024): 130892, https://doi.org/10.1016/j.ijbiomac.2024.130892.

226. V. A. Nang, L. Hoang Nguyen, K. Yoshimura, T. Duy Tran, and H. Van Le, "Cellulose Nanocrystals Isolated From Sugarcane Bagasse Using the Formic/Peroxyformic Acid Process: Structural, Chemical, and Thermal Properties," *Arabian Journal of Chemistry* 17, no. 8 (2024): 105841, https://doi.org/10.1016/j.arabjc.2024.105841.

227. M. Pagliaro, R. Ciriminna, M. Yusuf, et al., "Application of Nanocellulose Composites in the Environmental Engineering: A Review," *Journal of Composites and Compounds* 3, no. 7 (2021): 114–128, https://doi.org/10.52547/jcc.3.2.5.

228. S. M. Hussnain, S. Z. H. Shah, P. S. M. Megat-Yusoff, and M. Z. Hussain, "Degradation and Mechanical Performance of Fibre-Reinforced Polymer Composites Under Marine Environments: A Review of Recent Advancements," *Polymer Degradation and Stability* 215 (2023): 110452, https://doi.org/10.1016/j.polymdegradstab.2023.110452.

229. S. C. Das, A. D. La Rosa, S. Goutianos, and S. Grammatikos, "Effect of Accelerated Weathering on the Performance of Natural Fibre Reinforced Recyclable Polymer Composites and Comparison With Conventional Composites," *Composites Part C: Open Access* 12 (2023): 100378, https://doi.org/10.1016/j.jcomc.2023.100378.

230. K. Yorseng, S. M. Rangappa, H. Pulikkalparambil, S. Siengchin, and J. Parameswaranpillai, "Accelerated Weathering Studies of Kenaf/Sisal Fiber Fabric Reinforced Fully Biobased Hybrid Bioepoxy Composites for Semi-Structural Applications: Morphology, Thermo-Mechanical, Water Absorption Behavior and Surface Hydrophobicity," *Construction and Building Materials* 235 (2020): 117464, https://doi.org/10.1016/j.conbuildmat.2019.117464.

231. P. Davies, M. Le Gall, Z. Niu, et al., "Recycling and Ecotoxicity of Flax/PLA Composites: Influence of Seawater Aging," *Composites Part C: Open Access* 12 (2023): 100379, https://doi.org/10.1016/j.jcomc.2023.100379.

232. X. Zhao, K. Copenhaver, L. Wang, et al., "Recycling of Natural Fiber Composites: Challenges and Opportunities," *Resources, Conservation and Recycling* 177 (2022): 105962, https://doi.org/10.1016/j.resconrec.2021.105962.